Devising an Effective Biological Decolorization Approach for Synthetic Textile Effluents

Submitted in partial fulfillment of the requirement for the award of the degree of

DOCTOR OF PHILOSOPHY

in

CHEMICAL ENGINEERING

by

Mukkera Vamshi Krishna

Roll No: 718053

Under the Supervision of

Dr. K Srivani

(Supervisor)

Dr. K S Rajmohan

(Co-supervisor)

DEPARTMENT OF CHEMICAL ENGINEERING
NATIONAL INSTITUTE OF TECHNOLOGY WARANGAL
TELANGANA – 506004, INDIA.
AUGUST 2023

ABSTRACT

Water treatment processes are commonly employed to reduce the concentration of foreign particles in industrial effluents. Among various industries, textile industries release effluents containing azo dyes, which can increase the levels of Chemical Oxygen Demand (COD), Biological Oxygen Demand (BOD), and Total Organic Carbon (TOC) in water bodies, leading to adverse impacts on flora and fauna. To mitigate these environmental effects, it is essential to degrade azo dyes before discharging them into water bodies. While several physico-chemical methods have been studied for azo dye degradation, this research focuses on using bioremediation in a Fluidized Bed Bioreactor, which offers advantages over other methods.

The study primarily targets the reduction of dye content in synthetic solutions to the minimum possible levels. The main objectives of this research are (a) to study the biodegradation of azo dyes using microbes with response surface methodology to optimize decolorization, (b) to compare the decolorization rates of bacteria and yeast, (c) to develop an improved decolorization process by immobilizing Pichia pastoris, and (d) to compare the decolorization efficiency of a physical method (Adsorption) with a physical-biological method in a microbe-immobilized bioreactor (Fluidized Bed Bioreactor).

Pure cultures of bacteria "*Thalassospira frigidphilosprofundus*" and "*Erwinia chrysanthemi burkholder*" and yeast "Pichia pastoris" were employed for the above objectives. Experiments were conducted in shaking conical flasks to degrade Chrysophenine and Acid red 13, commonly used azo dyes in textile industries. Various environmental conditions such as pH, temperature, agitation, and dye concentration were observed to determine their impact on biodegradation. The kinetic models for dye degradation were obtained using MINITAB 14 software, and the results were analyzed.

The study found that *Thalassospira frigidphilosprofundus* (NCIM no. 5438) exhibited higher decolorization efficiency compared to *Erwinia chrysanthemi burkholder* (NCIM no. 5213), indicating the ease of dye decolorization by the former. Phytotoxicity tests using Phaseolus Mungo seeds confirmed the detoxification of simulated wastewater by microbial treatment.

For the biodegradation of Direct Yellow 12 and Acid Red 13 using yeast culture Pichia pastoris (NCIM 3632), response surface methodology was used to optimize the process factors, such as pH, inoculum dosage, and initial dye concentration. The modeled kinetic data were statistically significant, showing promising results for the biodegradation of azo dyes.

Further experiments were conducted in bioreactors with Pichia pastoris immobilized in activated carbon obtained from locally sourced coconut shells. This immobilization process improved the microbe's action on the degradation process. The Fluidized Bed Bioreactor showed higher decolorization rates compared to the Batch reactor tank.

Adsorption kinetics of the microbe-immobilized activated carbon on dye simulated solutions were studied using Langmuir, Freundlich, and Temkin adsorption isotherms. The results indicated that chemisorption assisted Langmuir adsorption isotherm favored physisorption assisted Freundlich adsorption isotherm for Direct Yellow 12 biodegradation compared to Acid Red 13.

Overall, this research demonstrates the efficacy of bioremediation and immobilization techniques for the efficient degradation of azo dyes in industrial effluents. The findings have promising environmental implications in cleaning up azo dye-containing effluents and promoting sustainable wastewater treatment practices.

Keywords: Azo dye degradation, Bioremediation, Fluidized Bed Bioreactor, Microbe immobilization, Sustainable wastewater treatment, *Thalassospira frigidphilosprofundus*, *Erwinia chrysanthemi burkholder*, *Pichia pastoris*

CONTENTS

List of Figures

List of Tables

Nomenclature

a	Agitation (rpm)
A	Equilibrium binding constant (L/g)
ANOVA	Analysis of Variance
AOP	Advanced Oxidation Process
ASP	Activated Sludge Process
B	Constant related to heat of sorption (J/mol)
BOD	Biochemical Oxygen Demand
BRT	Batch Reactor Tank
c	Concentration of dye (mg/L)
C	Inoculum dosage
CCD	Central composite design
CF	Control flask
COD	Chemical Oxygen Demand
CSAC	Coconut shell activated carbon
C_o	Initial concentration of adsorbate in solution (mg/L)
CFD	Computational Fluid Dynamics
D	Methanol content added
D1	Direct yellow 12
D2	Acid red 13
DO	Dissolved Oxygen
DCM	Dry Cell Mass

EGSB	Expanded granular sludge bed
$FADH_2$	Flavin adenine dinucleotide
FBBR	Fluidized bed Bioreactor
h	Initial adsorption rate (mol/(g.min))
HRT	Hydraulic Retention Time
IUPAC	International Union of Pure and Applied Chemistry
k_1	Rate constant of first-order adsorption (1/min)
k_2	Rate constant of second order adsorption (g/(mg/min))
K_L	Langmuir adsorption constant related to energy of adsorption (L/mg)
K_f	Freundlich adsorption constant
K_T	Temkin constant
K_m	Michaelis constant
m	The weight of adsorbent used per litre of solution (g/L)
MB	Methylene Blue
MBR	Membrane Bioreactor
MO	Methyl Orange
MFC	Microbial Fuel Cell
MGYP	Growth Medium for yeast
MSM	Minimal Salt Medium
n	Empirical constant of Freundlich isotherm
N	*Pichia pastoris*
NADH	Nicotinamide adenine dinucleotide

NADPH	Nicotinamide adenine dinucleotide phosphate
NCIM	National Collection of Industrial Microorganisms
NM1	*Thalassospira frigidphilosprofundus*
NM2	*Erwinia chrysanthemi burkholder*
OD	Optical Density
P	pH
PAC	Powdered Activated Carbon
PUF	Polyurethane foam
PVA	Polyvinyl alcohol
q_e	quantity of dye uptake from solution by mass of adsorbent (mg/g)
q_t	Amount of adsorbed dye on the adsorbent at time t min (mg/g)
q_m	maximum adsorption capacity of the solid (mg/g)
r	Reaction rate
RTD	Residence Time Distribution
S	Substrate concentration
SBR	Sequential batch reactor
SRT	Solids Retention Time
t	Temperature (°C)
TDR	Tire Derived Rubber
TOC	Total Organic Carbon
TSS	Total Suspended Solids
UASB	Upflow Aerobic Sludge Blanket

UF	ultrafiltration
V_{max}	Maximum rate of reaction
WB	Wheat Bran
y	% decolorization
λmax	Maximum wavelength in UV Vis spectroscopy

Chapter 1

Introduction

Chapter 1

1. Introduction

1.1 Background

Water is a finite and vital resource that sustains life on Earth. However, its availability is becoming increasingly scarce due to various factors, including population growth, urbanization, and industrialization. Currently, less than 1% of the world's freshwater is accessible for human use, and this demand is expected to rise by more than 35% by 2050. The textile industry, in particular, is a significant consumer of water during the process of converting fiber to textiles (R. G. Saratale et al., 2011). In addition to water usage, the industry also contributes to water pollution through the discharge of effluents containing dyes and chemicals. Plastic, trash, and chemicals have accumulated in our water resources, such as lakes, rivers, and reservoirs (Melissa Denchak, 2018). In the last few decades, there is an exponential increase in wastewater generation due to growing urbanization and industry needs (Shindhal et al., 2021). The exponential increase in wastewater generation, driven by rapid urbanization and industrial needs, has further aggravated the problem (Ngo et al., 2016). There are many industries that use dyes that contribute to pollution of water, including textile mills, food, pharmaceuticals, paper and printing, leather and cosmetics (Chang et al., 2001;Gharbani et al., 2008). Consequently, dyes inflict harm to water bodies due to their high solubility and the existence of chromophoric groups in their assembly. Moreover, they prevent light from penetrating the water, which can lead to the reduction in photosynthetic level, destroying the entire aquatic environment (Hassan & Carr, 2018). Speaking of worldwide economics, the textile industry is a significant division. Textile dyeing and dyestuffs manufacturing have experienced tremendous growth, resulting in increasing volumes and complexities of wastewater released into the habitat. A high amount of dye contaminated runoff is dumped to water straight away, which is predicted to be 0.7 to 2 lakh tonnes annually (Kurade et al., 2015; Chen et al., 2019; Foroutan et al., 2020). For the dying course, a group of dyes which are about 60 to 70% of all dyes, are utilized in many of the industries, of which, about 20% are discharged into the environment, particularly azo dyes (Lin et al., 2014) which cause severe damage to the habitat (Akpan & Hameed, 2009). According to (Martorell et al., 2018), nearly 3 lakh tons of dyes are released as industrial wastewater every year. When textiles are dyed, there is a loss of dyestuff directly into water, which that finally makes hits the environment. The waste water

characteristics of a dye house vary greatly based on the dye's layout and the concentration of the agents added. BOD, COD, suspended solids and alkalinity of dye wastewater become usually high, along with relatively high temperatures (H. S. Lade et al., 2012).

1.1.1 Color Dyes

In the past, individuals have tinted their fabrics using locally accessible materials by applying common, natural colorants to their environment, and their garments. In the Neolithic period, dyes were used in painting and dyeing. Earlier, dyes were got of plant, creatures or mineral sources. Spanish treasure ships brought cochineal bugs and timber dyes to Europe. Castillejo et al (2008) and they were then transported to America by the colonizers (Adrosko et al. 1971). In traditional dye manufacturing, all colorants were of natural origin until 1856, when W.H.Perkin managed to manufacture a die from quinine that had excellent dyeing properties. (Anthony 1990, Hubner 2006). During the early 1940s, synthetic dyes and organic chemistry as a whole were resurrected. Mauvine, fuchsine, saffranine and Induline are some examples of aniline dyes that have been discovered. Millions of other dyes have been created since (Hunger 2003, Zollinger 2003).

1.1.2 Classification of Dyes

There are mainly two classes of dyes

Natural dyes come from plants or animals such as roots, bark, leaves, berries wood and lichens and fungi. *Synthetic dyes* are human made and are artificial. Based on the particle charge, synthetic dyes can be divided into non-ionic (disperse dyes), anionic (direct, acidic, and reactive dyes), and cationic forms (basic dyes) (Varjani et al., 2020).

1. Direct dyes

There are many types of dyes available, including direct dyes which are utilized for dyeing cotton, paper, leather, wool, silk. They are also used as stains in microbiology as well as to indicate pH.

2. Mordant dyes

It is essential for natural dyes to contain a mordant, which improves the dyes resistance to water and light. 30% of wool is dyed with mordant dyes.

3. Vat dyes

The alkaline metal of salt of these dyes is soluble in water and thus can be used for dye textile fibres directly, but they are insoluble in water.

4. Acid dyes

It refers to colorants that are compatible with synthetic fibers like as silk, wool and acrylic fibers. Most synthetic food colours are anionic dyes.

5. Basic dyes

A basic dye is a water soluble, cationic dye that is most often found in acrylic fibre, though some are used with wool and silk. In addition to acrylic fibre, basic dyes are sometimes found in paper colouring.

6. Reactive dyes

For dyeing cotton and other cellulose fibres, reactive dyes use chromophores attached to substituents that react directly with substrate.

7. Azoic dyes

The use of insoluble hazardous is declining as the toxic nature of the chemicals is causing them to be wiped out. These guys are produced by treating cotton fibres with both diazoic and coupling components.

8. Disperse dyes

Dyeing polyester with these dyes is the most common use, but nylon, cellulose triacetate, an acrylic fiber can also be dyed with them. These dyes are actually developed for the coloring of cellulose acetate.

9. Sulfur dyes

Usually, these days are purchased at low prices and are used to color cotton with dark colors. A Nitro phenol derivative and polysulfide or sulphide solution are used in the dyeing process. Some of the typical examples of dyes are shown in the following Fig. 1.1

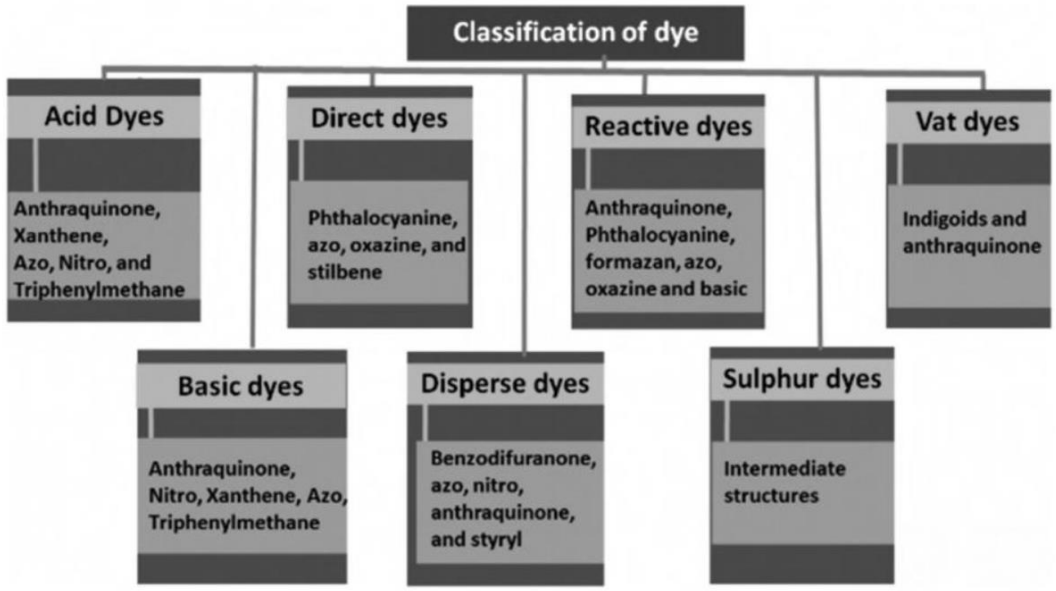

Figure 1.1 Classification of dyes (From Rajmohan et al., 2019)

1.2 Azo dyes

Azo dyes are the synthetic dyes which can be any of the above classifications with different chromophores and auxochromes. Azo dyes have the functional group (-N=N-) (Olukanni et al., 2009). Azo dyes are seen in textiles, food, food packaging printing and cosmetic sectors. It is defined by the IUPAC that azo groups are outcomes of diazine, HN=NH, which contain hydrogens replaced by hydrocarbons, typically which is shown in Fig. 1.1. They are composed of 2 aryl in groups and the N=N group is known as azo group.

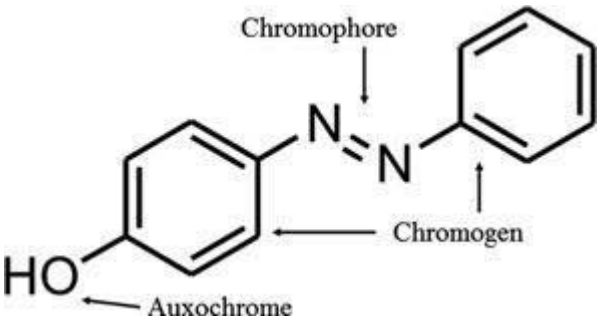

Figure 1.2 Structure of a typical azo dye

A dye has of two constituents:

1.2.1 Chromophore

Colour is provided by chromophores, groups present in Azo dyes that absorb light in the UV region of spectrum. Some of the examples of the chromophores are given in the Table 1.1

Table 1.1 Common chromophores present in dyes with their absorption range

Chromophore	**Compound**	**λ_{max} (nm)**
Methyl	CH_4	122
C-C	C_2H_6	135
Ethyl	C_2H_4	103
Propyl	C_3H_4	170
Carbonyl	R-O-R	180
C-S	R-S-H	195
COOH		200
C=N	$(NH_2)_2C=NH$	265
$CH_3C=N$		170
N=O	Me_3NO	300
C-Cl		173

Several important chromophores are N-O, azo, carbon–nitrogen, -NO2, C=O, -C=S. Individual chromophores can affect by colour by absorption and reflection such as visible light and UV light (Zollinger 1991).

1.2.2 Auxochrome

Several di groups called auxochrome attached to fibres through stable chemical bonds. Examples include OH, COOH, SO_3H, NH_2, NR_2 and a few configurations are shown in Table 1.2.

Table 1.2 Common auxochromes and their configurations

Type of Auxochrome	Configurations
Sulfonic group	$-SO_3H$
Amino group	$-NH_2$
Carboxylic group	-COOH
Hydroxyl group	-OH

In addition to primary colorants, azo dyes are the most common form of synthetic colorants, accounted for about 60 to 70% (Elbanna et al., 2017), followed by anthraquinone colours (Vandevivere et al., 1998). In 1858, Gries discovered a mechanism for producing azo compounds, diazotization followed by coupling (Zollinger 1987). Amino, hydroxy groups are normally used for pairing. Because die components are available for synthesis in a wide variety of ways, many structurally different acids are used in industry.

1.2.3 Hazardous Effects of Azo dyes as Effluents

As a result of improper treatment of textile effluents (mainly comprising of azo dyes) and leaving it to the water bodies, surface and groundwater will be severely contaminated. The existence of even a trivial amount of dyes in water has an adverse impact on aesthetic value, transparency of water and solubility of gases in lakes and rivers (Vandevivere et al., 1998). Consequently, bacteria and plants are disrupted in receiving water, causing ecological disruption. Dye me reduce the light penetration during photosynthesis process of aquatic life (Sharma, 2009). Release of untreated effluents into habitat water changes its pH, BOD and COD values (H. S. Lade et al., 2012). As well as being toxic, mutagenic, and carcinogenic in nature, a few dyes and their bio transformative spin-offs like aromatic amines me bioaccumulate in the food chain and harm aquatic and human life (Lourenco et al., 2000). They can cause albinism (physiological condition) (Dubey et al., 2007). It is therefore essential to

treat such waste waters in order to prevent hypopigmentation. Hence, to reduce the harmfulness, pollution, and to guard the habitat the dye effluent water is to be treated before its release.

1.3 Problem Statement

1.3.1 Challenges Posed by Azo Dye Contaminated Effluents

The discharge of untreated or partially treated industrial effluents containing azo dyes presents several challenges for environmental protection. The complex molecular structures of azo dyes make them resistant to conventional treatment methods, leading to their persistence in the environment.

1.3.2 Impacts of Azo Dyes on Water Bodies and Ecosystems

The presence of azo dyes in water bodies can lead to a range of adverse effects, including reduced light penetration, altered oxygen levels, and disrupted food chains. These impacts can result in the deterioration of aquatic habitats and the decline of various aquatic species.

1.3.3 Need for Effective and Sustainable Azo Dye Degradation Methods and Techniques Available

Given the potential environmental and health risks associated with azo dyes, there is a pressing need to develop efficient and sustainable methods for their degradation and removal from industrial effluents. The development of eco-friendly and cost-effective treatment approaches is crucial to address this problem and safeguard the integrity of water resources and ecosystems.

This is achieved by treating the water of the contaminants and is explained in the subsections below

1.3.3.1 Overview of Water Treatment in Industries

The textile and dye processing industries were driven to create cutting-edge new technologies in order to decolorize colors in effluents due to regulatory requirements for pollution management (Banat et al., 1996). The primary objective of treatment systems is to remove harmful substances and minimize the impact of industrial wastewater on the environment. However, the efficient removal of azo dyes from industrial effluents remains a challenging task due to their complex chemical structures and resistance to conventional treatment methods. (Solís et al., 2012) listed the prominent techniques of decolorization and is shown below as Fig. 1.3

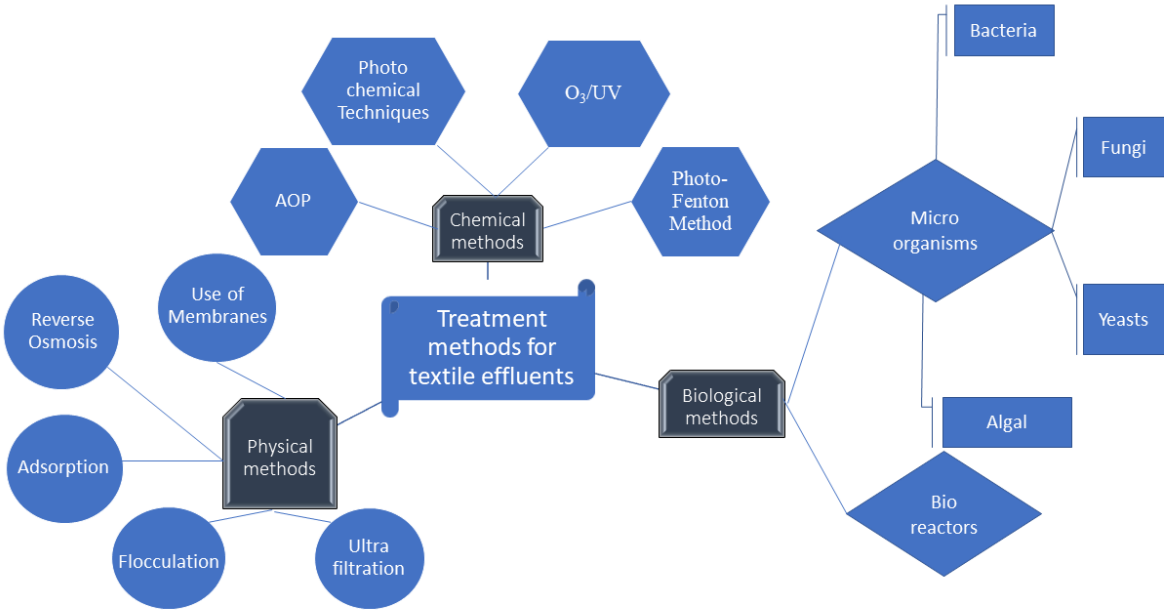

Figure 1.3 Various treatment methods of dye removal from waste water

According to Easton (1995), each of the above methods has its own specific colour removal results, capacity to remove volume, speed of operation and capital cost. Historically, dyes have been eliminated from effluent predominantly by physical or chemical processes (Forgacs et al., 2004). Some of these methods have been demonstrated to be successful, but they also had drawbacks, such as excessive chemical use, sludge production with apparent disposal issues, high-priced plant requirements or functioning costs, deficiency in real colour lessening, especially for sulfonated azo dyes (Atalay & Ersöz, 2016). Moreover, some of the disadvantages of Physical and Chemical methods used in decolorization are tabled below as Table 1.3.

Table 1.3 Disadvantages of some of the physical and chemical methods of treatments

Physical & Chemical methods	**Disadvantages**
$FeH_4O_6S^{+2}$	Sludge production
Ozonation	Very less half-life (20 min)
Photochemical	generation of by-products
Membrane filtration	Strenuous sludge production and highly expensive
Ion exchange	Not effective for all dye types
Silica gel	Side processes prevent marketable application
Electro-kinetic coagulation	High sludge production

There are a few pollutants which have very high concentrations and also complex chemical makeups, so physicochemical methods are unable to achieve a complete mineralization.

1.3.3.2 Bioremediation

In contrast, bioremediation using microorganisms is a promising alternative to physicochemical methods (Garg et al., 2020) In literature, different strains of microorganisms and enzymes have been reported for the detoxification of water contaminated with textile dyes (H. S. Lade et al., 2012). By biologically degrading organic waste under control conditions, environmental contaminants are degraded into forms less toxic by microorganisms. Bacteria, filamentous fungi, yeasts, and algae have all been explored as degraders of dyes during past few decades (Syed et al. 2009). Biochemical Wastewater Treatment has several advantages over physicochemical wastewater treatment which includes eco-friendly and cost effective, physical and chemical reduction of sludge, mineralization of effluents and reduced use of water for dilution of effluents (Hayat et al., 2015). The bio methods of completely degrading textile effluents have numerous benefits, including being (a) environmentally benign, (b) economically competitive, (c) producing a smaller amount sludge (d) creating non-hazardous metabolites or complete mineralization (e) a smaller amount water is used compared to other oxidation techniques for dye degradation (Telke et al., 2008;Khalid et al., 2008). cost competitive, less sludge creation, providing non-hazardous metabolites, or full mineralization are all possible outcomes. (e) less water is used compared to other oxidation techniques for dye degradation (Telke et al., 2008;Khalid et al., 2008). Further degradation of several days, many microorganisms and enzymes have been isolated and tested. Their efficiency depends on the compliance of selected microbes. In textile wastewater treatment potent microbes can be isolated and used to degrade dies. A wide variety of microbes including bacteria, fungi and algae are capable of degrading a wide range of dyes (Praveen et al. 2009). According to (Lie et al., 1998), microbes are essential for mineralization of biological polymers and xenobiotic compounds, such as azo dyes. Microbial cell-based decolorization is one of the several bioremediation techniques that has found widespread use. Decolorizing industrial wastewater from dyeing industries and removing dyes from contaminated ecosystems may be possible with the use of microbial enzymes in a newer approach.

1.3.3.3 Biosorption

In biosorption, molecules of gas, liquid or dissolved solids adhere toa surface, resulting in the formation of a bio sorbate film (the molecules or atoms that are accumulated) at the surface of the adsorbent. The term biosorption refers to a group of metabolically unrelated activities that

primarily occur in cell walls, including physical and chemical adsorption, electrostatic contact, ion exchange, complexation, chelation, and micro precipitation. The key benefits of biosorption include its low cost, great efficiency and selectivity, and effective removal from huge quantities. Activated carbon is widely employed as an adsorbent for the efficient reduction of colours from textile effluents (Chen et al., 2019).

1.3.3.4 Biosorption by Immobilization

Because of the less particle dimensions, deprived mechanical strength, a little density, low stiffness of the adsorbent particles, the separation of the adsorbent after adsorption is exceedingly challenging. The solution to this problem is to immobilize the particles on a solid matrix. Their stability and reuse are increased by immobilization. There are a number of benefits, including the preservation of the biomass' natural features, increased strength, ease of handling, decreased obstruction, lower head-loss during column operation, and enhanced regeneration characteristics. During continuous operation in various processes, it has been observed that cells trapped in natural polymers are more stable than loose cells. The adsorbent material is preferred over others due to its natural origin, low density, mechanical stability, biodegradability, hydrophilicity, carboxylic groups, and its stability in all pH levels (Bustos-Terrones et al., 2022).

Summary

In light of the challenges posed by azo dye-contaminated effluents and the significance of addressing this issue, this dissertation aims to investigate and propose effective bioremediation strategies using fluidized bed bioreactors for the degradation of azo dyes. The subsequent chapters will expound the review of relevant literature, experimental methodologies, results, discussions, and conclusions drawn from the study. By understanding and mitigating the environmental impact of azo dyes, this research endeavors to contribute to sustainable water treatment practices and environmental conservation efforts.

Chapter 2

Literature Review

Chapter 2

2. Literature Review

A complete literature on the dye decolorization and treatments that are present for the same, dye adsorption methods, their usages is done and are described.

The health of human population is significantly impacted by the environmental pollution. The pollution has a major negative impact on not only humans by causing diseases, but also on animals, plants, and trees. As a result, now it has become a responsibility of international organizations, national governments, local authorities, and the general public to utilize resources to balance the living environment and to live sustainably. One of the most significant environmental concerns is water pollution. Various human activities, including industrial, agricultural, and residential ones, lead to water contamination. Water is severely polluted by industrial effluents, hazardous industrial waste, and agricultural runoff containing excessive amounts of fertilizers and pesticides. Such cases are runoff from agriculatural fields are referred as the non point sources whereas the point sourses are referred to the industrial effluents where the pollutants are left directly to the water habitats. Environmental pollution brought on by wastewater discharge from textile industry is an increasing global concern. A significant amount of effluents, predominantly dyes, are produced by the textile industry. Such effluents pollute the aquatic environment when they are released, which negatively impacts aquatic life. Synthetic dyes are intricate aromatic chemical compounds causing to elevate BOD and COD, as well as carcinogenic and mutagenic characteristics of the waterbodies to which the effluents are released. This intricate aromatic structure is resistant to normal methods of deterioration. When textile dye waste is improperly dumped into water bodies, the water becomes intensely coloured. As a result, light cannot penetrate the aquatic environment, which ultimately has an impact on photosynthetic activity. It has become compulsory to industrialists for the protection of environment based on the value requirements of COD, BOD of effluents that are being released into the water bodies. Textile effleuents can be decolorised in three ways before letting into the water bodies. They can be in (i) Physical methods (ii) Chemical methods (iii) Biological methods

2.1 Various Methods of Decolorization

In the work of (Corona-Bautista et al., 2021), Advanced Oxidation Processes which is a Physical Method is used, in which a 0.16 L of batch electrochemical tank with Boron Doped Diamond electrodes was used for the decolorization of azo dye Brown HT using Na_2SO_4 (0.05 M) electrolyte solution and Fe^{2+} (0.5 mM), pH 3.0 and 500 rpm, achieved 100% decolouration and 80% reduction of COD after 1 hour. The process had a current efficiency of 30% and energy consumption of 2.25 kWh (per g of COD). Although Advanced Oxidation Processes have demonstrated promise in the treatment of wastewater containing azo dyes, it is crucial to take into account their drawbacks and difficulties before adopting them wholeheartedly as a solution. The significant energy consumption of AOPs is one potential restriction. Carvalho et al., (2007) have Sludge originally collected from a pulp and paper wastewater treatment plants

Actual effluents from experiments in an up-flow anaerobic sludge blanket reactor fed with a simulated textile effluent containing acid orange 7, working in mesophilic or thermophilic conditions, were used for testing. In the presence of liposomes, which accelerated dye uptake by anaerobic biomass and caused a rapid decolorization, 96% of the color was removed. Boron doped Diamond electrodes were used for this process.

(Harichandran & Prasad, 2016) studied the Fenton process and its congregation with sonolysis where Direct Red 81 degraded more quickly in aqueous solutions because of the synergistic effects of the Fenton process and sonolysis, and the process was a hydroxyl radical oxidation one. The impact of the initial substrate concentration, pH, and catalyst loading were investigated on the rate of decolorization. A pH of 3, $[Fe^{2+}]$ = 0.2 g/L, $[H_2O_2] = 5.1*10^{-3}$ mol/L, and ultrasonic frequency = 120 kHz were the ideal decolorization conditions. The amount of decolorization peaked to 98% but with the expense of addition of more H_2O_2 than required where H_2O_2 has a strong oxidizing effect and can interact with a variety of chemicals. When it comes into contact with the eyes, it irritates.

This procedure's primary drawback is the ongoing loss of the catalyst in the effluent, which makes it necessary to remove the catalyst from the effluent before disposal. Additionally, as the optimal operating pH for this process is around 3, which corresponds to the highest concentration of the active Fe^{2+} species and the slowest rate of parasitic H_2O_2 breakdown, acidification of the starting solution is necessary. Bhad et al., (2022) have worked on the Ozonation method which is a Chemical Method for the degradation of Procyon blue dye. For a 20 mg/L dye solution with an initial pH value of 12, the highest dye degradation was seen at

roughly 92%. At higher pH, the dye degradation increased as the rate of formation of hydroxyl radical increased with pH. But, when dye concentration in synthetic solution was increased from 20 to 70 mg/L, the rate of dye degradation decreased. With the addition of 1, 2, and 5 g/L H_2O_2, respectively, for dye concentrations of 60 mg/L and pH 10 solutions, the percent elimination of dye solutions was 87.3, 90.3, and 91.5, respectively. This resulted due to the increased hydroxyl radical production. Hydroxyl radical has its own disadvantages. The water consumed which is treated with ozone is carcinogenic because of the presence of Bromate due to its conversion from bromide y ozone

Hence when compared to physical and chemical methods, there is a chance of higher decolorization along with less drawbacks in biological methods. Yang et al., (2022) used the microbe *Stenotrophomonas acidaminiphila* EFS1 to decolorize Methyl orange dye.

- ✓ *S. acidophilus* decolored Methyl Orange completely in a less time and its metabolites had less phytotoxicity.
- ✓ The dye's decolorization continued to increase with the increase in time, and it was higher than 95%.

Many researchers have worked on the decolorization studies of azodyes using physical, chemical, and biological methods. But due to its cost effectiveness and ease of handling for the sludge production, biological decolorization methods can be chosen for the effectiveness.

2.1.1 Latest Research Trend

Much of the latest research has shown the practicality of use of bioremediating techniques for the treatment of textile effluents, such as textile effluent bioremediation using bacterial, algal, fungal and yeast (Bhatia et al., 2017) and lately research on the bioremediation of dyes has grown significantly and is shown in the Fig. 2.1.

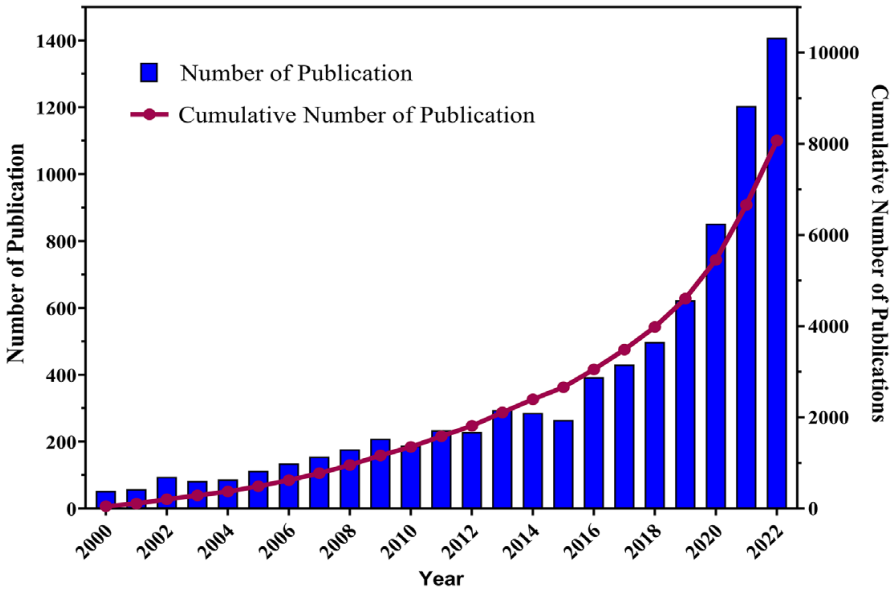

Figure 2.1 Number of articles on bioremediation of dyes from 2000 to 2022

It is believed that yeast may be one of the potential decolorizing agents replacing the majority of other biological entities in wastewater treatment after carefully reviewing the literature. The biological removal of hazardous pollutants from industrial effluents is known as the bioremediation method. Biological treatment techniques are economical, effective, and harmless to the environment. They also produce little or no sludge (Sudarshan et al., 2023). Microorganisms, primarily bacteria and microalgae, but occasionally also yeast and fungus are used decolorize textile dye molecules to innocuous chemical compounds. "Mauvine" the first synthetic dye was invented by Perkin, in 1856. Since then, many dyes have been produced in massive amounts and are highly used for a variety of commercial reasons (Ajaz et al., 2019).

2.2 Decolorization Approach

Biological decolourization can be divided to biosorption as well as biodegradation depending on the approach followed (Kaushik and Malik 2009). Dye-resistant strains emerge spontaneously as microorganisms adapt to the dangerous chemical environment and change a variety of extremely toxic compounds into less or harmless forms (G. D. Saratale et al., 2011). Generally, the dye molecules are broken down by microorganisms in order to use them as a source of carbon (Bheemaraddi et al., 2014). By focusing on the cell wall, biological adsorption quickly eliminates dyes, whereas enzyme-mediated biodegradation takes. Microorganisms are effectively used as adsorbing agents for waste removal due to their innate capacity to degrade and to endure in the harshest environments (Bai et al., 2022). This biological adsorption and biodegradation are empowered by usage of microorganisms such as bacteria, Fungi, yeast and

algae (Solís et al., 2012) whereas applying dead cells to aqueous solutions can get rid of nonbiodegradable dyes. The adsorption capacity is influenced by the chemistry of the dye, the kind of biomass, the dose of biosorbent, its surface characteristics, and environmental variables including temperature, pH and the ionic strength (Aksu & Tezer, 2005). Biosorption is highly recommended due to its high removal performance and economical process, but pH control of the water is crucial because it can affect both the ionization level of the contaminants and the adsorbent surface properties (Vijayaraghavan and Yun 2008). Adsorption isotherm models like Freundlich, Langmuir, Temkin, and others are used to mathematically describe the biosorption isotherm and determine the kind of adsorption (Vijayaraghavan and Yun 2008). The dried biomass of Chlorella vulgaris was used to adsorb reactive dyes, such as Remazol red and Remazol golden yellow, according to the Langmuir model (Aksu & Tezer, 2005) where on the algal cell wall, dye molecules were adsorbing as a monolayer or homogeneously. The Freundlich model has been confirmed in the biosorption of malachite green dye onto Pithophora sp. biomass, it implied the possibility of a heterogeneous or multilayer sorption of dye compounds on the algal cell wall.

2.3 Literatures Showing Action of Different Microbes on Decolorization

The majority of research on the biodegradation of azo dyes has been centered on bacteria and fungi, with bacteria being frequently employed to decolorize azo dyes because to their high activity, wide distribution, and great adaptability Pearce et al., (2003);dos Santos et al., (2007). However, products like aromatic amines can stop bacteria from growing (Qu et al., 2010). The extracellular ligninolytic enzymes laccase, manganese peroxidase, and lignin peroxidase, on the other hand, are used by fungi to catalyze the degradation of complex organic molecules (Gomi et al., 2011).

In the work done by (Franciscon et al., 2012) the biodegradation of azo dyes Reactive Black 5, Reactive Yellow 107 and Direct Blue 71 was done by bacteria *Brevibacterium* sp. Although laccase and peroxidase were inactive during the biotreatment process, tyrosinase activity was seen, suggesting that this enzyme played a part in the process of decolorization and degradation.

Hassan & Carr (2018) have studied that Novacron dyes, viz orange W3R, red FNR, yellow FN2R, blue FNR, navy WB were decolored with the help of micro-organisms *Micrococcus*

luteus, *Listeria denitrificans* and *Nocardia atlantica*. After 7 days of incubation, all bacteria had showed their peak decolourizing activity with little variation. This study also showed that some bacteria live in textile wastewater and use the dyes as a source of nutrition and energy, indicating the significance of such organisms in the treatment of industrial effluents. When other sources of energy are scarce or unavailable, *Micrococcus luteus*, *Listeria denitrificans*, and *Nocardia atlantica* can thrive in the poisonous dye environment by using them as their source of energy.

R. L. Singh et al., (2015) reviewed on the enzymatic decolorization and degradation of azo dyes. The breakdown of dyestuffs by several kinds of microorganism generated enzymes has been explained in this review using various enzymatic pathways. Only in the presence of reducing agents like NADH, NADPH, and $FADH_2$, the azoreductases catalyze the reaction. It has been doubted lately whether intracellular azoreductase plays a role in bacterial decolorization because many azo dyes have complicated structures and high polarity, making it challenging for colors to diffuse across cell membranes. The enzymes including azoreductases, laccases, peroxidases, and polyphenol oxidase can decolorize and break down textile dyes.

Sen et al., (2016) **s**tudied on the biological degradation of the azo dyes. Bioremediation techniques that too usage of fungi has been useful in the decolorization when compared with the Advanced Oxidation Processes and MFCs, since usage of fungi is economical, ecologically friendly, yield less sludge. Decolourization using fungus can happen by adsorption or enzymes or the combination of both. However, it's usage has some of the drawbacks like nitrogen limiting conditions, lengthy growth cycles. It is difficult to preserve fungi in bioreactors for longer time (Stolz, 2001). Hence the bacteria can be used in the degradation since they have a quick growth rate, elevated hydraulic retention stretch.

According to the (Popli & Patel, 2015), for the complete mineralization of azo dyes, sequential anaerobic-aerobic biological treatment is thought to be one of the most economical approaches. The reductive breakage of the dye's azo linkages during the anaerobic stage results in decolorization and the creation of typically colourless but potentially dangerous aromatic amines. Degradation of the aromatic amines occurs during the aerobic phase. Since dye adsorption takes place on developing, alive, and dead biological material, the process is known as biosorption.

Different reactor designs have been reported for effective dye decolorization, including the popular UASB, EGSB, SBR, and ASP. Varied types of dyes have varied colour removal efficiencies in analogous reactors and under analogous experimental settings. A diazo dye is more resistant to decolorization than a mono azo dye. With an increase in the values of HRT there was an increase in the decolorization activity whereas the reduction in SRT, and less initial concentration resulted in the reduction in the colour removal efficiency. Accordingly, a biological reactor with a higher capacity for biomass retention, like a UASB, would be more effective in decolorizing azo dyes than one with a lesser capacity, like an SBR, according to (Van Der Zee & Villaverde, 2005). The difference in redox potential between the electron acceptor and electron donor determines how an electron accepts an electron (dos Santos et al., 2007). As a result of the azo dye's potential competition with other electron acceptors for reducing equivalents, such as oxygen, nitrate, sulphate, and ferric ion, there may not be enough color removal occurring in anaerobic conditions. The number of azo linkages in the dye's chemical structure is discovered to correlate with the concentration and number of aromatic amines produced (Franciscon et. al., 2012). Reduction of azo bonds may be aided by biogenic reductants produced under anaerobic conditions, such as sulphide, ascorbate, or Fe^{2+}. Aromatic amines or the products obtained after the biodegradation may be poisonous (Chung & Stevens, 1993;DeVito, 1993). Additionally, reversal colorization may occur when the anaerobic breakdown products are exposed to oxygen (Knapp & Newby, 1995). These issues prevent the widespread use of bacterial decolorization. According to the work done by (Kapdan et al., 2000) when the dyestuff Everzol Turquoise Blue G was degraded by fungi *Coriolis versicolor* MUCL, pH 5 was found to be the most suitable one with the addition of glucose which is he most suitable carbon source for the microbe for decolorization. Here the research has concluded that the nitrogen concentration has to be lower for the requirement of the effective decolorizaion. Moreover, the adsorption of the dye on the fungi's surfaces was negligible. White-rot fungus species can effectively degrade lignin, xenobiotics, and dyestuffs with the help of their extracellular ligninolytic enzyme system. The three main strains of white-rot fungi utilized for delignification and decolorization are *Phanerochaete chrysosporium*, *Trametes versicolor*, and *Coriolus versicolol* (Knapp et al., 1997; Heining et al., 1997). The three extracellular enzymes lignin peroxidase, Mn peroxidase, and H_2O_2 dependent peroxidases are involved in the biodegradation of dyestuffs (Jim et al., 1993). An external source of urea was also needed for the use of energy source by fungi here in the form of nitrogen.

The below Table 2.1 shows the biological decolorization studies of few of the researchers

Table 2.1 A few studies of biological decolorization

Culture	Dye	Result	Reference
Bacillus firmus H4 (Bacteria)	Novacron Red	80–89% (24 h)	(Guembri et al., 2021)
Bjerkandera adusta CX-9 (Filamentous fungi)	Remazol Brilliant Blue R	~90%	(Bouacem et al., 2018)
Saccharomyces cerevisiae (Yeast)	Remazole blue	100% in 1 h	(Mahmoud, 2016)
Nostoc muscorum (Algal)	Naphthol Green B	98.5%	Sawsan abdallatif et al., 2021

These biological methods can be done in batch studies or in microbial reactors or adsorption and even by immobilization techniques.

2.4 Batch Studies

Researchers of (Krishnan et al., 2017) have isolated microbes from sludge and have used for the decolorization of dyes Reactive brilliant red X-3B, Direct blue-6, Direct black-19. Among these, the reactive dye was found to be less degraded when compared to the other Direct azo dyes. Hence it can be concluded that among azodyes direct ones can inhibit degradation a more than other type of azo dyes. (Rajamohan & Rajasimman, 2013) have worked on the kinetic modelling of the biodegradation of textile effluent using *Pseudomonas stutzeri* where 93% of COD removal of the effluent under anoxic conditions at an optimal pH of 8 was achieved Among the various environmental parameters that effect the biodegradation it is said that pH is essential for microbial cultures to function at their best, because it influences how nutrients are transported across cells membrane (Kumar Garg et al., 2012). The dye house effluent was collected from a dyeing unit situated in Tirupur region (Tamilnadu, India) (Rajamohan &

Rajasimman, 2013) with a specific degradation rate (COD removal rate) found to be 0.1417 l/g Dry Cell Mass at 32°C and obtained that the biokinetics of the COD removal was found out to be first order. (Pannerselvam et al., 2012) have studies on the bioaccumulation of dye reactive red 11 using yeast *Rhodotorula glutinis* where it was said that, with an increase in dye concentration, *R. glutinis'* dye absorption ability was shown to increase. Saravanan et al., (2021) have studied the bioremediation of Reactive Red 11 (RR11) and Acid Green (AG1) using yeast *Pichia pastoris*. At 5% inoculum volume, the highest dye absorption capacities for RR11 and AG1 dye, respectively, were reported to be 5.43 and 6.87 mg/g. Here AG1 is an anionic dye whereas RR11 is a cationinc dye. The number of binding sites (positive charged amines) rises when the media pH drops, leading to an increase in the absorption of the anionic dye (G. Singh et al., 2020). When comparing the accumulation of AG1 dye using *P. pastoris* to the accumulation of RR11 dye using *P. pastoris*, it was discovered that the percentage color removal was higher. (Xu et al., 2007) have biodegraded Fast Acid Red GR using *Shewanella decolorationis* S12. It has been reported that under anaerobic conditions, more than 90% of the color was lost, but aerobic and microaerophilic environments showed decolorizing rates of 12.8 and 33.7%. Hence anaerobic conditions were more useful in the decolorization than aerobic or microaerophilic conditions because of the initial step of the cleaving of the azo bonds where anaerobic conditions are required for the formation of aromatic amines for the removal of electrons on the azo bond without the presence (removal) of electrons from the oxygen molecule. Kalyani et al., (2009) have studied the decolorization of azo dye Reactive red 2 using a single microbe, *Pseudomonas* sp. SUK1 and achieved 96% decolorization. In this research it has been concluded that even a single microbe can completely decolorize dye, when used.

2.5 Employing Bioreactors

In the work done by (Hai et al., 2006), for the treatment of textile dye effluent, a submerged microfiltration membrane bioreactor using the white-rot fungus *Coriolus versicolor* was created. An effective system was calibrated by fusing the superior degrading capacity of white-rot fungi with the inherent benefits of a MBR, which resulted in less sludge generation. The fungi were immobilized on polyurethane foam cubes in an effort to reduce scattered growth (Fujita,'* Akira Era,' et al., 2000) and the cubes were fed to the reactor as stable seed. The reactor successfully removed about 97% TOC and 99% color from the synthetic wastewater under controlled temperature (29±1°C) and pH (4.5±0.2). The main disadvantage of the usage of this reactor is that there was a lot of problem of membrane fouling but this problem was reduced by the addition of external chemical cleaning dosage (100 mL/m^2) frequently which is

another drawback i.e., the addition of chemicals. The smaller footprint and reduced reactor volume of MBR technology over conventional activated sludge systems are its key benefits. The main drawbacks of MBRs are their high installation and operating costs, frequent membrane inspections, and need for maintenance (Melin et al., 2006). The creation of specific methods (such as a specifically designed reactor) to prevent excessive sludge formation is important given the intense distributed growth of fungi. Contrary to the results of aseptic batch tests, the use of fungi in continuous bioreactors for the treatment of dye wastewater has been limited by issues like the overgrowth of fungi that clogs the reactor and the loss of extracellular enzymes and mediators that are crucial for dye degradation in treated effluent (Hai et al., 2012). The reduction in enzyme activity and decolorization efficiency brought on by bacterial contamination is extremely concerning. Fungi grow more slowly than bacteria do. It is obvious that systematic and careful optimization studies are necessary, along with metabolite and microbe (or enzyme) or mediator) research, as it is still unclear how and why some dyes are degraded while others are not. The biosorbents are very capable of biodegrading and biosorbing colors from wastewater due to the presence of a range of functional groups. According to (Naz et al., 2014) the use of tire-derived rubber (TDR) in fixed biofilm reactors for wastewater treatment is long-term and successful in developing biofilms. Under aerobic conditions as opposed to anaerobic ones, TDR incubated at (30°C) with activated sludge demonstrated substantially stronger biofilm production. A crucial component growth processes is the production of biofilm on support media; the microbial populations and their metabolic pathways are unique in aerobic and anaerobic processes, which led to their individual strategies for removing contaminants. In the work done by (H. Lade, Govindwar, et al., 2015) an azo dye congo red was mineralised in an upflow Column bioreactor with PUF immobilized microbial consortium under microaerophilic conditions. A microbial consortium isolated from the soil of textile industry, was immobilized on the PUF cubes and this immobilized carrier is used in the decolorization of congo red dye which was obtained to be 92%. Here the real textile effluent was also used for the decolorization and the reduction of COD 0f 78% was obtained for it. When compared with 78% that was obtained for the decoorization of congo red dye. Hence it can be concluded that biological decolorization can also be employed for the real textile effluents rather than dye solutions with the nearly same amount of reduction of COD values. (Kaskote et al., 2019) have worked on the removal of COD and BOD from the Granular sludge obtained from a South African brewery's UASB treating brewery effluent using the bioreactors SGBR and EGSB. The SGBR showed better COD removal performance with a COD removal of 78% as opposed to 66% for the EGSB. For the anaerobic degradation of brewery wastewater,

(Narayanan & Narayan, 2019) compared the efficacy of a fluidized bed biofilm reactor and UASB. They claimed that the UASB bioreactor contributed 77% of the COD removal, while the other could had contributed more than 90%. Moreover, operations in UASB are very sensitive to temperature and pH. In the studies done by (Firmino et al., 2010) one- and two-stage anaerobic treatment systems in UASB reactors were used to degrade anaerobic sludge from a brewery mesophilic reactor in Brazil. Both systems had extremely high color removal efficiency, with values of 95% and 99%. Two stage system was shown a marginally higher degree of stability, where decolorization was the predominantly caused, demonstrating the contribution of fermentative microbes to dye reduction. Hence it was concluded that recycle system was needed for the effective colour removal to occur. (Basitere et al., 2017) have coupled the Static granular bed reactor coupled with ultrafiltration (UF) membrane system. The system's overall COD and TSS removal was 98% and 99.8%, respectively when compared to 93% and 95% when only SGBR was used. The results of this work concluded that there will be an increase in the removal when there is coupling of more than one reactor. (Song et al., 2021) have used Fluidized-bed bioreactor for the treatment of Polyacrylate containing wastewater which are the textile effluents. The reduction of COD was more than that achieved by previous chemical techniques and they reached 95.2% and 96.6%, respectively where High-throughput sequencing study revealed that Proteobacteria, Firmicutes, and Bacteroidetes, which aid in the breakdown of effluents, rose in relative abundance.

2.6 Literatures Pertaining to Adsorption and Immobilization

The researchers in (Miao et al., 2022) have claimed that, nanoscale iron-based compounds are widely employed as photocatalytic materials for catalytic oxidative degradation, which were used for biosorption (Physico-Biological Combination). Methyl Orange, Congo Red, Malachite Green, Rhodamine B, and Neutral Red are the azo dyes that were used in this study. The findings of this study revealed that the interaction between physical and adsorption processes may offer fresh ideas for the removal of organic contaminants from wastewater. The immobilization of microbial cultures on carriers has expanded the decolorization applications, allowing these to be reused and improving their performance by offering greater stability towards a wide range of temperature and pH values as well as exposure to higher dye concentrations (Ramsay et al., 2005). Immobilization can also lessen the chance of biomass wash-out. The employment of immobilized cultures in a continuous reactor to treat significant amounts of wastewater containing dye has been encouraged by these improved properties. Making the right choices for whole cell immobilization matrices is crucial to maintain dye-

degrading bacteria in the reactor. Due to its high porosity, strong mechanical strength, resistance to microbial attack, vast surface area, and ease of availability at a cheap cost, polyurethane foam with macropores has drawn a lot of interest as the most ideal support for the immobilization of bacteria (Patil et al., 2006). The primary barrier to widespread usage of bioreactors for dye removal is the high expense of the growing medium employed. Studies on dye-degrading bioreactors often employ prescribed growth media, like nutrient broth, which is prohibitively expensive for usage in commercial settings (R. G. Saratale et al., 2011). Decolorization has increased in the studies employing the PUF immobilized microbial consortium present in the soil samples obtained from the industrial estate in Ichalkaranji, MS, India when compared to the just aerobic incubation conditions (H. Lade, Govindwar, et al., 2015). Jayapal et al., (2018) have used the decolorization of studies of azo dye methyl red using microbes isolated from cow dung slurry. The dye solution was directly decolorised with the microbe as well as decolorised with microbes immobilised on vetiver. Decolorization of 59.7% was achieved for the decolorization of vetiver-microbe which was higher than decolorization of 2.4% achieved for the direct decolorization obtained just the microbe. This study gave the idea of effective decolorization of the dye is possible with immobilization rather than with the normal biological decolorization. In the work done by (Chakravarthi et al., 2021) congo red-21 was decolorized by *Streptomyces sviceus* microbe. Laccase enzyme was purified from the microbe and is immobilized by calcium alginate method. Purified and immobilized laccase represented 78% and 92% of color removal after 24 hours, respectively, but crude laccase enzyme from microbe produced 69% of decolorization of dye after 48 hours. A solid must meet certain criteria in order to be used as a media, including providing attention to substrate adsorption (be immersed inside the cell), a comfortable particle size, and a surface sense for ensuring bacterial colonization. Barragán et al., (2007) investigated the outcomes of several solid medium on which different microorganisms were immobilized. They chose to utilize Kaolin, Bentonite, and powdered activated carbon with cultures of Enterobacter, Pseudomonas, and Morganella sp. since these microbes have the ability to break down a variety of textile colours. The PAC particles exhibited these qualities of a perfect solid for adsorption among the ones that are used. They suggested that dye degradation was feasible, whereby anaerobic and aerobic slots in the PAC particle carried out azo bond cleavage and generated amine oxidation. H. Lade, Kadam, et al., (2015) according to their work, where Benzidine dyes are frequently employed in the manufacture of textiles and It's important to consider the potential use of agricultural waste as a cheap supply of carbon and nitrogen. Wheat bran was assessed as a growing medium as a representation of agricultural waste since it is easily accessible,

inexpensive, and includes a range of nutrients. Using WB as a growing medium, a microbial community developed from soils contaminated with textile dyes and tested for biodegradation of the dye Trypan Blue. The complete removal of 50 mg/L of Trypan Blue dye within 24 hours at 30±0.2°C and pH 7, decolorization assays revealed that the microbial consortia has strong metabolic activity towards this dye. Mineralization was confirmed by a decrease in TOC (64%) and COD (88%) of dye-decolorized metabolites. In the work done by (Kamdod & Kumar, 2022), the adsorbent coconut shell activated carbon (CSAC) was checked for the adsorption capacity of cationic Dye Methylene Blue and anionic dye Methyl orange. maximum adsorption capacity values were obtained at a pH of 10 and 3 for the cationic dye and anionic dyes respectively. This primarily occurred because the adsorption mechanism studies for the cationic dyes MB included rate-limiting steps other than intra-particle diffusion. The main rate-limiting step in the instance of the anionic dye (MO) adsorption was discovered to be intra-particle diffusion. In the work done by (Bustos-Terrones et al., 2022), sodium alginate was used as a support material for pollutant biodegradation in wastewater to immobilize a microbial consortium that was isolated from an activated sludge tank of a typical wastewater treatment facility using a fluidized bed bioreactor. A basic blue 9 textile dye was tested for degradation by immobilized bacteria in a setting that resembled textile wastewater. After 2 hours, it was discovered that the degradation process was up to 99.5% effective. Hence from this study it can be concluded that immobilized microbes in a fluidized bed bioreactor can be used for obtaining the maximum degradation of the textile dyes.

2.7 Motivation

Surface water availability per capita in India in 1991 and 2001 was 2300 m^3 (6.3 m^3/day) and 1980 m^3 (5.7 m^3/day) respectively and these are projected to reduce to 1400 and 1200 m^3 by 2025 and 2050 respectively. The proper handling of wastewater ensures that water quality remains tolerable. The broad and critical literature review on the present research work excited me to identify the following gaps.

- Most of the biological degradation works carried out so far involve either aerobic or anaerobic conditions and few works involve both.
- Existing research works require more in-depth knowledge of the process.
- The studies on textile dye wastewater treatment using bioreactor integrated with the physical processes for degradation are limited in the literature.

- Hence, it has been motivated to take up the wastewater treatment studies of azo dyes by (i) Comparing with various microbes and (ii) Combined process of biological and physical (Adsorption) decolorization processes.

2.7.1 Aim

- To find an efficient microbe for the process of biological decolorization
- The aim of this research work is to devise an efficient way in order to combine the biological and the physical approaches for the decolorization of the azo dyes.

2.7.2 Objectives

- To study the biodegradation of azo dyes using microbes with their response surface methodology along with the optimized conditions for obtaining the maximum decolorization.
- Comparison of decolorization rates of bacteria with that of yeast.
- Developing an improvised decolorization process by immobilization of *Pichia pastoris.*
- Comparing the decolorizing extent of physical method (Adsorption) to that with the physical-biological method in a microbe immobilised bioreactor (Fluidized Bed Bioreactor)

2.8 Dissertation structure

Chapter 2 This chapter provides a critical appraisal of previous work published in the literature pertaining to the degradation of azo dyes, bioremediation techniques, and biosorption methods.

Chapter 3 The experimental setups, procedures, and methodologies adopted for the investigation will be detailed in this chapter.

Chapter 4 explains the decolorization studies of Direct yellow 12 and Acid red 13 with *Thalassospira frigidphilosprofundus, Erwinia chrysanthemi burkholder* and *Pichia pastoris* along with the developing of improvised decolorization process by immobilization of *P. pastoris* on activated carbon along with its integration to Batch Reactor Tank and Fluidized Bed Bioreactor.

Chapter 5 includes the mechanisms of the biodegradation reaction. The conclusions drawn from the study, along with significant contributions and recommendations for future research, will be presented here.

Chapter 6 provides the summary and conclusions.

Thesis work map is shown in the next page where the process is moved from **A** to **B** to **C**, where **A** denote the batch decolorization of simulated solutions of Direct yellow 12 and Acid red 13 using *T. frigidphilosprofundus*, *E. Burkholder* and *P. pastoris*. **B** denote the process of immobilization of *P. pastoris* on Activated carbon. **C** denote the decolorization experiments in Bioreactors

2.9 Thesis Work Map

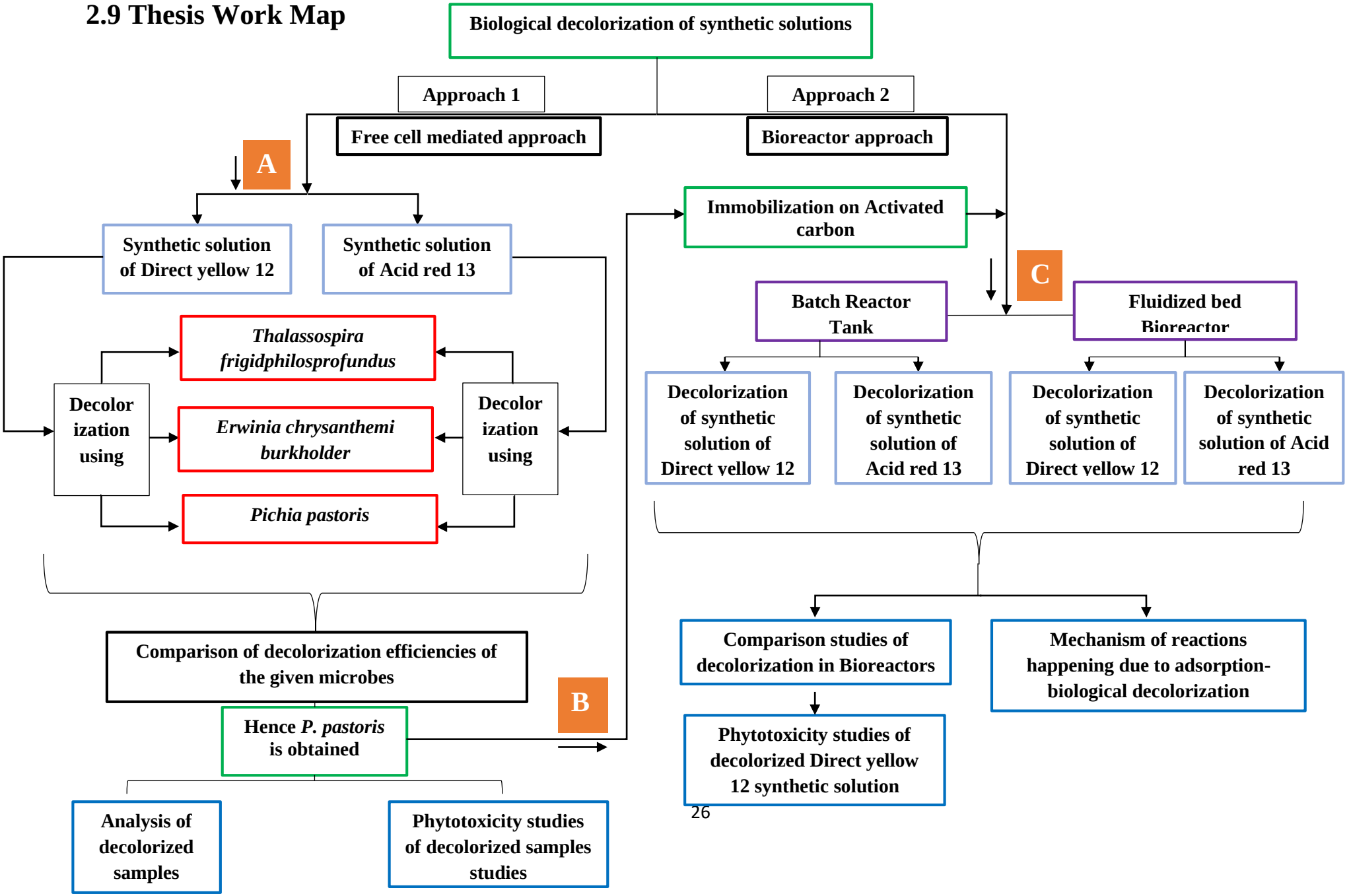

Chapter 3

Materials and Methods

Chapter 3

3. Materials and Methods

Some of the materials that were used in the studies are shown in the below Fig. 3.1.

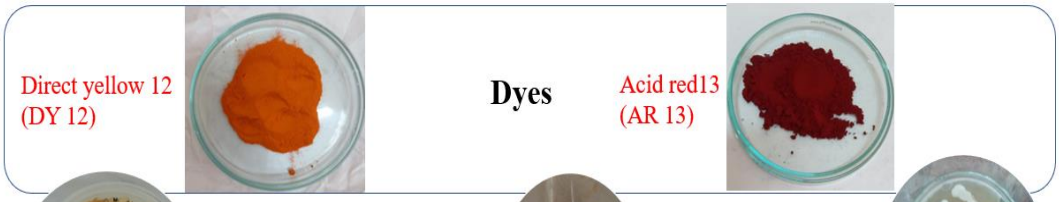

Thalassospira frigidphilosprofundus
NCIM no 5438 (Bacteria)

Thalassospira medium	
Bactopeptone	5 g/L
Yeast extract	1 g/L
$FeCl_3$	0.1 g/L
$MgCl_2$	5 g/L
NaCl	1.8 g/L
$CaCl_2$	1.8 g/L
KCl	0.55 g/L
pH of the media was adjusted to 7.6	

Erwinia chrysanthemi burkholder
NCIM no 5213 (Bacteria)

Nutrient medium	
Beef extract	10 g/L
Nacl	5 g/L
Peptone	10 g/L
pH of the media was adjusted to 7.0-7.5	

Pichia pastoris
NCIM no 3632 (Yeast)

MGYP medium	
Glucose	10 g/L
Malt extracts	3 g/L
Yeast extracts	3 g/L
Peptone	5 g/L
pH of the media was adjusted to 6.4-6.8	

Figure 3.3.1 Materials used

3.1 Dyes Employed

i. Chrysophenine (Direct yellow 12) :

According to IUPAC it is called sodium 5-[(4-ethoxyphenyl) diazenyl] – 2 - [(E) – 2 - [4- [(4-ethoxyphenyl) diazenyl]-2- sulfophenyl] ethenyl] benzene sulfonic acid. Its molecular formula is $C_{30}H_2N_4Na_2O_8S_2$. It is a deep yellow evenly powder and is used for dyeing cotton, wool, viscose, PVA and its blended textile coloring. It can also be used in leather, paper colorizations and bio screening. Chrysophenine is commonly accepted since it has high usefulness and a larger shelf lifespan.

ii. Acid red 13 (Tertracid Red E):

According to IUPAC it is called disodium; 6-hydroxy-5-[(4-sulfonatonaphthalen-1-yl) diazenyl] naphthalene-2 sulfonate. Its molecular formula is $C_{20}H_{12}N_2Na_2O_7S_2$. It is pale red light purple powder and is used for dyeing wool, silk and also for feathers, paper,

soap, leather, wood, cosmetics and pharmaceutical colour. It is also called as Fast red E, CI Food Red 4, Acidal Red E, Cilefar Red E.

3.2 Microbial Culture Employed

3.2.1 Bacterial culture

i. *Thalassospira frigidphilosprofundus* (NCIM no 5438).

It is a lineage cellular proteobacteria which belongs to the family of *Rhodospirillaceae*. The microbe in consideration is an aerobic bacterium**.** The enzyme produced by it is β-galactosidase. The optimum temperature for its growth is 37°C (Pulicherla et al., 2013).

ii. *Erwinia Chrysanthemi burkholder* (NCIM no 5213).

The microbe in consideration is a facultative anaerobe in (Kaneshiro et al., 2008)**.** Gram-negative bacterium, that lives alone or wholes to pairs and a mesophilic bacterium. It produces a number of extracellular cell wall degrading enzymes such as pectic enzymes to degrade pectin, cellulase to degrades cellulose, hemi cellulases, arabanases, cyanoses and a protease. It flourishes in the temperature range between 27 and 30 degrees Celsius.

3.2.2 Yeast culture

Yeasts, a unicellular microorganism have immense potential to treat water contaminated with azo dyes, in comparison to unicellular bacteria and multicellular filamentous fungus (Saravanan et al., 2021).

Pichia pastoris (NCIM no 3632).

Pichia pastoris is a well-known industrial-scale fermentation strain for recombinant protein synthesis. Interestingly, numerous, strong, inducible and constitutive promoters, and signal peptides that present in *P. Pastoris* provide beneficial characteristics which include the ability to produce recombinant proteins (r-proteins) to the extracellular media, its expeditious growth to very high cell densities in a definite mineral medium. Moreover, it performs post-translational alterations (Torres & Dickson, 2021). All these facilitate *P. Pastoris* to synthesize protein more effectively. However, there is hardly any literature to explore the functionality of *P. Pastoris* in the dye decolorization except one by (Saravanan et al., 2021). It opens the ample opportunity for researchers to establish the scope of biodegradation of dye contaminated water by employing *P. Pastoris*. It has two alcohol oxidase genes, Aox1 and Aox2, that also comprise

strong inducible promoters (Daly & Hearn, 2005). These genes let the microbe to utilise methanol as an energy source, but they are repressed by glucose.

3.2.3 Inoculation

The bacterial cultures *Thalassospira frigidphilosprofundus* (NCIM no 5438) and *Erwinia chrysanthemi burkholder* (NCIM no 5213) were obtained from NCIM Pune as pure cultures in agar slants. The cultures were grown on Thalassospira medium and Nutrient agar medium respectively. Cultures were recultivated at their optimal growth temperatures of 20°C and 30°C respectively in the respective nutrient agar media. The Yeast culture *Pichia pastoris* (NCIM no 3632) was obtained from NCIM Pune as pure culture. Culture was grown at their optimal growth temperature of 37°C in MGYP medium and preserved in Refrigerator at 4°C. These nutrient media were used for the suitable medium for microbial decolorization of the dyestuff with their compositions shown in Fig. 3.1 and they are preserved in Refrigerator at 4°C. All chemicals and reagents used in this work were of analytical grade. Direct Yellow 12 and Acid Red 13 were procured from Aniline Dyes, Mumbai, India. Chemicals peptone, Yeast extract, Malt extracts, glucose, H_2SO_4, NaOH were procured from Sigma-Aldrich (Mumbai, India). Methanol was procured from Changshu Hongsheng Fine Chemical Co. Ltd, China. All the glassware used were procured from Borosil and sterilized before use. All the experiments were conducted in triplicate and the average value is reported. For experiments, laminar chamber (Alpha Linear, 186H), autoclave (Precious Techno Engineering, India), centrifuge (Eppendorf, M-5418) and incubation chamber (CIS-24 Plus (LCD Version), REMI India) and UV-Vis Spectrophotometer (XD 7500, Lovibond®) were used. Agar of 20 g/L is added to the media for subcultures.

3.3 Synthetic Textile wastewater

Synthetic textile wastewater was prepared by adding the dyes to the minimal salt medium, the composition of which is shown in the Table 3.1.

Table 3.1 Composition of synthetic textile wastewater

MSM (g/L) with dyes	
K_2HPO_4	6.3
KH_2PO_4	1.8
$NaNO_3$	1
$MgSO_47H_2O$	0.006
Yeast Extract	5
Dyes	Varied Concentration

The grown culture is acclimatized (on the simulated solutions of the same concentration of experimental studies) for one day.

3.4 Decolorization

In Bacterial decolorization,

The Synthetic textile wastewater was decolorized in the 250 ml shake flasks with the addition of inoculum. Samples were removed after 48 hours of incubation and centrifuged at 800 rpm for 10 min. The experiments were also carried out in control flasks that comprised only synthetic solution, but no bacteria.

In Yeast decolorization,

The Synthetic textile wastewater was decolorized in the 250 ml shake flasks with the addition of 10% v/v inoculum. Samples were removed after 48 hours of incubation and then centrifuged at 13000 rpm for 7.5 min.

3.4.1 Decolorization studies

For bacterial decolorization, the experiments were done at various concentrations of the dye, maintained at different pH of solutions, operating at different temperatures and the agitation

values of the incubator shaker. The experiments were performed as free cell mediated decolorization. The studies were utilized in the MINITAB 14 software to model the equations which best fit the influence of the values of variables on the decolorization percentage. For yeast decolorization, the experiments were done at various concentrations of the dye, maintained at different pH of solutions with varying inoculum dosage at the various levels of methanol content. The experiments were performed as the free cell mediated decolorization and immobilized cell decolorization. The studies were utilized in the Design expert 7 software to obtain the modelled equation of decolorization. To fit the data, a Second-degree polynomial was obtained. Surface plots, contour plots can be used to investigate the synergic effects of factors on the outcome, as well as to optimise dye decolorization (Zhao et al., 2012). All the experiments carried out in shaking conical flasks i.e., one substrate reaction followed the Michaelis Menten equation shown in equation (3.1) for the determination of kinetics of the biodegradation.

$$r = (V_m S)/(K_m + S) \quad (3.1)$$

P. pastoris immobilized activated carbon is used as the solid support in the continuous Fluidized Bed bioreactor for the decolorization studies.

3.5 Immobilization of *P. pastoris* on Activated carbon

3.5.1 Preparation of Activated Carbon

Coconut shells were obtained from the market in the vicinity and made into small parts of nearly 5 mm. They were heated to about 100°C for an hour in an oven. These hot and dried samples were heated to about 500°C for 12 hours for the pyrolysis to take place. These lumps were moved to ball mill and pulverized for 2 hours. This sample was sieved under 300 μm size and were taken into beakers containing 1M H_2SO_4. This mix is stirred with a stirring rod and is left for 2 hours. This acid activated shell material was rinsed in the deionized water and then moved into a beaker containing KOH of 1M concentration. This mix was stirred with a stirring rod and is left for 2 hours. This activated carbon material was rinsed in the deionized water and then dried in an oven to remove the moisture completely.

3.5.2 Immobilization

The yeast microbial cells are aseptically inoculated in the media and then the mixture is incubated for two days. Later, the support (which is autoclaved and sterilized with UV in Laminar chamber) was added to the inoculum and then incubated for two days.

3.6 Dye Decolorization in Reactor

Modelling saves the time and effort required to conduct real-world tests while also reducing experimentation errors. RSM extracts the most information from a limited number of studies. Furthermore, the graphical outputs are user-friendly, making it simple to comprehend and analyse the impact of factors on the final result. Central composite design can be used to investigate the synergistic effect of numerous variables in order to find settings that favour optimal dye degradation.

3.7 Bioreactors

3.7.1 Arrangement

Fig. 3.2 shows the Fluidized-bed bioreactor which is used for the studies. It is fabricated with glass. Air flow input into the reactor was done by sparger (Built-in glass sparger) at 200 mL per minute through air pump (MODEL HSV (2), 230/50 Hz 1PH, AMP MAX 0.8; Air filter: Built in micro air filter). A jacket is fabricated for the water to flow to uphold the temperature in the reactor. Two locks are fixed, one at the outlet for sample collection and the other at air input tube. Lock 1 would be applied when the air pump was switched on and Lock 2 would be fixed while the sample is being collected. The specifications of FBBR used are shown in Table 3.2.

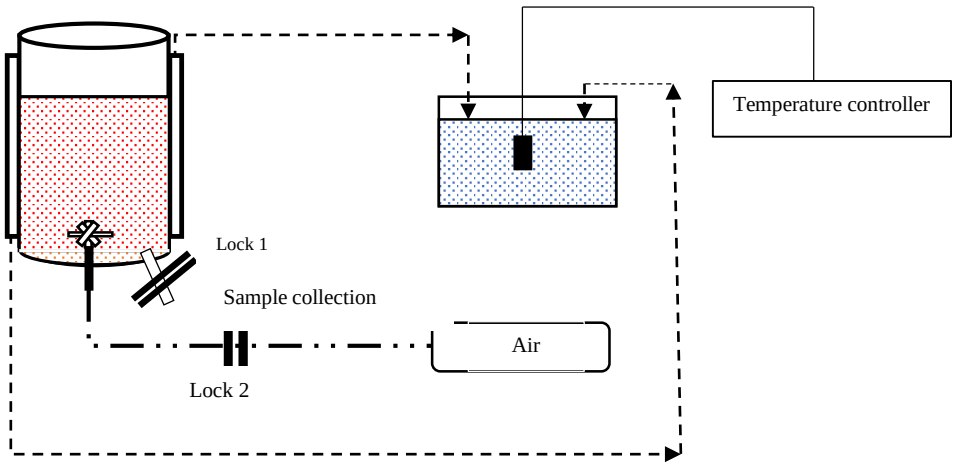

Figure 3.2 Fluidized bed Bioreactor

The specifications of FBBR are given in Table 3.2(a) Table 3.2(b)

Table 3.2 Specifications and Draft tube dimensions of FBBR

Specifications of Fluidized Bed Bioreactor			
Outer Diameter of Glass column	100 mm	**Draft Tube Dimensions**	
Inside Diameter of Glass column	93 mm	Outer Diameter	70 mm
Height	500 mm	Inside Diameter	65 mm
Jacket diameter (Inside)	118 mm	Length	365 mm
Jacket diameter (Outside)	122 mm		

Pictorial depiction of Batch reactor tank (BRT) used in the studies is in Fig. 3.3 and its specifications are in Table 3.3

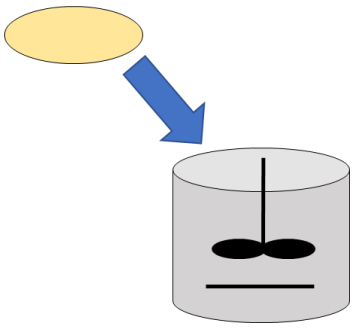

Figure 3.3 Batch Reactor Tank

Table 3.3 Specifications of Batch reactor Tank	
Length	305 mm
Breadth	235 mm
Height	227 mm
Air pump	0.3 MPa, 5W, 1.1 lpm

3.7.2 Decolorization works in Reactors

Two synthetic dye solutions of Direct yellow 12 and Acid Red 13 were biodegraded using yeast immobilized activated carbon in a Fluidized bed Bioreactor as well as in a Batch reactor tank. The complete volume of the reactor that is used (1400 ml), having synthetic solution along with MGYP medium. Results due to varying dye concentration (100, 125, 150, 175, 200 mg/L), varying amount of Activated carbon (10, 20, 30, 40, 50 mg/L), varying pH values (5, 6, 7, 8, 9) on decolorization were examined. The samples were removed, and absorbance was found using UV Spectrophotometer.

3.8 Scope of the Study

This research focuses specifically on the degradation and removal of azo dyes from textile industry effluents. While the scope is limited to this particular class of dyes, the methods and approaches explored in this study have the potential for broader applicability in other industries facing similar water pollution challenges. The study's geographical scope encompasses a representative sample of textile mills and wastewater treatment facilities, allowing for a comprehensive analysis of the effectiveness of the proposed treatment methods under various conditions.

3.9 Analysis

3.9.1 UV Visible Spectrophotometric analysis

The obtained centrifuged supernatant was treated to extract metabolites with same amount of $C_4H_8O_2$ and dried with anhydrous Na_2SO_4, and then it was used for analyzing. Absorbance measurements were done by using 'analytikjena SPECORD 205' spectrophotometer. Wavelengths resulting in maximum absorbance were used for each dyestuff. Samples were diluted so as to ensure the correct results were given by spectrophotometer. The decolorization % was estimated by using the formula given as equation (3.2).

$$Decolorization\ \% = \frac{Initial\ absorbance - Final\ absorbance}{Initial\ Absorbance} \times 100 \qquad (3.2)$$

3.9.2 FTIR analysis

FTIR analysis was done to know the functional groups of the obtained metabolites after the decolorization which is compared with the before decolorization functional groups. This analysis was made on PERKIN ELMER Spectrum 100 FT-IR Spectrometer in section of 400-4000 cm^{-1}.

3.9.3 Statistical analysis

In Yeast decolorization experiments, data was analyzed by one-way ANOVA by Tukey Kramer multiple comparison test (H. S. Lade et al., 2012).

3.10 Toxicity studies

3.10.1 Phytotoxicity Effect of Dye Degradation Products

The discharge of untreated or insufficiently treated industrial effluent is the primary cause of contamination of ocean and river water quality. Hence the biological method of decolorization is employed in this study. Many studies have suggested using bioassays such as phytotoxicity to consider the hazardous impact of dyes and their treated samples on plants (Jadhav et al., 2011). Furthermore, seedlings grown with dye and effluents had shorter gemule and radicle lengths than seeds grown with pure water.

The discharge of improperly treated industrial effluent is the primary cause of contamination in ocean and river water quality. Hence this method of decolorization is employed and both the dyes, their metabolites are assessed for the toxicity by conducting phytotoxicity experiments on the agricultural seeds, (i) Spinacia oleracea, (ii) Capsicum frutescens, (iii) Trigonella foenum. Each crop's ten seeds were planted independently in a plastic vessel with 50 g clean and oven dry sand. The toxicity test was carried out by spraying 5 ml of Dye solutions and their metabolites daily at room temperature, i.e., 28°C. Spraying is done even with the distilled water in the other set. Germination (%), length of gemule, length of root were noted after 14 days.

The phytotoxicity tests of the bacterial decolorization metabolites in shake flasks and the yeast decolorization metabolites in shake flasks as well as for the reactor studies were done.

Chapter 4

Results and Discussion

Chapter 4

4. Results and Discussion

The results and discussion chapter is divided based on the approach of the biodegradation viz.

1. Free cell mediated approach: In this approach, biodegradation is done on synthetic solutions using bacteria and yeast cells directly in conical flasks
2. Bioreactor approach: In this approach, decolorization of the solutions is done in Bioreactors.

The studies which were done are tabulated as below Table 4.1.

Table 4.1 Studies done in this work

S.no	Studies	Approach
4.1	Decolorization studies of Direct yellow 12 solution with bacteria and yeast	1
4.2	Decolorization studies of Acid red 13 solution with bacteria and yeast	1
4.3	Response surface methodology of decolorization for various works is done with finding the optimized conditions for maximum removal	1
4.4	Comparison of decolorizing efficiencies of both the bacteria	1
4.5	Comparison of decolorization rates of bacteria and yeast.	1
4.6	Comparison of decolorization of yeast on both the dyes	1
4.7	Immobilization of the microbe on the prepared activated carbon.	1
4.8	Decolorization with immobilized yeast in Fluidized bed bioreactor (FBBR) with preliminary studies with Batch reactor tank	2
4.9	Comparison of decolorization rates in Batch reactor tank with FBBR	2

Approach 1

A free cell mediated approach

4.1 Finding the Maximum Absorbance

In UV visible spectroscopy graph, the wavelength at which maximum value of OD is observed at the various concentrations is considered to be the wavelength at which maximum absorbance will be observed for the unknown concentration.

The wavelength at which maximum absorbance of each dye is obtained is found and tabled the experimental findings in Table 4.2.

Table 4.2 Wavelength values at maximum absorbance of dyes

S.no	Concentration of dye (mg/L)	Direct yellow 12		Acid red 13	
		Wave length (nm)	Absorbance	Wave length (nm)	Absorbance
1	10	398	0.3184	492	0.9035
2	30	398	0.429	494	1.7268
3	50	402	0.611	492	2.388
4	90	398	1.41	492	6.367
5	150	398	2.037	492	9.581
6	200	398	2.35	492	12.45
7	250	398	2.859	492	1.685

Hence from the above table,

i. for Direct yellow 12, the wavelength for the maximum absorbance is the average of the wavelengths of all the considered concentrations and its value is 398 nm.
ii. for Acid red 13, the wavelength for the maximum absorbance is the average of the wavelengths of all the considered concentrations and its value is 492 nm.

Batch Decolorization Studies of Direct yellow 12 simulated solution

Experimental studies were done for decolourization of Direct yellow 12 solution with bacteria and yeast and Response surface methodology of decolorization is done for finding the optimized conditions for maximum removal

Bacterial decolorization of Direct yellow 12 was published in (Vamshi a et al., 2022)

4.2 Decolorization of Direct yellow 12 Using Bacteria *Thalassospira frigidphilosprofundus*

Table 4.3 shows the observations which were made from the batch experiments of the decolorization of corresponding dye solutions and calculated percentage decolorization.

The experimental matrix conducted is shown below as Table 4.3 and the following observations were obtained.

Table 4.3 Experimental matrix and the percentage decolorization calculations

					% decolorization	
S.no	**C(mg/L)**	**pH**	**T(°C)**	**A(rpm)**	**In Control Flask**	**In Microbial Flask**
1	30	4	15	0.1	7.10	55.52
2	50	6	20	20	2.29	77.41
3	150	10	30	60	8.79	73.15
4	200	12	40	80	6.76	43.84
5	30	6	20	40	7.10	58.11
6	200	10	15	0.1	6.76	46.88
7	30	8	30	40	7.10	64.06
8	150	12	15	20	8.79	30.29
9	50	6	25	0.1	2.29	73.78

10	90	12	20	80	14.99	34.32
11	200	10	15	40	6.76	47.07
12	30	4	30	80	7.10	67.11
13	150	12	40	0.1	8.79	32.99
14	50	6	25	80	2.2	64.68
15	200	8	30	30	6.76	60.21
16	30	12	40	60	7.10	71.63
17	90	12	20	0.1	14.9	64.48
18	150	4	30	40	8.79	52.31
19	50	8	15	20	2.29	69.85
20	30	4	25	60	7.10	59.95
21	200	12	20	0.1	6.76	56.20
22	150	4	25	80	8.79	64.02
23	200	8	30	20	6.76	60.32
24	30	10	20	80	7.10	59.37
25	90	12	25	40	14.99	56.38
26	50	6	15	60	2.29	72.06

4.2.1 Triumph attained

The experiments were also done in control flasks. Their results of percentage decolorizations were compared along with the experiments of decolorization of Direct yellow 12 solution using *Thalassospira frigidphilosprofundus* and the following graphs were obtained.

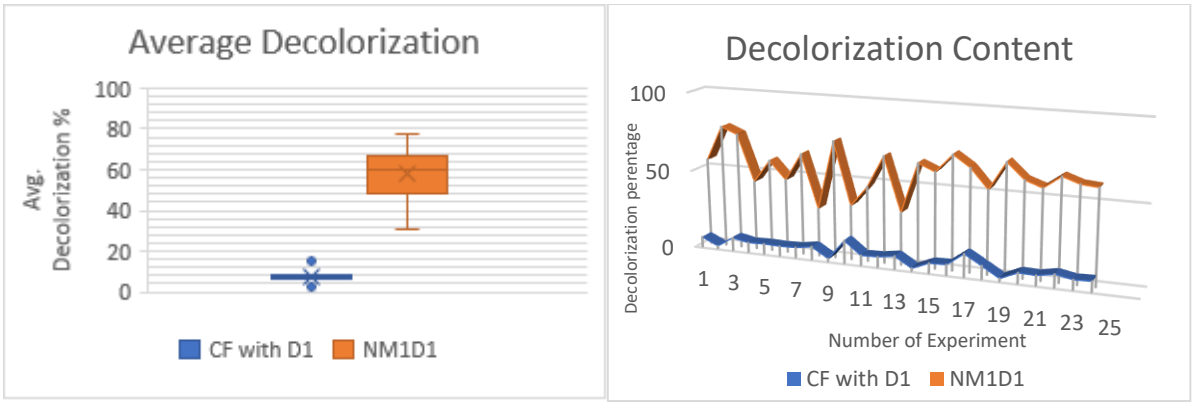

(a) Average Decolorization (b) Decolorization Content

Figure 4.1 Comparison of amount of photodecolorization to microbial decolorization of Direct yellow 12 solution using *T.frigidphilosprofundus*

In Fig. 4.1(a) the average decolorization in control flask for all the runs performed is nearly 8 whereas for microbial decolorization, it is nearly 60 and from Fig. 4.1(b), it is evident that the decolorization in control flask for each run was very less when compared with microbial decolorization.

4.2.2 Decolorization process

Using the results of Table 4.3 in Minitab software, an equation was obtained for the natural logarithm of y and later, it is worked mathematically to obtain the following equation (4.1). This equation corresponds to the effect of the independent variables on the dependent variable which is decolorization percentage.

$$y = exp(1.59) \times C^{0.882} \times P^{-5.28} \times T^{-0.18} \times A^{-0.93} \times$$
$$e^{C\times(-0.0214+0.000024\times P-0.00061\times T-0.000064\times P\times A} \times$$
$$e^{\times(1.9-0.0615\times P-0.0116\times T+0.0002\times C+0.000175\times T\times A} \times$$
$$e^{A\times(0.0069+0.00089\times C-0.00277\times P+0.0003\times T-0.000033\times C\times T} \quad (4.1)$$

The above equation was obtained with 93.7% of Rsq.

From Minitab 14, various results were obtained like Surface plots, Contour plots, Analysis of variance (ANOVA), Residual plots and Scatter plots. The surface plots of the runs indicated that the decolorization do not just have a linear relationship or any known curve regressions. They had a lot of local maximums and local minimums. The contour plots indicated many regions which are indicated with respect to their decolorization percentages.

- Surface plot and Contour plots of influence of concentration of the synthetic solution and pH of the synthetic solution on the decolorization percentage are shown in Fig. 4.2.

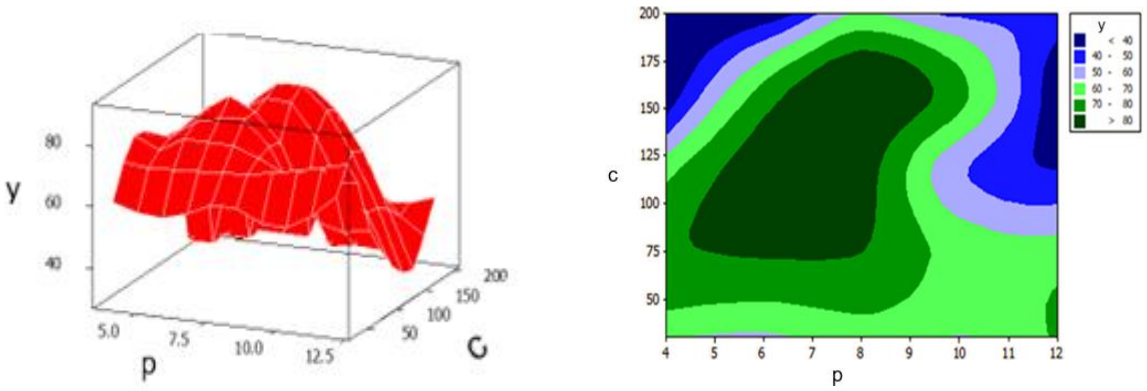

(a) Surface plot of y vs c, p (b) Contour plot of y vs c, p

Figure 4.2 Effect of Concentration and pH on decolorization

Fig. 4.2(b) shows us that maximum amount of decolorization percentage (i.e., greater than 80%) is possible in the regions of approximately 5 to 9 pH values and 75 mg/L to 175 mg/L concentrations of the sample. Similar results were shown in the Fig. 4.2(a), but in a 3D view.

- Surface plot and Contour plots of influence of Temperature of operation and concentration of the synthetic solution on the decolorization percentage are shown in Fig. 4.3.

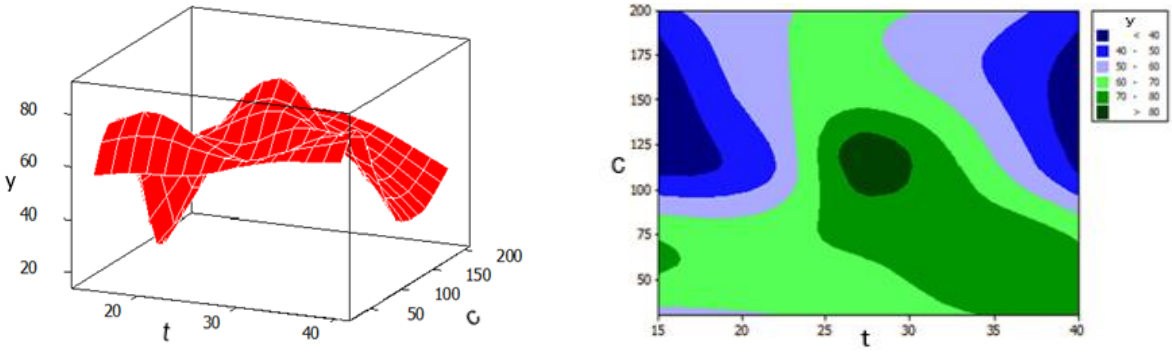

(a) Surface plot of y vs c, t (b) Contour plot of y vs c, t

Figure 4.3 Effect of Concentration and temperature on decolorization

Fig. 4.3(b) shows us the information that maximum amount of decolorization percentage (i.e., greater than 80%) is possible in the regions of approximately 26°C to 30°C values and 95 mg/L to 130 mg/L concentrations of the sample. Similar results were shown in Fig. 4.3(a), but in a 3D view.

- Surface plot and Contour plots of influence of agitation of the chamber and concentration of the synthetic solution on the decolorization percentage are shown in Fig. 4.4.

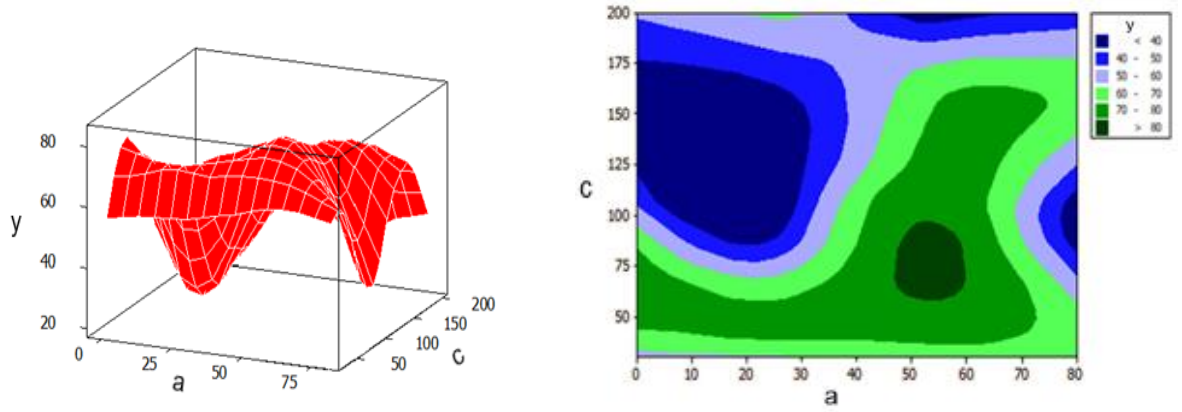

(a) Surface plot of y vs c, a (b) Contour plot of y vs c, a

Figure 4.4 Effect of Concentration and agitation on decolorization

Fig. 4.4(b) shows us the information that maximum amount of decolorization percentage (i.e., greater than 80%) is possible in the regions of approximately 45 rpm to 60 rpm values and 60 mg/L to 90 mg/L concentrations of the sample. Similar results were shown in Fig. 4.4(a), but in a 3D view.

- Surface plot and Contour plots of influence of pH of the synthetic solution and the temperature of operation on the decolorization percentage are shown in Fig 4.5

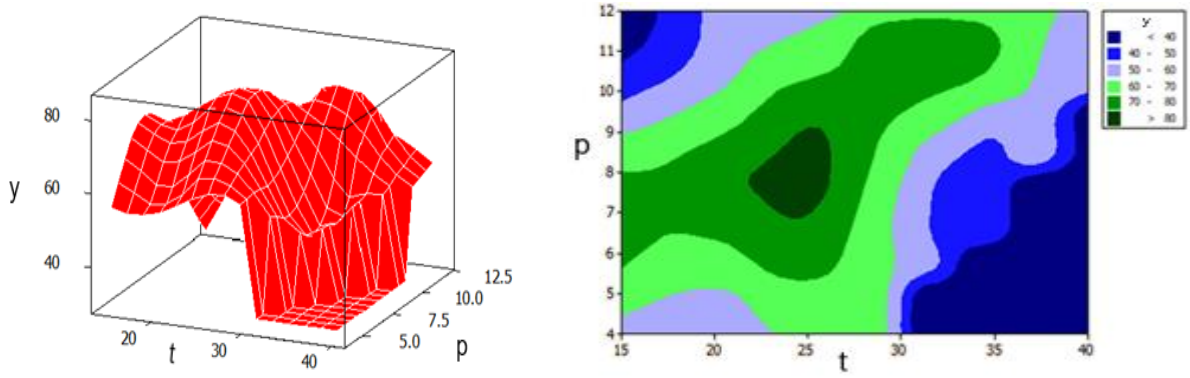

(a) Surface plot of y vs p, t (b) Contour plot of y vs p, t

Figure 4.5 Effect of pH and Temperature on decolorization

Fig. 4.5(b) shows us the information that maximum amount of decolorization percentage (i.e., greater than 80%) is possible in the regions of approximately 22.5°C to 26.5°C values and 6.9 to 8.5 pH values. Similar results were shown in Fig. 4.5(a), but in a 3D view.

- Surface plot and Contour plots of influence of agitation of the chamber and pH of the synthetic solution on the decolorization percentage are shown in Fig. 4.6

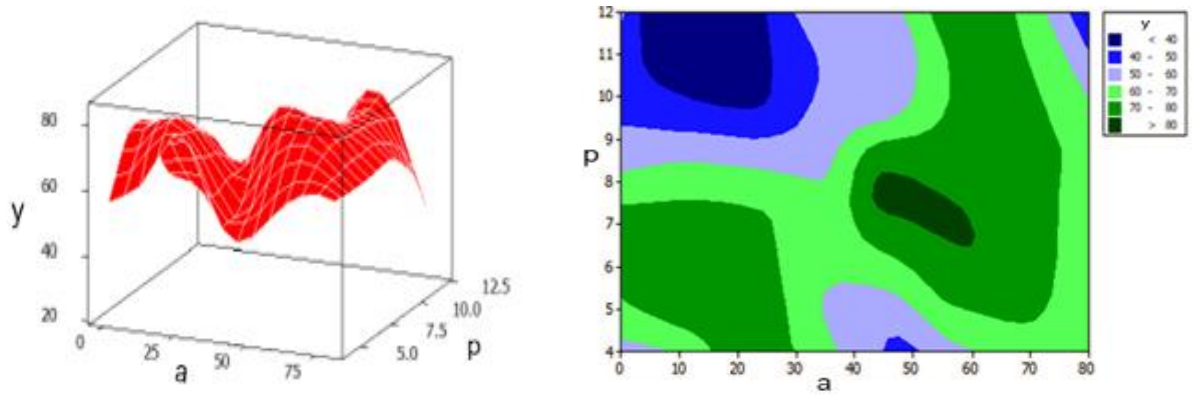

(a) Surface plot of y vs p, a (b) Contour plot of y vs p, a

Figure 4.6 Effect of pH and agitation on decolorization

Fig. 4.6(b) shows us the information that maximum amount of decolorization percentage (i.e., greater than 80%) is possible in the regions of approximately 45 rpm to 60 rpm values and 6.5 to 8 pH values. Similar results were shown in Fig. 4.6(a), but in a 3D view.

- Surface plot and Contour plots of influence of temperature of operation and agitation of chamber on the decolorization percentage are shown in Fig. 4.7.

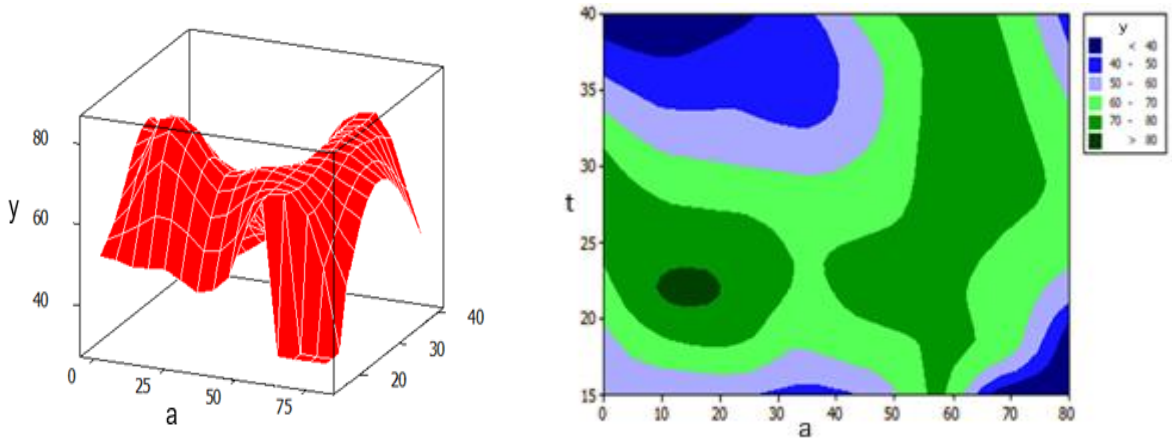

(a) Surface plot of y vs t, a (b) Contour plot of y vs t, a

Figure 4.7 Effect of temperature and agitation on decolorization

Fig. 4.7(b) shows us the information that maximum amount of decolorization percentage (i.e., greater than 80%) is possible in the regions of approximately 10 rpm to 20 rpm values and 21^{o}C to 24^{o}Cvalues. Similar results were shown in Fig. 4.7(a), but in a 3D view.

From the above info, it can be deduced that the maximum amount of decolorization (greater than 80%) can be obtained at the conditions of 90 mg/L of concentration, pH of 7.2, 26°C of temperature, agitation of higher value like at 40 rpm.

ANOVA tables of decolorization of Direct yellow *12 solution is given in Appendix A.* Appendix tables A1, A2 shows the Analysis of variance of decolorization of Direct yellow 12 using *T. frigidphilosprofundus,* Appendix table A3 shows the Degrees of freedom, seq SS of the individual parameters of decolorization of Direct yellow 12 using *T. frigidphilosprofundus.* The scatter plots at the various experimental conditions were also obtained and shown in Fig. 4.8. They denote the correlation between the result obtained and the input variables (Barker and Westfall 2022). Here 3D plots were obtained, where the points indicate the percentage decolorization obtained at two particular input variables.

a

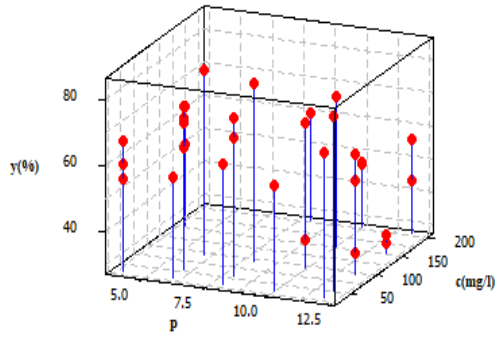

3D Scatter plot of y vs c(mg/L) vs p

b

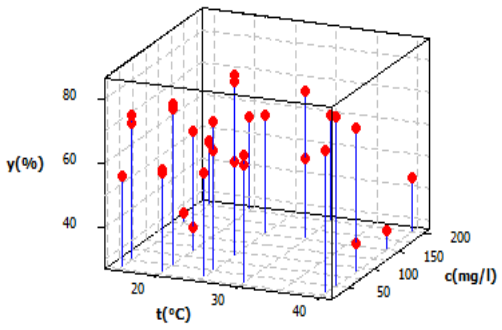

3D Scatter plot of y vs c(mg/L) vs t(°C)

c

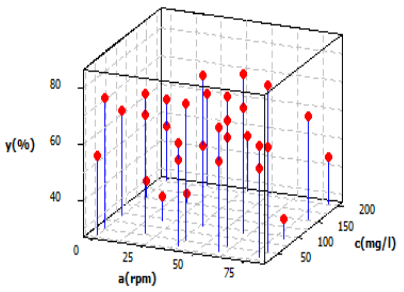

3D Scatter plot of y vs c(mg/L) vs a(rpm)

d

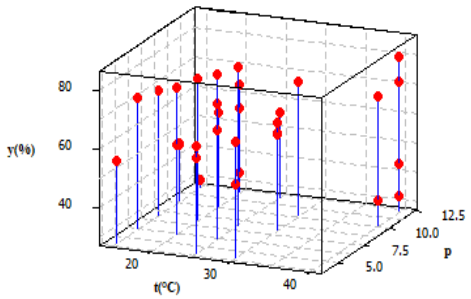

3D Scatter plot of y vs p vs t(°C)

e

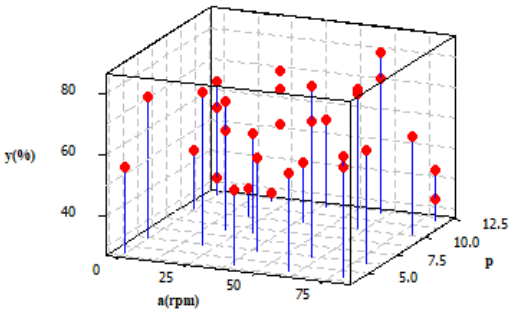

3D Scatter plot of y vs p vs a(rpm)

f

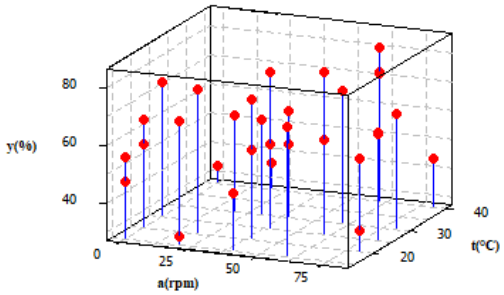

3D Scatter plot of y vs t(°C) vs a(rpm)

Figure 4.8 Scatter plots of biodegradation of Direct yellow 12 using *Thalassospira frigidphilosprofundus*

In the above figure, (a) denote the figure of scatter plot of y vs c (mg/L) vs p, (b) denote the figure of scatter plot of y vs c (mg/L) vs t(°C), (c) denote the figure of scatter plot of y vs c(mg/L) vs a(rpm), (d) denotes the figure of scatter plot of y vs p vs t(°C), (e) denotes the scatter plot of y vs p vs a(rpm), (f) denote the scatter plot of y vs t(°C) vs a(rpm). From the above plots, the majority of the data points tend to rise or fall.

The residual plots of the runs for degradation of D1 using *T. Frigidphilosprofundus* are shown in Fig. 4.9.

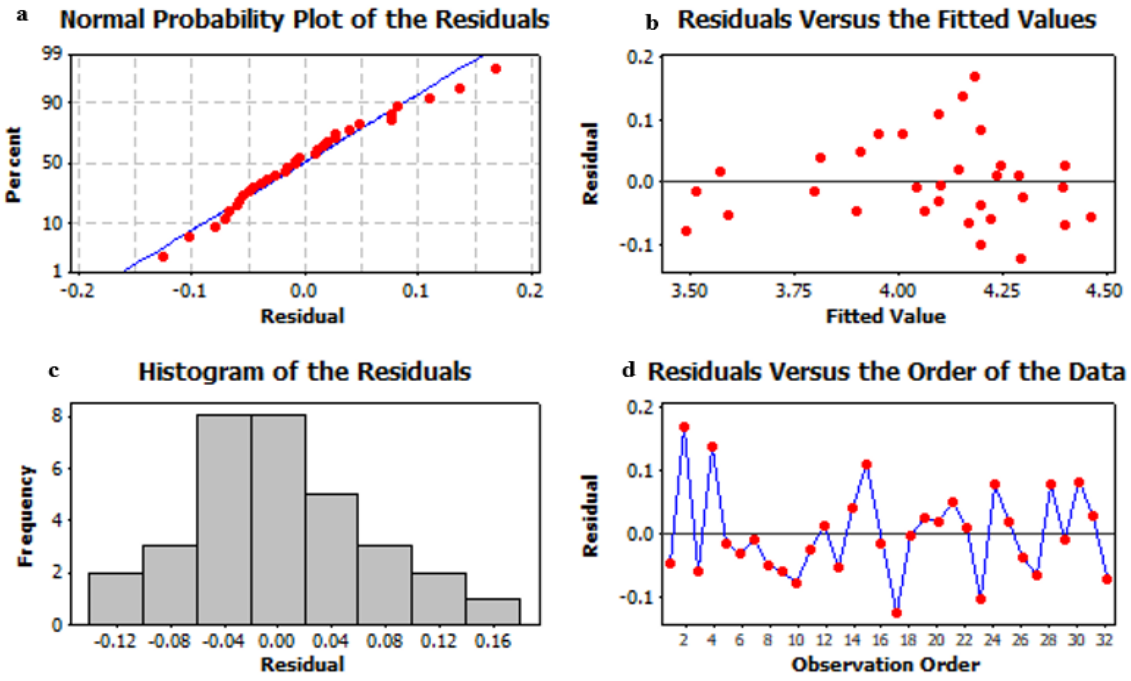

Figure 4.9 Plots showing (a) Normal probability plot of the residuals, (b) Residuals versus the order of the data, (c) Histogram of the residuals, (d) Residuals versus the fitted values of decolorization of direct yellow 12 using *T. frigidphilosprofundus*

A residual is a difference between the predicted value and the obtained value. The obtained value is the experimental result and the predicted value is of the software (Olawoye, 2020). The normal probability plot was shown if the acquired data follows the normality distribution and whether the gathered data from the trials form a good fit. It depicts the deviation between points and detects deviation. Fig. 4.9(a) explains that residuals obtained from experiments form a nearly straight line which implies that the errors were distributed normally. The acceptable limit for the residual value is $\leq \pm 2$ (Ibrahim et al., 2022) and the obtained residual is very less within the limit. Hence it can be stated that the values did not depart from the approved limitations (Ibrahim et al., 2022). The assumption of constant variance is tested by plotting the residuals against the ascending fitted response values. According to (Olawoye, 2020), the plot should be random scatter (constant range of residuals across the graph). This has been seen in plot b above. The number of trials that match the residual produced is shown in the histogram of the residuals graph, and when the frequency is connected by a straight line, it follows a bell curve, which can describe it as a good fit. There will be a random dispersion on the plot (Olawoye, 2020). From c, the residuals don't show a clear form. It implies that there is very little error in the collection of results of the experiment order (Patidar and Sharma 2021). Since from the above points, the work done in this study complies with the work to be done, to obtain

very few errors, this is said to be a valid work to understand the biodegradation of direct yellow 12 using *T. frigidphilosprofundus*. The residual work is published in (Vamshi b et al., 2022)

4.3 Decolorization of Direct yellow 12 Using Bacteria *Erwinia chrysanthemi burkholder*

The values of observations were taken from Table 4.4 which is shown below.

Table 4.4 Experimental matrix and the percentage decolorization calculations

					% decolorization	
S.no	**c(mg/L)**	**pH (p)**	**t(°C)**	**a(rpm)**	**In Control Flask**	**In Microbial Flask**
1	30	4	15	0.1	7.10	53.14
2	50	6	20	20	2.29	74.50
3	150	10	30	60	8.79	69.46
4	200	12	40	80	6.76	42.48
5	30	6	20	40	7.10	71.33
6	200	10	15	0.1	6.76	45.43
7	30	8	30	40	7.10	70.28
8	150	12	15	20	8.79	35.69
9	50	6	25	0.1	2.29	40.43
10	90	12	20	80	14.99	47.33
11	200	10	15	40	6.76	50.26
12	30	4	30	80	7.10	74.64
13	150	12	40	0.1	8.79	30.41
14	50	6	25	80	2.2	65.62

15	200	8	30	30	6.76	57.96
16	30	12	40	60	7.10	44.06
17	90	12	20	0.1	14.9	61.05
18	150	4	30	40	8.79	51.94
19	50	8	15	20	2.29	70.25
20	30	4	25	60	7.10	72.42
21	200	12	20	0.1	6.76	53.98
22	150	4	25	80	8.79	64.20
23	200	8	30	20	6.76	58.14
24	30	10	20	80	7.10	61.19
25	90	12	25	40	14.99	45.21
26	50	6	15	60	2.29	69.62

4.3.1 Triumph attained

The same observations as NM1D1 can be made when the control flask decolorization is compared with the combination NM2D1.

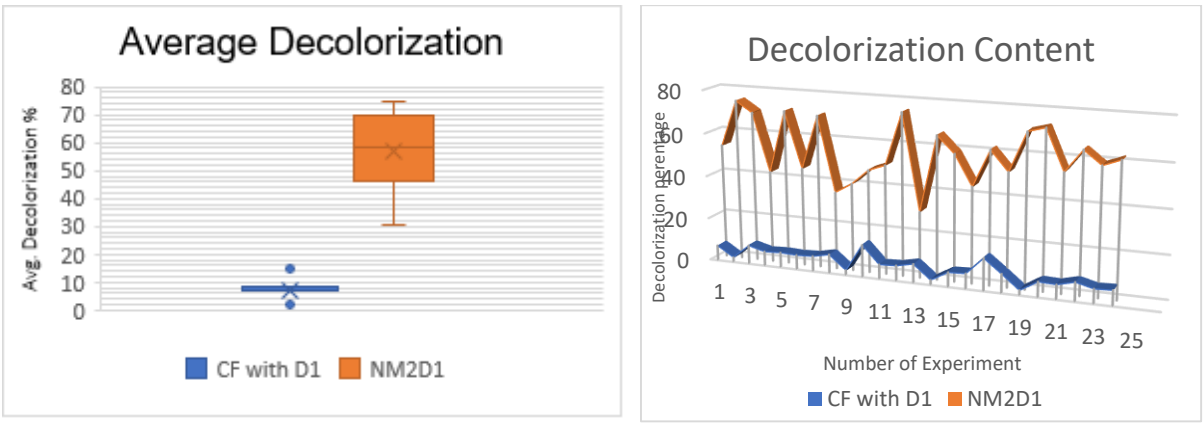

(a) Average Decolorization (b) Decolorization Content

Figure 4.10 Comparison of amount of photo decolorization to microbial decolorization of Direct yellow 12 solution using *E. burkholder*

From Fig. 4.10(b) it is evident that the decolorization in control flask for each run was very less when compared with microbial decolorization and from Fig. 4.10(a) the average decolorization in control flask for all the runs performed is nearly 8 whereas for microbial decolorization, it is nearly 58.

4.3.2 Decolorization process

Using these results shown in Table 4.3 in Minitab software, an equation was obtained for the natural logarithm of y and later, it is worked mathematically to obtain the following equation (4.2). This equation corresponds to the effect of the independent variables on the dependent variables which is decolorization percentage.

$$y = c^{6.64} \times p^{-7.36} \times t^{3.64} \times e^{c\times(-0.053+0.000182\times c-0.00216\times p} \times e^{p\times(2.11-0.065\times p+0.000112\times c+0.000062\times c\times a} \times e^{t\times(-0.196+0.00073\times t-0.000963\times c} \times e^{a\times(-0.000216\times a-0.000664\times c-0.000003\times c\times p\times t} \times e^{-6.57} \quad (4.2)$$

The above equation was obtained with 92.1% of Rsq. The surface plots and contour plots of the experimental observations corresponding to the modelled equation were obtained from the Minitab software. The surface plots of the runs indicate that the decolorization do not just have a linear relationship or any known curve regressions. They have a lot of local maximums and local minimums. The contour plots indicated many regions which are indicated with respect to their decolorization percentages.

- Surface plot and Contour plots of influence of concentration of the synthetic solution and pH of the synthetic solution on the decolorization percentage are shown in Fig. 4.11.

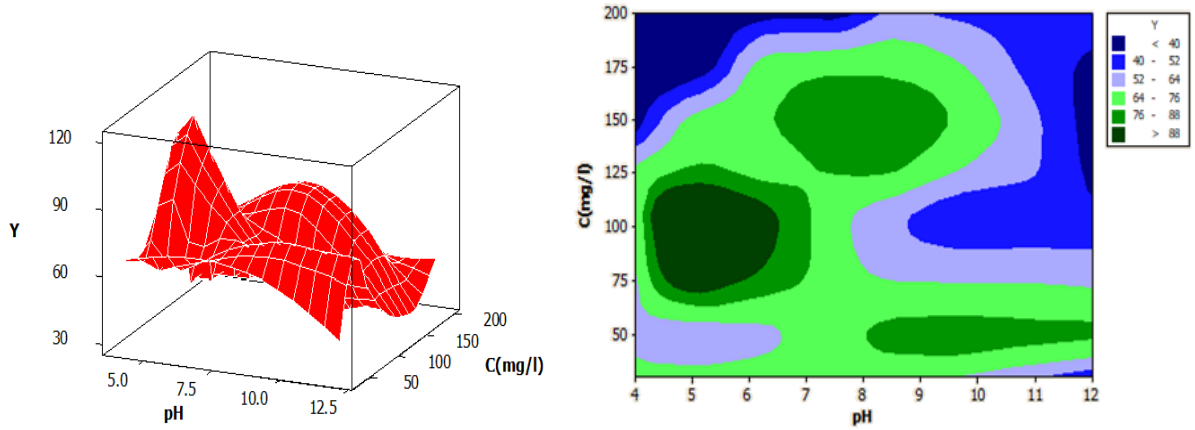

(a) Surface plot of y vs c, p (b) Contour plot of y vs c, p

Figure 4.11 Effect of Concentration and pH on decolorization

Fig. 4.11(b) shows us that maximum amount of decolorization percentage (i.e., greater than 80%) is possible in the regions of approximately 4.5 to 6.5 pH values and 75 mg/L to 120 mg/L concentrations of the sample. Similar results were shown in Fig. 4.11(a), but in a 3D view.

- Surface plot and Contour plots of influence of Temperature of operation and concentration of the synthetic solution on the decolorization percentage are shown in Fig. 4.12.

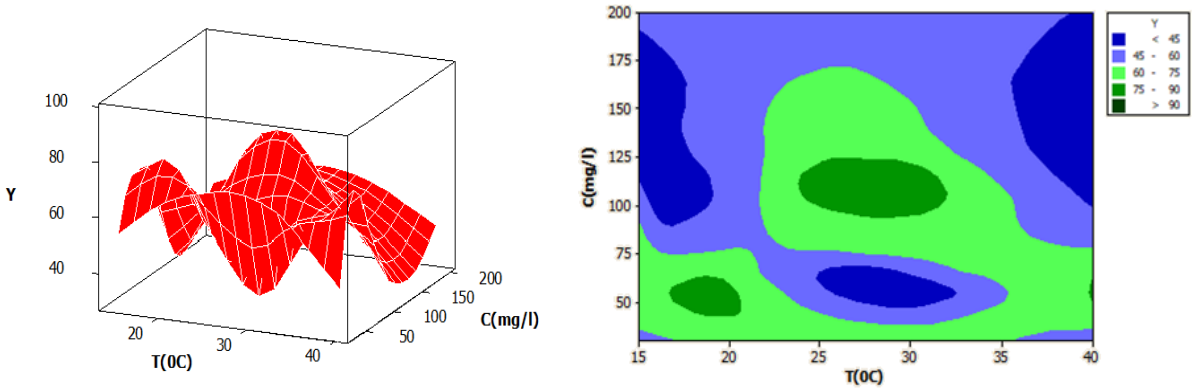

(A) Surface plot of y vs c, t (b) Contour plot of y vs c, t

Figure 4.12 Effect of Concentration and temperature on decolorization

From Fig.4.12(b), the relationship between concentration of the sample and Temperature maintained with the decolorization percentage is obtained. The contour plot shows us the information that maximum amount of decolorization percentage (i.e., 75% to 90%) is possible in two regions) approximately 16°C to 20°C values and 30 mg/L to 60 mg/L concentrations of the sample. ii) approximately 24°C to 32°C values and 90 mg/L to 125 mg/L concentrations of the sample Similar results were shown in Fig. 4.12(a), where first region showed the high decolorization content.

- Surface plot and Contour plots of influence of agitation of the chamber and concentration of the synthetic solution on the decolorization percentage are shown in Fig. 4.13.

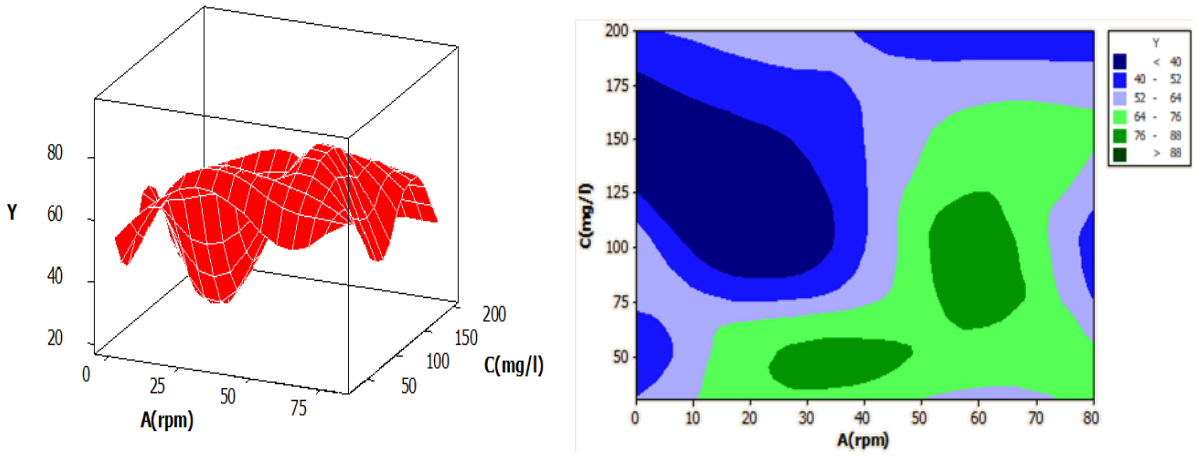

(a) Surface plot of y vs c, a (b) Contour plot of y vs c, a

Figure 4.13 Effect of Concentration and agitation on decolorization

From Fig. 4.13(b), the relationship between concentration of the sample and Agitation created with the decolorization percentage is obtained. The contour plot shows us the information that maximum amount of decolorization percentage (i.e., 76% to 88%) is possible in two regions i) approximately 25 rpm to 50 rpm values and 10 mg/L to 60 mg/L concentrations of the sample. ii) approximately 50 rpm to 70 rpm values and 60 mg/L to 125 mg/L concentrations of the sample Similar results were shown in Fig. 4.13(a), but in a 3D view.

- Surface plot and Contour plots of influence of pH of the synthetic solution and the temperature of operation on the decolorization percentage are shown in Fig. 4.14.

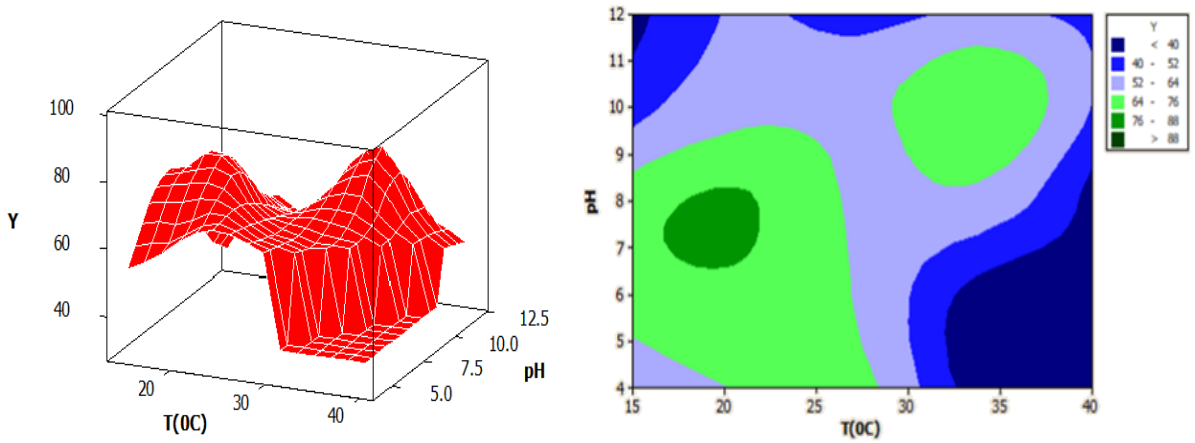

(a) Surface plot of y vs p, t (b) Contour plot of y vs p, t

Figure 4.14 Effect of pH and Temperature on decolorization

From Fig. 4.14(b), the relationship between pH of the sample and Temperature maintained with the decolorization percentage is obtained. The contour plot shows us the information that maximum amount of decolorization percentage (i.e., 76% to 88%) is possible in the regions of approximately 16^{o}C to 22^{o}C values and 6.5 to 8 pH values. Similar results were shown in Fig. 4.14(a), but in a 3D view.

- Surface plot and Contour plots of influence of agitation of the chamber and pH of the synthetic solution on the decolorization percentage are shown in Fig. 4.15.

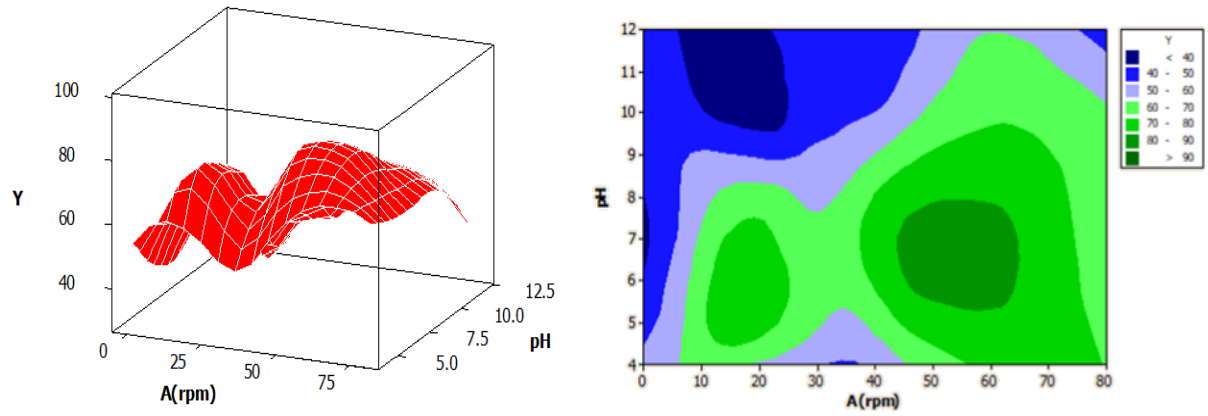

(a) Surface plot of y vs p, a (b) Contour plot of y vs p, a

Figure 4.15 Effect of pH and agitation on decolorization

From Fig. 4.15(b), the relationship between pH of the sample and Agitation created with the decolorization percentage is obtained. The contour plot shows us the information that maximum amount of decolorization percentage (i.e., 80% to 90%) is possible in the regions of approximately 45 rpm to 65 rpm values and 5 to 8 pH values. Similar results were shown in Fig. 4.15(a), but in a 3D view.

- Surface plot and Contour plots of influence of temperature of operation and agitation of chamber on the decolorization percentage are shown in Fig. 4.16.

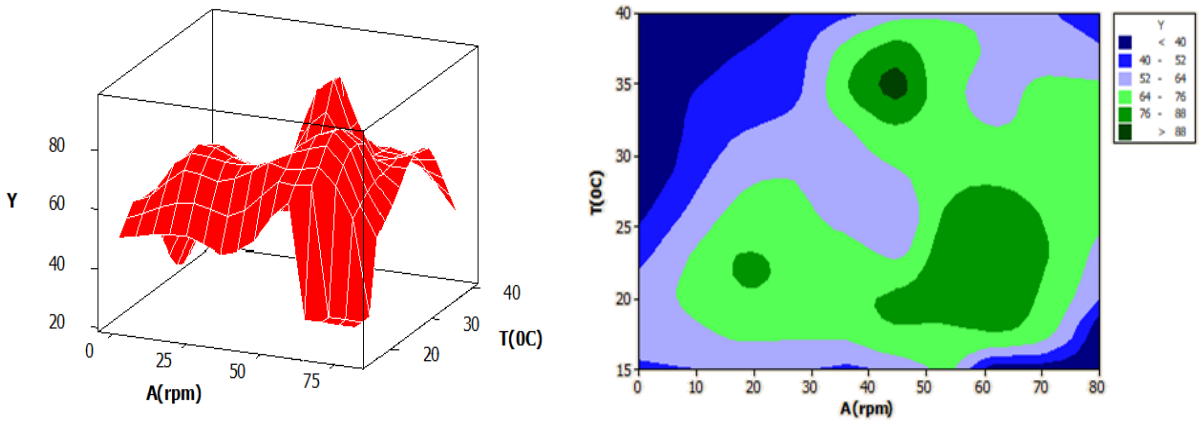

(a) Surface plot of y vs t, a (b) Contour plot of y vs t, a

Figure 4.16 Effect of temperature and agitation on decolorization

From Fig. 4.16(b), the relationship between Temperature of the sample and Agitation created with the decolorization percentage is obtained. The contour plot shows us the information that maximum amount of decolorization percentage (i.e., greater than 88%) is possible in the regions of approximately 40 rpm to 45 rpm values and 32ºC to 35ºCvalues. Similar results were shown in Fig 4.16(a), but in a 3D view.

From the above info, it can be deduced that the maximum amount of decolorization (greater than 80%) can be obtained at the conditions of 90 mg/L of concentration, pH of 6.5, 22°C of temperature, agitation of higher value like at 50 rpm.

ANOVA tables of decolorization of Direct yellow 12 solution is given in Appendix A. Appendix tables A4, A5 shows the Analysis of variance of decolorization of Direct yellow 12 using *E. burkholder*, Appendix table A6 shows the Degrees of freedom, seq SS of the individual parameters of decolorization of Direct yellow 12 using *E. burkholder*. Fig. 4.17 below shows the scatter plots that were obtained. They represent the relationship between the

acquired result and the input variables (Barker and Westfall 2022). The points reflect the percent percentage decolorization obtained at two specific input variables in these 3D plots.

a

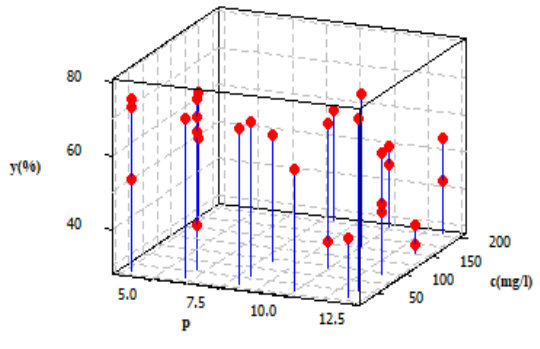

3D Scatter plot of y vs c(mg/L) vs p

b

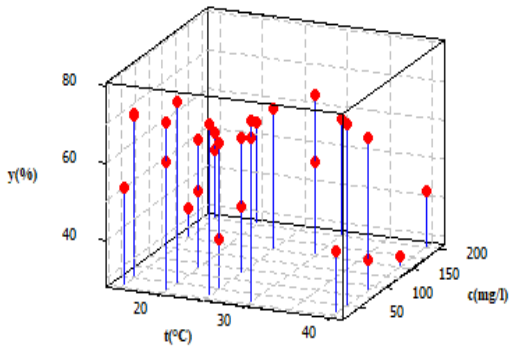

3D Scatter plot of y vs c(mg/L) vs t(°C)

c

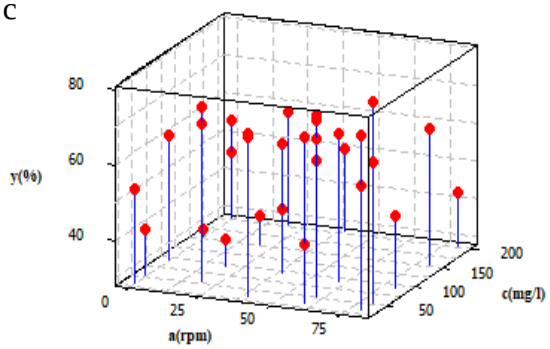

3D Scatter plot of y vs c(mg/L) vs a(rpm)

d

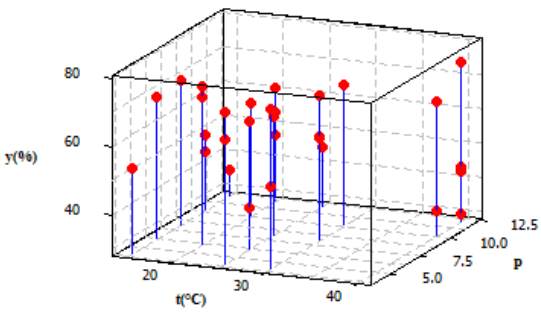

3D Scatter plot of y vs p vs t(°C)

e

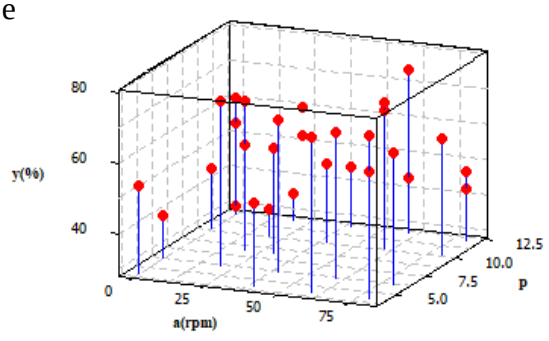

3D Scatter plot of y vs p vs a(rpm)

f

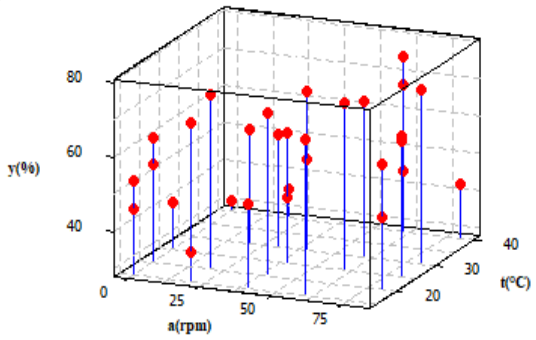

3D Scatter plot of y vs t(°C) vs a(rpm)

Figure 4.17 Scatter plots of decolorization of Direct yellow 12 using *Erwinia chrysanthemi burkholder*

In the above figure, (a) denote the figure of scatter plot of y vs c (mg/L) vs p, (b) denote the figure of scatter plot of y vs c(mg/L) vs t(°C), (c) denote the figure of scatter plot of y vs c(mg/L) vs a(rpm), (d) denotes the figure of scatter plot of y vs p vs t(°C), (e) denote the scatter plot of y vs p vs a(rpm), (f) denote the scatter plot of y vs t(°C) vs a(rpm). From the above plots, majority of the data points tend to rise or fall. The residual plots of the runs for degradation of Direct yellow 12 using *E. chrysanthemi burkholder* are shown in Fig. 4.18.

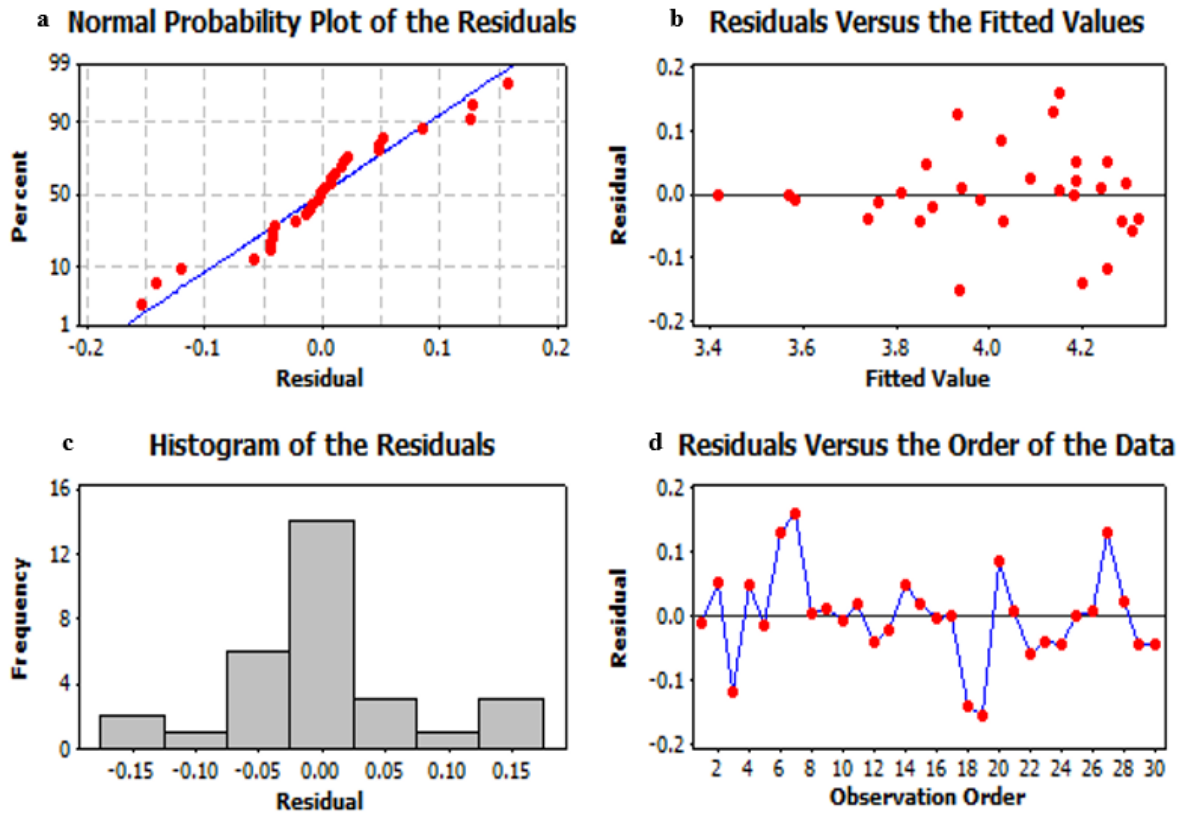

Figure 4.18 plots showing (a) Normal probability plot of the residuals, (b) Residuals versus the order of the data, (c) Histogram of the residuals, (d) Residuals versus the fitted values of decolorization of direct yellow 12 using *E. burkholder*

The disparity between the predicted and actual value is called a residual. The obtained value is the result of the experiment, whereas the predicted value is the result of the software (Olawoye, 2020). The Normal Probability plot illustrates if the acquired data follows a normal distribution and whether the data from the trials fits together well. It shows the difference between two locations and detects the difference. Our model's residual values did not deviate from approved limitations ($\leq \pm 2$) and fell on a straight line with only a few exceptions, implying that the errors were distributed normally, as the residuals form a nearly straight line (Ibrahim et al., 2022). By displaying the residuals against the ascending fitted response values, the assumption of constant

variance is checked. The plot should be random scatter, according to (Olawoye, 2020). This can be seen in plot b. The histogram of the residuals graph shows the number of trials that match the residual created, and when the frequency is connected by a straight line, it follows a bell curve, which may be described as a good fit. On the plot, there will be a random dispersion (Olawoye, 2020). The residuals shown in plot c don't have a distinct form. It suggests that the experiment order's results are collected with relatively minimal inaccuracy (Dashrath Patidar and Suman Sharma 2021). Because the work done in this study corresponds with the work that needs to be done to achieve very few errors, it is considered a valid study to investigate the biodegradation of D1 utilizing *E. Chrysanthemi Burkholder*.

4.4 Decolorization of Direct yellow 12 Using Yeast *Pichia pastoris*

Table 4.5 shows the observations which were made from the batch experiments of the decolorization of corresponding synthetic solution and calculated percentage decolorization. The experimental matrix conducted is shown below and the following observations were obtained.

Table 4.5 Experimental matrix and percentage decolorization calculations

					% decolorization	
S.no	**Concentration mg/L**	**pH**	**Inoculum dosage (%v/v)**	**Methanol (ml)**	**In Control Flask**	**In Microbial Flask**
1	184.09	7	10	10	0.79	64.155
2	15.91	7	10	0	15.60	81.515
3	150	10	5	5	5.61	62.095
4	184.09	7	10	0	0.79	42.123
5	50	4	5	0	7.39	79.799
6	100	7	10	10	5.26	67.08

7	50	4	5	5	7.39	78.376
8	100	1.95	10	0	5.02	47.383
9	15.91	7	10	10	15.60	85.758
10	100	7	10	10	5.26	67.08
11	100	7	18.4	18.4	5.02	84.435
12	100	7	10	0	5.02	60.055
13	100	7	10	10	5.26	67.08
14	150	4	15	0	5.61	46.632
15	100	1.95	10	10	5.02	55.207
16	100	7	1.5	0	5.02	62.603
17	50	4	15	15	7.39	87.931
18	100	7	1.5	1.5	5.02	45.11
19	100	7	10	0	5.02	60.055
20	150	10	5	0	5.61	50.694
21	50	10	5	5	7.39	73.276
22	150	4	5	0	5.61	47.847
23	50	10	15	0	7.39	75
24	100	7	18.4	0	5.02	75.069
25	150	4	15	15	5.61	80.451
26	100	7	10	0	5.02	60.055
27	50	10	15	15	7.39	77.802
28	100	7	10	0	5.02	60.055

29	50	4	15	0	7.39	73.779
30	150	4	15	0	5.61	46.632
31	150	10	15	15	5.61	89.132
32	150	4	15	0	5.61	46.632
33	150	10	15	0	5.61	72.257
34	100	7	10	0	5.02	60.055
35	100	7	10	0	5.02	60.055
36	100	12.04	10	0	5.02	79.256
37	50	10	5	0	7.47	66.379
38	150	4	5	5	5.61	61.227
39	150	4	15	0	5.61	46.632
40	100	12.04	10	10	5.02	85.041

4.4.1 Biodegradation perspective

The advantage of biodegradation techniques over degradation due to light is shown as Fig. 4.19.

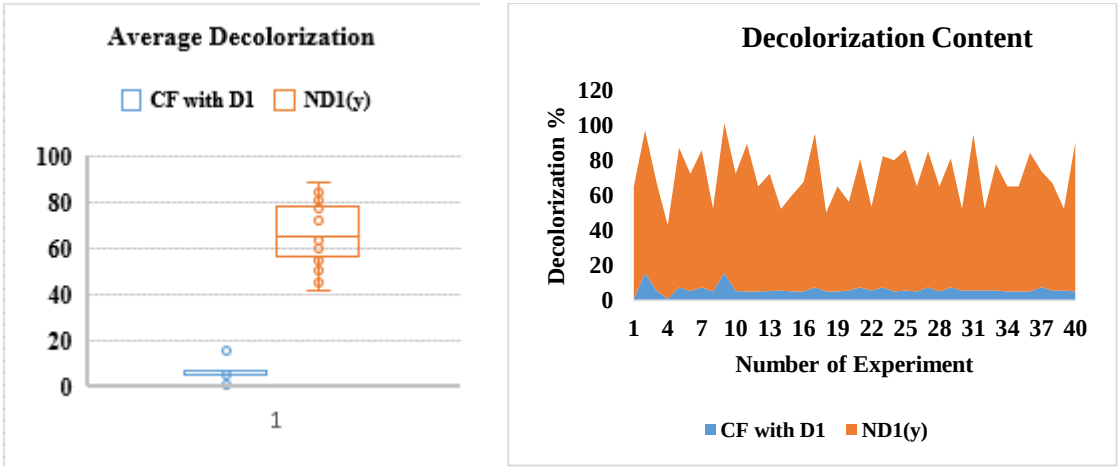

(a) Average decolorization (b) Decolorization Content

Figure 4.19 Comparison of amount of photo decolorization to microbial decolorization i.e., decolorization of direct yellow 12 solution by *P. pastoris*

In Fig 4.19(a), the graph depicting the average decolorization of the system is shown and in Fig. 4.19(b), the amount decolorization of dye of control flask and microbial flask is shown. It can be clearly seen that the complete decolorization in the microbial flask is higher than the flask of photo decolorization. From the plots a, b we can understand that the bio decolorization is better than that of decolorization in control flask i.e., due to sun light. The average bio decolorization (obtained from plot b) for microbial is 65% whereas for control flask decolorization of direct yellow 12 is 5%.

4.4.2 Response surface methodology

A regression analysis was done using the result in Design expert 7 software. The following model equations (4.3) and (4.4) were obtained.

When the content of methanol added to the culture is low i.e., the volume added is 0 ml,

$$y = 149.96 - 0.84 \times c - 8.005 \times p - 4.53 \times C + 0.027 \times cp + 0.012 \times cC + 0.16 \times pC + 0.0016 \times c^2 + 0.38 \times p^2 + 0.14 \times C^2 \quad (4.3)$$

When the content of methanol added to the culture is high i.e., its volume is equal to the volume of the inoculum added,

$$y = 135.58 - 0.72 \times c - 8.62 \times p - 3.32 \times C + 0.027 \times cp + 0.012 \times cC + 0.16 \times pC + .00016 \times c^2 + 0.37919 \times p^2 + 0.13768 \times C^2 \quad (4.4)$$

Table 4.6 ANOVA for decolorization of Direct yellow 12 using *P. pastoris*

	Sum of Squares	DF	Mean Square	F-value	p-value
Model.	5381.28	13	413.94	5.51	0.0001
c	1532.75	1	1532.75	20.4	0.0001
p	478.84	1	478.84	6.37	0.0180
C	1063.02	1	1063.02	14.15	0.0009
D	304.92	1	304.92	4.06	0.0544

cp	267.65	1	267.65	3.56	0.0703
cC	*155.88*	1	*155.88*	20.8	0.1617
cD	252.07	1	252.07	3.36	0.0785
pC	101.1	1	101.1	1.35	0.2565
pD	23.63	1	23.63	0.31	0.5797
CD	249.51	1	249.51	3.32	0.0799
c^2	461.69	1	461.69	6.15	0.02
p^2	335.69	1	335.69	4.47	0.0433
C^2	341.45	1	341.45	4.55	0.0426
Residual	1953.13	26	75.12		
Lack of fit	1325.83	16	82.86	1.32	0.3341
Total	7334.41	39			

From ANOVA table shown as Table 4.6, we can observe that the linear terms of the equation along with the squares of the linear terms have p value of less than 0.05.The Model F value of 5.51 suggests the model can be significant. There is only a 0.01% probability that a "Model F Value" this high could happen because of noise. "Lack of Fit F-value" equaling 1.32 means that it is not significant, comparative to pure error. There is a 33.41% probability that high "Lack of Fit F-value" could happen because of noise. Non-significant lack of fit is good. The model had an R^2 value of 93% which explains that the experimental results were found to be agreeing satisfactorily with the model results. The graphical representation of the model is shown as the surface plots and the contour plots in Fig. 4.20 where A denotes the concentration of dye in the solution in mg/L, B denotes the pH value adjusted and C denote the inoculum dosage in %v

(a) Hold value: Inoculum Dosage (%v)=10 (b)

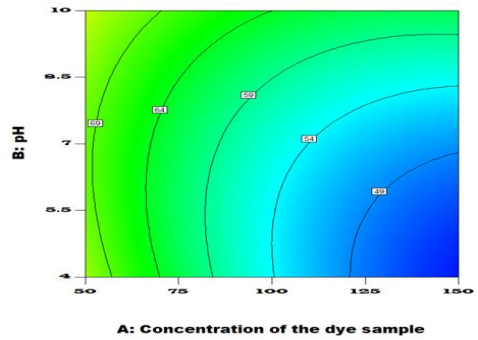

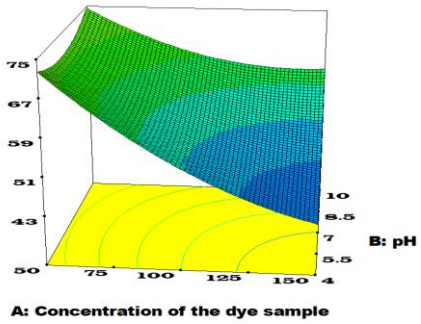

(c) Hold value: Concentration of the dye sample (mg/L)=100 (d)

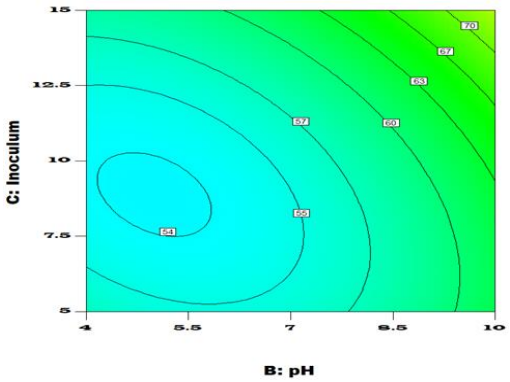

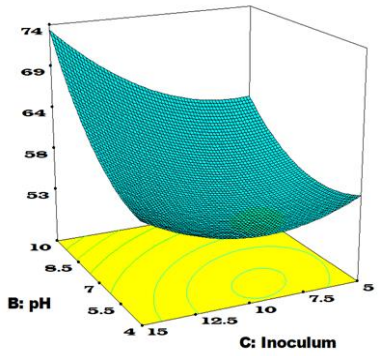

(e) (f)

Hold value: pH=7

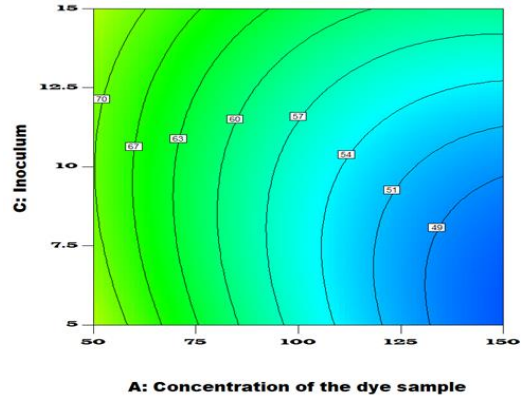

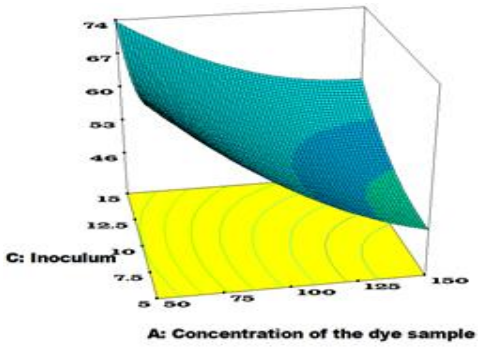

Figure 4.20 (a) Contour plot of B vs A. (b) Surface plot of B vs A. (c) Contour plot of C vs B. (d) Surface plot of C vs B. (e) Contour plot of C vs A. (f) Surface plot of C vs A

The plots were obtained at the hold value of low methanol content to be added along with other hold value as mentioned in the figure. From Contour plots, it can be observed that the % decolorization increases when the two factors are increased by keeping the third factor unchanged. From Surface plots, Fig. 4.20(b) showed that maximum decolorization was observed at high concentrations and low pH where as in the other cases of (high A and high B), (Low A, High B), (low A, low B) showed the minimum decolorization, Fig. 4.20(d) showed that maximum decolorization was observed only at the high inoculum dosages and high pH values, Fig. 4.20(f) showed that maximum decolorization was observed at the conditions of high inoculum whereas minimum was observed at low inoculum.

The residual plots of the runs for degradation of D1 using *P. pastoris* are shown in Fig. 4.21

a b

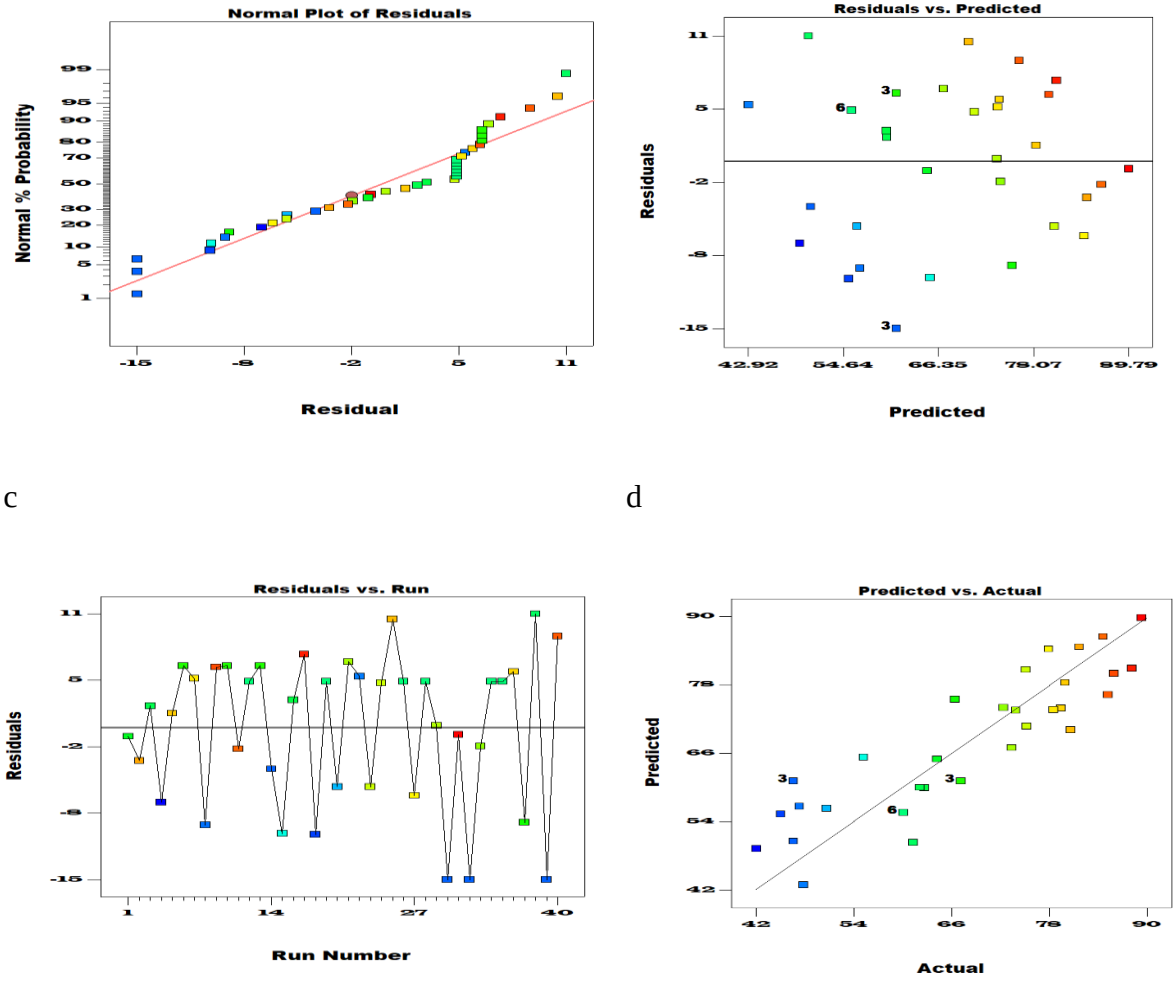

c d

Figure 4.21 Residual plots of Decolorization process of direct yellow 12 using *P. pastoris* (a) Normal Plot of residuals (Normal % Probability vs Residuals) (b) Residuals vs Predicted (c) Residuals vs Run (d) Predicted vs Actual

The optimum values of the degradation reaction of D1 were found out (and shown in Fig. 4.22) and are A of 149.05 mg/L, B of 9.93, C of 14.99 %v and D of 15 ml with a desirability of 1.

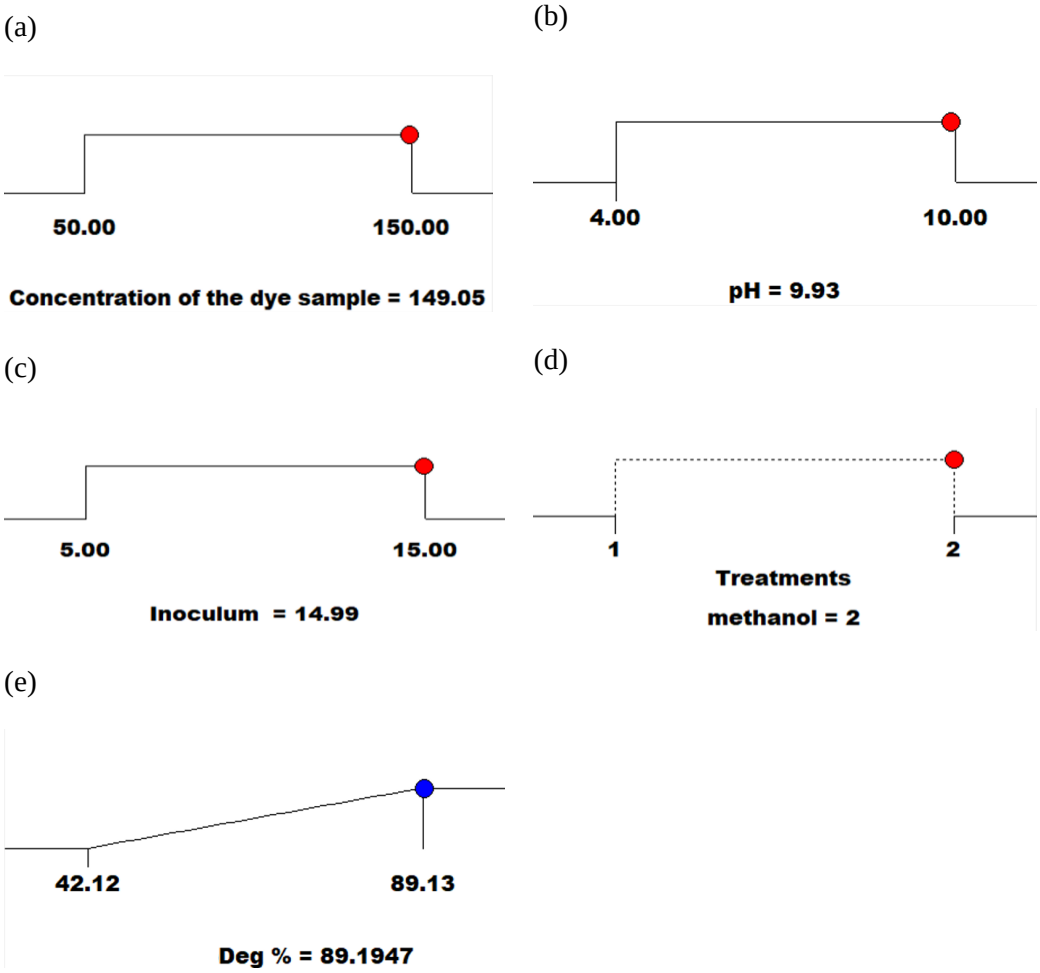

Figure 4.22 Optimal values required for (a) concentration of the dye sample to take (b) pH (c) dosage of inoculum needed (d) Methanol required (e) Decolorization of dye obtained at given optimal conditions

The experimental validation yielded decolorizing percentage of 83.3. (Hema and Suresha, 2014) have obtained the biodegradtion of 63.5% of chrysophenine optimized value. In their report even though the bacteria was isolated from the effluent of the textile industry, its biodegradation percentage was not up to the mark that is obtained in the present study using yeast culture. (Adnan et al., 2015) demonstrated 91.1% biodegradation of Reactive black 5 utilising *Trichoderma Atroviride* F03 at a starting amount of 50 mg l^{-1} in their study. Glucose and N_2 supplements were also suppled, which increased the microbe's capability to degrade. The figure explaining the residual plots of N1D can be found in the supplementary material

4.4.3 Biodegradation analysis

FTIR spectrum was used to analyse samples before and after decolorization and it is shown below as Fig. 4.23.

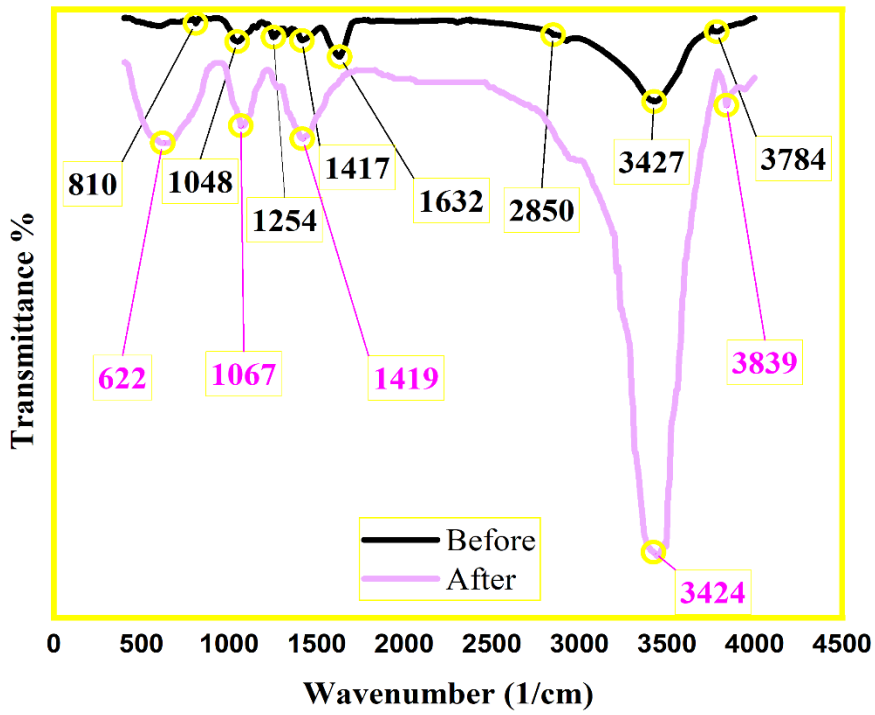

Figure 4.23 FTIR spectrum of decolorized direct yellow solution by yeast *P. pastoris*: before and after microbial degradation

Before decolorization as shown in Fig. 4.23, the wavenumbers 2923 cm^{-1}, 2854cm^{-1} corresponded to the presence of methyl CH asymmetric bonds and 1325 cm^{-1} for the Methyne CH bend and 810 cm^{-1} for the para disubstituted aromatic ring and 1632 cm^{-1} for the presence of azo bond C-S stretch and 1048 cm^{-1} for primary amine i.e., CN stretch and 1254 cm^{-1} for aromatic primary amine CN stretch and 1417 cm^{-1} for vinyl CH in plane bend and 2850 cm^{-1} for Methoxy (methyl ether O-CH3) (CH stretch) and peak at 3427 cm^{-1} with broad peak corresponding to OH group and 3784 cm^{-1} with medium sharp peaks corresponding to OH . So, it might be ONa group. Whereas after decolorization, a new bond of thiol might be formed with wavenumber of 622 cm^{-1} corresponding to disulfides (CS stretch) and 1067 cm^{-1} for primary amine i.e., CN stretch and 1419 cm^{-1} for phenol or OH bond and peak at 3424 cm^{-1} with broad peak corresponding to OH group and 3839 cm^{-1} with medium sharp peaks corresponding to OH. So, it might be ONa group. There is no peak for azo bond for the after decolorization curve. Hence the azo bond is completely reduced after decolorization.

4.4.4 Experimental Validation

The regression models were used to compare the experimentally validated optimal values of both the dyes. The variation in the experimental and model values was less than 10% which can be considered to be acceptable. Table regarding the depiction of error of degradation is briefly shown as Table 4.7.

Table 4.7 Error between optimized model and experimental values

					% decolorization		
Dye	Concentration of Dye solution (mg/L)	pH	Inocolum Dosage (%v/v)	Methanol (ml)	model value	expt value	error %
Direct yellow 12	149.52	9.94	14.97	14.97	89.2	83.3	6.6

4.4.5 Toxicity studies

Dyes decolorized by microbes when compared to those of seedlings treated with water, were substantially higher than the seedlings treated with the dye simulated water. Many researchers like (Jadhav et al., 2011) have suggested using bioassays such as phytotoxicity to consider the hazardous impacts of dyes and their treated samples on plants. Furthermore, seedlings grown with dye and effluents had shorter plumule and radicle lengths than seeds grown with pure water. The dyes were harmful to these plants, but the metabolites generated after microbial degradation was less harmful, indicating that the dyes were detoxified by *Pichia Pastoris*. These outcomes mention the significance of yeast for bioremediation of dye as decolorization and detoxification. Biodegradation results in the development of simpler, harmless chemicals. With the formation of reasonably mild toxic sludge, this procedure of biodegradation is more cost-effective (Krishnan et al., 2017). After 48 hours, the decolorization rate of dyes decolorized by *Pichia Pastoris* reached approximately 90%. Phytotoxicity Table 4.8 show that both the dyes have different biological characteristics of the considered agricultural seeds when compared to water-treated seedlings.

Table 4.8 Phytotoxicity of direct yellow solution and their metabolites formed after degradation by microbe

		Germination %	plumule(cm)	Radical(cm)
Spinacia Oleracea	Distilled water	100	2.56±0.1	1.22±0.3
	Dye	30	0.57*±0.3	2.05±0.25
	Metabolites	90	0.56**±0.3	0.97±0.13
Capsicum Frutescens	Distilled water	100	2.4±0.06	3.45±0.34
	Dye	20	1.43±0.59	$0.28^{@}$±0.19
	Metabolites	90	$1.8^{@}$±0.21	$1.71^{@}$±0.41
Trigonella Foenum	Distilled water	100	3.22±0.2	7.46±0.73
	Dye	40	$1.43^{\#}$±0.59	$1.61^{\#\#}$±0.66
	Metabolites	90	2.44±0.34	5.6±0.91

The tabled values taken are mean of 10 seeds in 3 sets SEM (±). Spinacia oleracea seeds grown in Direct yellow 12 are dissimilar from the seeds grown in pure water at *P<0.05, **P<0.05. Capsicum frutescens kernels grown in Direct yellow 12 as well as metabolites of the treated water are dissimilar from those grown in pure water at $^{@}$P<0.005. Trigonella foenum seeds grown in Direct yellow 12 as well as metabolites of the treated water are dissimilar from those grown in pure water at $^{\#}$P<0.05 and $^{\#\#}$P<0.005 using 1-way ANOVA with Tukey Kramer analysis.

Batch Decolorization Studies of Acid red 13 simulated solution

Experimental studies were done for decolourization of Acid red 13 solution with bacteria and yeast and Response surface methodology of decolorization is done for finding the optimized conditions for maximum removal

4.5 Decolorization of Acid red 13 Using Bacteria *Thalassospira frigidphilosprofundus*

Table 4.9 shows the observations which were made from the batch experiments of the decolorization of corresponding dye solution D2 using *Thalassospira frigidphilosprofundus* and calculated percentage decolorization.

Table 4.9 Experimental matrix and the % decolorization calculations

					% decolorization	
S.no	c(mg/L)	pH (p)	t(°C)	a(rpm)	In Control flask	In microbial flask
1	30	4	15	0.1	13.71	53.60
2	50	6	20	20	7.62	67.48
3	150	10	30	60	16.31	61.90
4	200	12	40	80	10.08	38.38
5	30	6	20	40	13.72	67.52
6	200	10	15	0.1	10.08	42.08
7	30	8	30	40	13.72	69.65
8	150	12	15	20	16.31	55.02
9	50	6	25	0.1	8.29	71.25
10	90	12	20	80	2.25	62.09

11	200	10	15	40	10.08	42.28
12	30	4	30	80	13.72	74.10
13	150	12	40	0.1	16.31	40.79
14	50	6	25	80	14.63	33.81
15	200	8	30	30	10.11	53.39
16	30	12	40	60	13.72	66.18
17	90	12	20	0.1	2.25	55.56
18	150	4	30	40	16.31	46.23
19	50	8	15	20	7.62	57.59
20	30	4	25	60	13.72	38.47
21	200	12	20	0.1	10.07	52.84
22	150	4	25	80	16.31	50.70
23	200	8	30	20	10.07	53.39
24	30	10	20	80	13.72	48.89
25	90	12	25	40	2.25	62.87
26	50	6	15	60	7.62	68.37

4.5.1 Triumph attained

The decolorization in control flask for each run was very less when compared with microbial decolorization and the average decolorization in control flask for all the runs performed is nearly 12 whereas, it is nearly 53 for microbial decolorization.

4.5.2 Decolorization process

Using the results in Minitab software, the following equation (4.5) was obtained. This equation corresponds to the effect of the independent variables on the dependent variables which is decolorization percentage.

$$y = [\exp(-1.18)] \times c^{-0.651} \times p^{3.42} \times t^{3.42} \times a^{0.189} \times \left[\exp\left(c \times \left(0.0206 + (0.000838 \times p) - (0.000404 \times t)\right)\right)\right] \times \left[\exp\left(p \times \left(-1.2 + (0.0376 \times p) + (0.0104 \times t)\right)\right)\right] \times \left[\exp\left(t \times \left(-0.191 + (0.00255 \times a) - (0.00028 \times p \times a)\right)\right)\right] \times [\exp\left(a \times \left(-0.107 + (0.00643 \times p) + (0.000294 \times a)\right)\right)\right) \quad (4.5)$$

The above equation was obtained with 90.7% of Rsq and 81.6% of Rsq(adj). The surface plots and contour plots of the experimental observations corresponding to the modelled equation were obtained from the Minitab software. The surface plots of the runs indicated that the decolorization do not just have a linear relationship or any known curve regressions. They had a lot of local maximums and local minimums. The contour plots indicated many regions which are indicated with respect to their decolorization percentages.

- The plots shown below in Fig. 4.24, show the relationship between decolorization% (y) and concentration of the sample(c), pH (p) of the sample maintained.

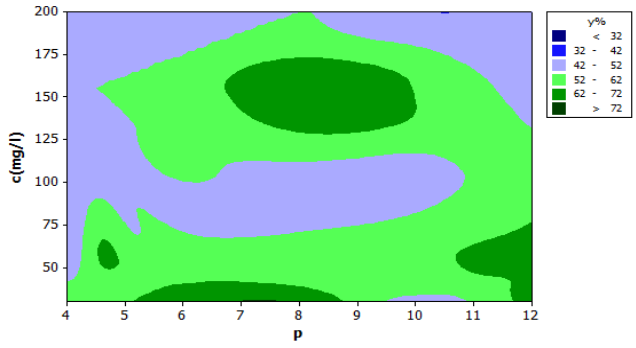

(a) Contour Plot of y vs c(mg/L), p

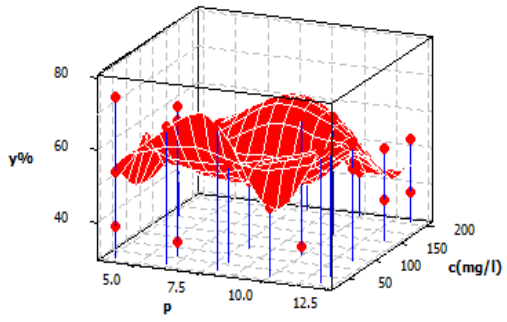

(b) Surface Plot of y vs c(mg/L), p

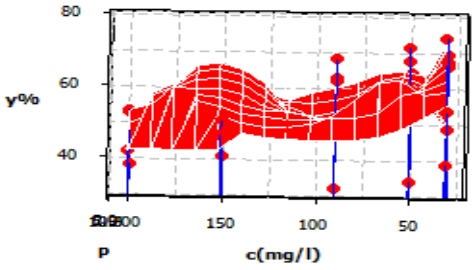

(c) Surface Plot of y vs c(mg/L), p

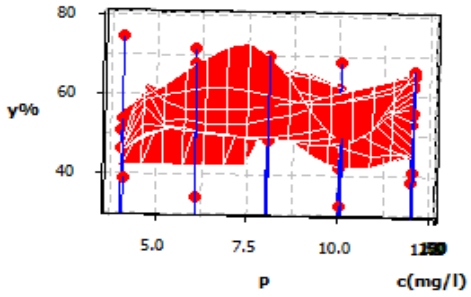

(d) Surface Plot of y vs c(mg/L), p

Figure 4.24 Effect of Concentration and pH on decolorization

Fig. 4.24(a) depicts the contour plot and explains that the maximum amount of decolorization percentage (i.e., greater than 72%) is possible in the region of approximately low concentrations of up to 5 (mg/L) concentrations of the sample and 7.5 pH. Similar result of maximum decolorization (i.e., 72.3%) was shown in Fig. 4.24(b), (c), (d) but in a 3D view.

- Surface plot and Contour plots of influence of Temperature of operation and concentration of the synthetic solution on the decolorization percentage are shown in Fig. 4.25.

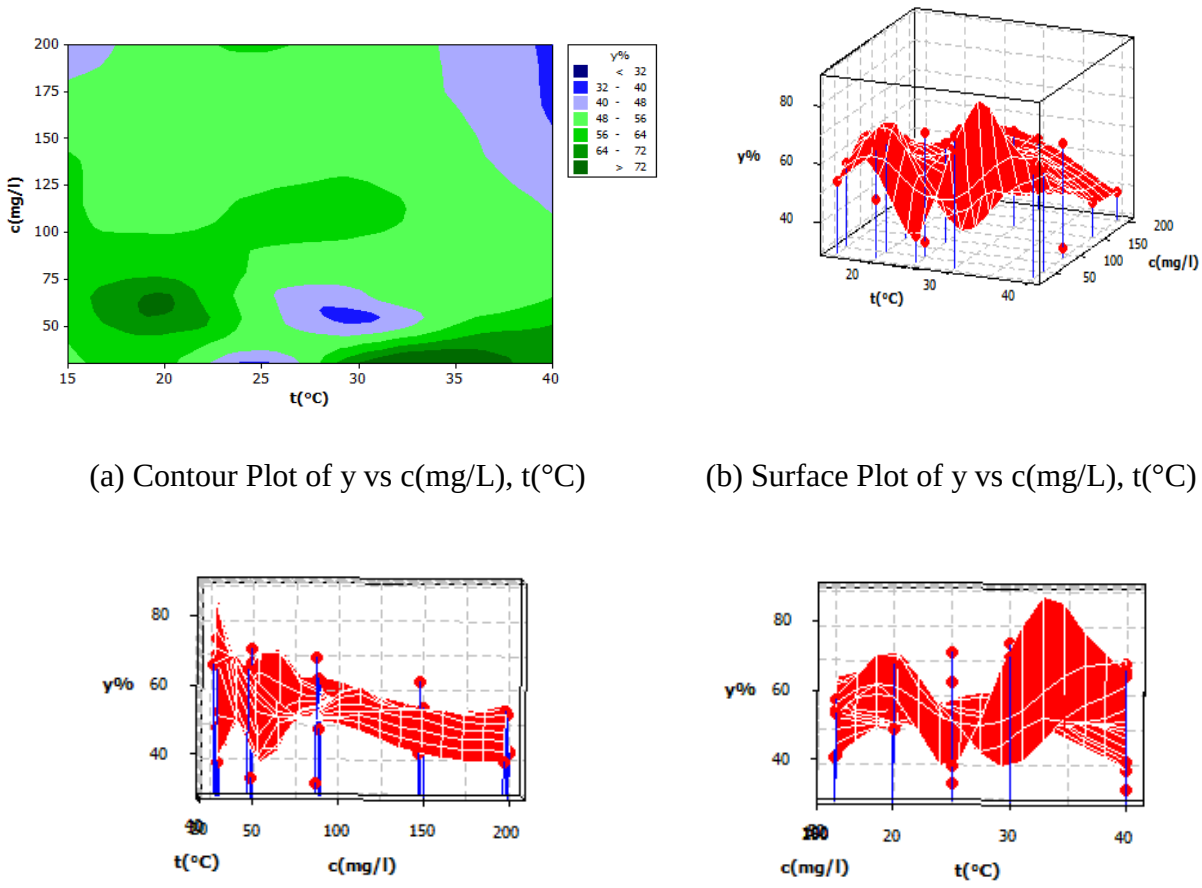

(a) Contour Plot of y vs c(mg/L), t(°C)

(b) Surface Plot of y vs c(mg/L), t(°C)

(c) Surface Plot of y vs c(mg/L), t(°C)

(d) Surface Plot of y vs c(mg/L), t(°C)

Figure 4.25 Effect of Concentration and temperature on decolorization

Fig. 4.25(a) shows the contour plot and explains that maximum amount of decolorization percentage (i.e., greater than 72%) is possible in two regions of approximately 55 (mg/L) to 70 (mg/L) concentration of the sample, 17.5°C to 21°C temperature, and 3concentrations up to 30 (mg/L) concentration of the sample, 0°C to 37.5°C temperature. Surface plots (from Fig. 4.25(b)) showed 3D view of the result (decolorization of greater than 85%) and from Fig. 4.25(c), (d) it can be deduced that maximum decolorization among the both regions were

observed at three concentrations of up to 33.33(mg/L) concentration of the sample and 3.33°C temperature.

- Surface plot and Contour plots of influence of agitation of the chamber and concentration of the synthetic solution on the decolorization percentage are shown in Fig. 4.26.

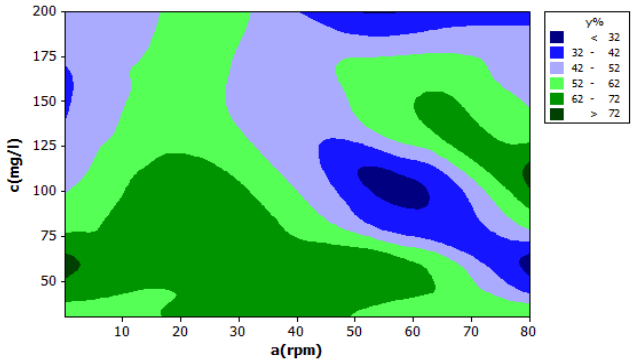

(a) Contour Plot of y vs c(mg/L), a

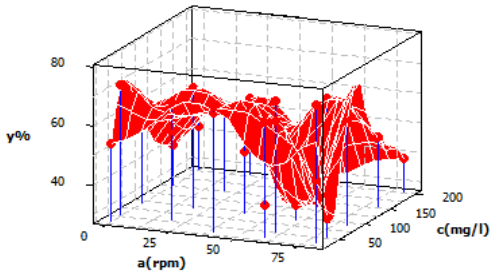

(b) Surface Plot of y vs c(mg/L), a

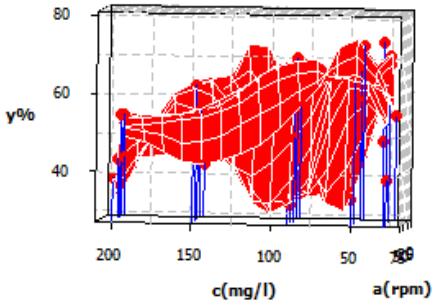

(c) Surface Plot of y vs c(mg/L), a

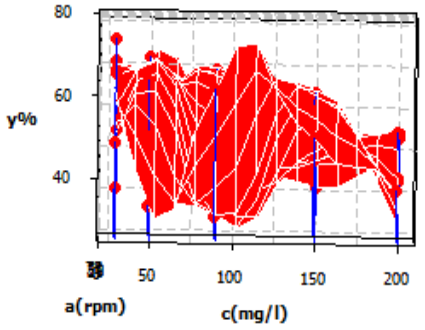

(d) Surface Plot of y vs c(mg/L), a

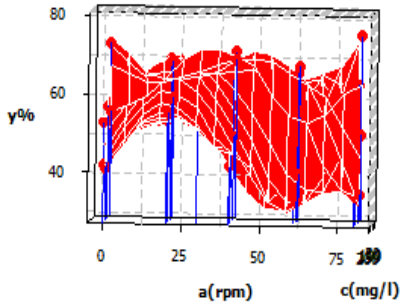

(e) Surface Plot of y vs c(mg/L), a

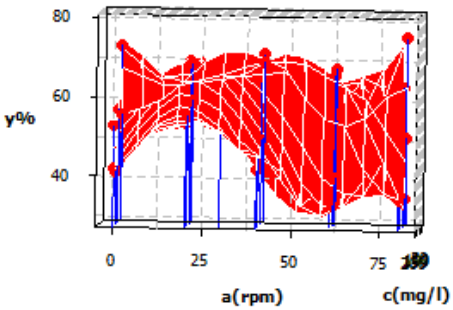

(f) Surface Plot of y vs c(mg/L), a

Figure 4.26 Effect of Concentration and agitation on decolorization

Fig. 4.26(a) explains that the contour plot obtained gave the information that maximum amount of decolorization percentage (i.e., greater than 72%) was possible in two regions of 52 (mg/L) to 60.5 (mg/L) concentrations of the sample, 0 rpm to 2.5 rpm and 100 (mg/L) to 112.5 (mg/L) concentrations of the sample, 78 rpm to 80 rpm. Surface plot (Fig. 4.26(b)) showed 3D view of the result and it depicted that decolorization (78.33%) among the both regions was shown in both the ranges at 50 (mg/L), 0 rpm and 106.25 (mg/L) of the sample,75 rpm. Concentration values are obtained from Fig. 4.26(c), (d) and agitation values were obtained from Fig. 4.26(e), (f)

- Surface plot and Contour plots of influence of pH of the synthetic solution and the temperature of operation on the decolorization percentage are shown in Fig. 4.27.

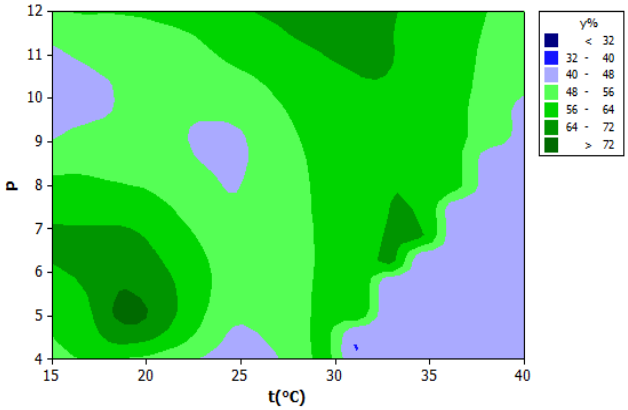

(a) Contour Plot of y vs p, t(°C)

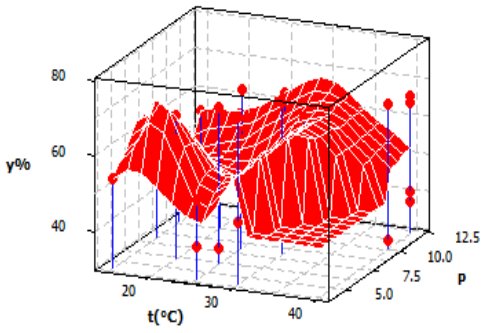

(b) Surface Plot of y vs p, t(°C)

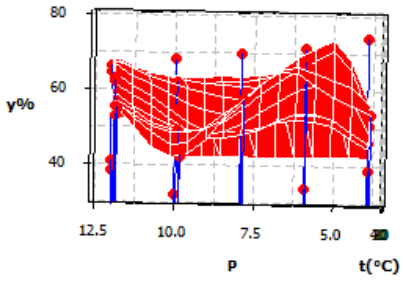

(c) Surface Plot of y vs p, t(°C)

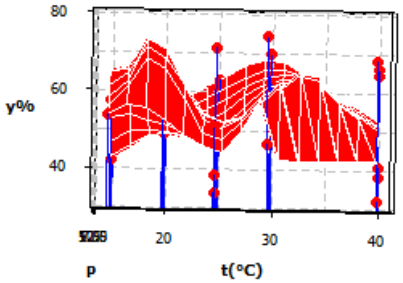

(d) Surface Plot of y vs p, t(°C)

Figure 4.27 Effect of pH and Temperature on decolorization

Fig. 4.27(a) gave the contour plot that showed us that maximum amount of decolorization percentage (i.e., greater than 72%) was possible in the region of approximately 4.8 to 5.5 pH

values and 18°C to 20°C Temperature values. Similar results were shown in the surface plots but in a 3D view (72.5%) at 5 pH and 18.33°C (obtained from Fig. 4.27(b), (c), (d)).

- Surface plot and Contour plots of influence of agitation of the chamber and pH of the synthetic solution on the decolorization percentage are shown in Fig. 4.28.

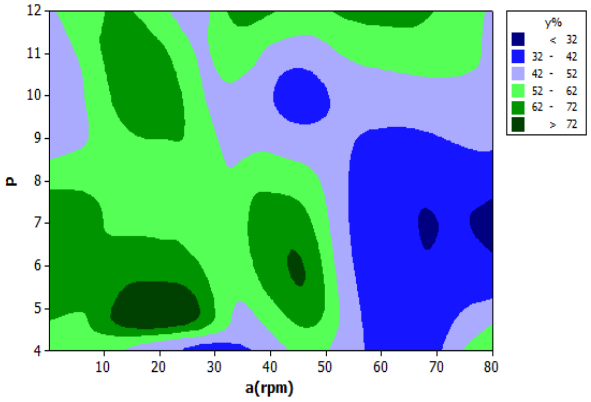

(a) Contour Plot of y vs p, a(rpm)

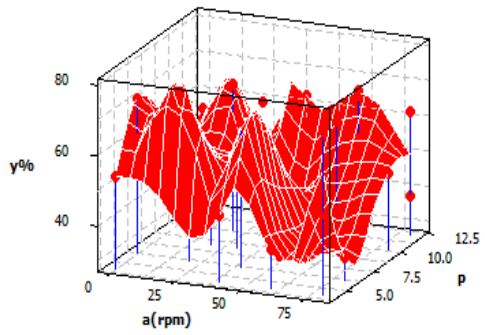

(b) Surface Plot of y vs p, a(rpm)

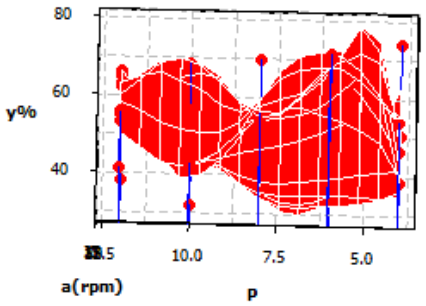

(c) Surface Plot of y vs p, a(rpm)

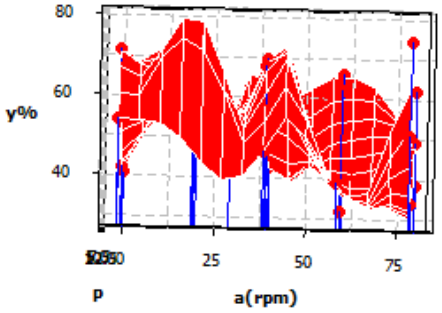

(d) Surface Plot of y vs p, a(rpm)

Figure 4.28 Effect of pH and agitation on decolorization

Fig. 4.28(a) gave the contour plot which showed that maximum amount of decolorization percentage (i.e., greater than 72%) was possible in two regions of 4.5 to 5.5 pH values,10 rpm to 28 rpm values and 5.5 to 6.5 pH values,42 rpm to 46 rpm. From Fig. 4.28(b) surface plot showed 3D view of the result and it depicted that decolorization (78%) among the both regions were shown at 5.5 pH values and 18.75 rpm (pH values are obtained from Fig. 4.28(c) and agitation values are obtained from Fig. 4.28(d)

- Surface plot and Contour plots of influence of temperature of operation and agitation of chamber on the decolorization percentage are shown in Fig. 4.29.

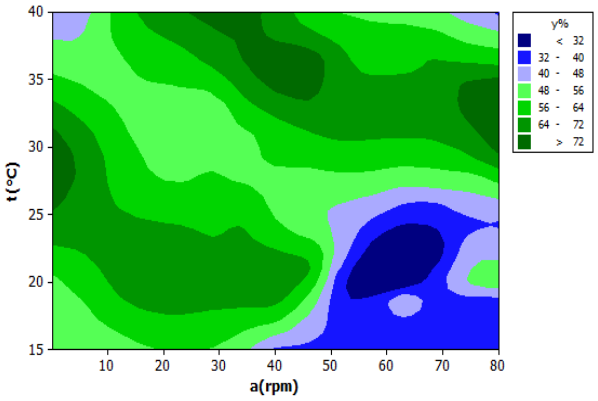

(a) Contour Plot of y vs t(°C), a(rpm)

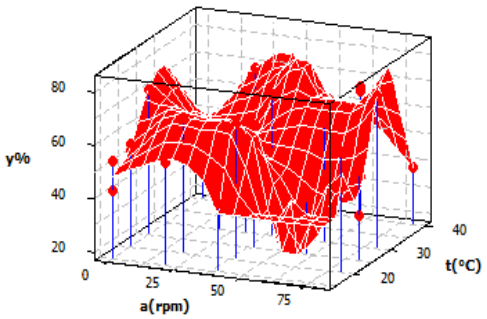

(b) Surface Plot of y vs t(°C), a(rpm)

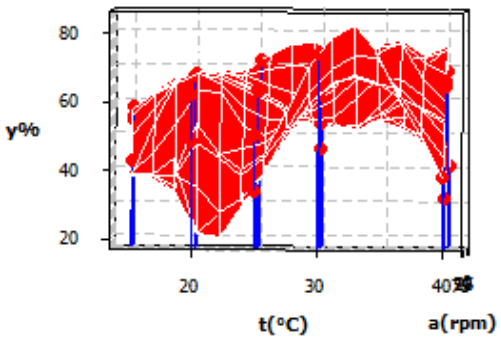

(c) Surface Plot of y% vs t(°C), a(rpm)

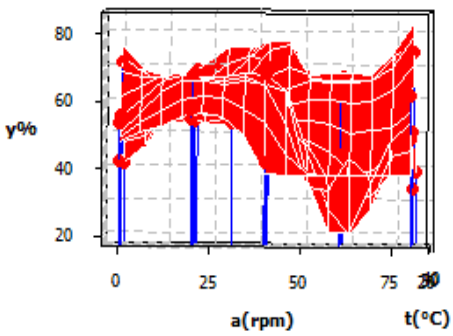

(d) Surface Plot of y% vs t(°C), a(rpm)

Figure 4.29 Effect of temperature and agitation on decolorization

Fig. 4.29(a) shows the contour plot which gives us the information that maximum amount of decolorization percentage (i.e., greater than 72%) was possible in three regions of 26°C to 31°C values,0 rpm to 5 rpm and 34°C to 40°C, 30 rpm to 50 rpm, and 30°C to 35°C ,72 rpm to 80 rpm. Surface plot showed 3D view of the result (from Fig. 4.29(b)) and it depicted that decolorization (84%) among the regions was shown as temperature at 32.8125°C (from Fig. 4.29(c)) and 79.166 rpm (from Fig. 4.29(d)).

From the above obtained data, the maximum amount of decolorization can be achieved at the conditions of 29.44 (mg/L) concentration, pH 6, temperature of 33.07125°C, and agitation of 77.083 rpm, according to the data obtained.

ANOVA tables of decolorization of Acid red 13 solution is given in Appendix B. Appendix tables B1, B2 shows the Analysis of variance of decolorization of Acid red 13 using *T. frigidphilosprofundus*, Appendix table B3 shows the Degrees of freedom, seq SS of the individual parameters of decolorization of Acid red 13 using *T. frigidphilosprofundus*. The scatter plots were also obtained and shown in Fig. 4.30. They denote the correlation between the result obtained and the input variables (Barker and Westfall 2022). Here 3D plots were obtained, where the points indicate the percentage decolorization obtained at two particular input variables.

a

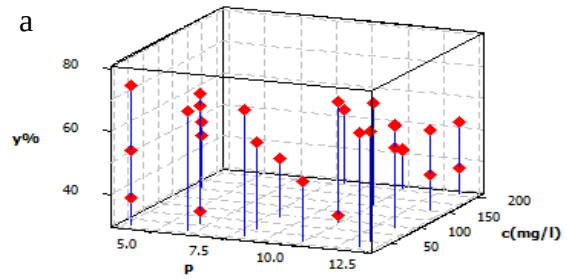

3D Scatter plot of y vs c(mg/L)vs p

b

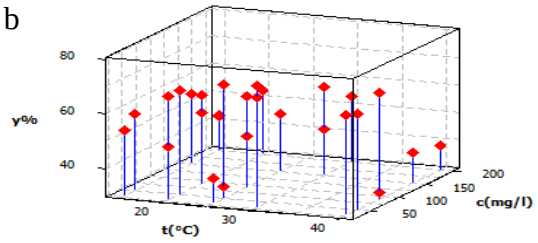

3D Scatter plot of y vs c(mg/L) vs t(°C)

c

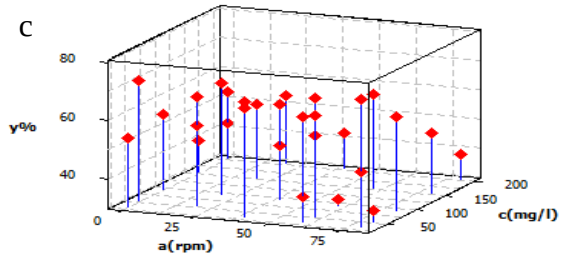

3D Scatter plot of y vs c(mg/L) vs a(rpm)

d

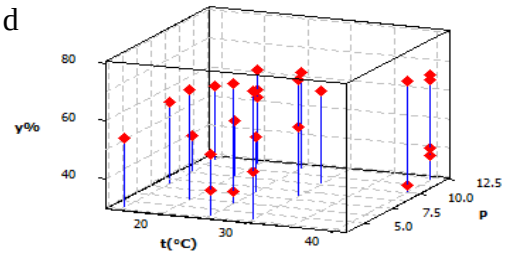

3D Scatter plot of y vs p vs t(°C)

e

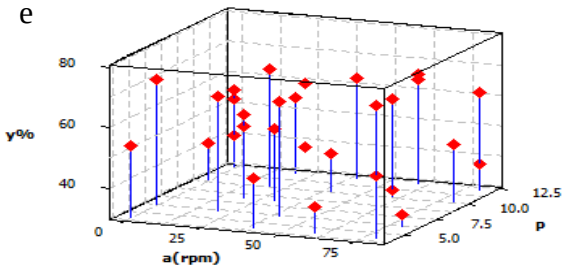

3D Scatter plot of y vs p vs a(rpm)

f

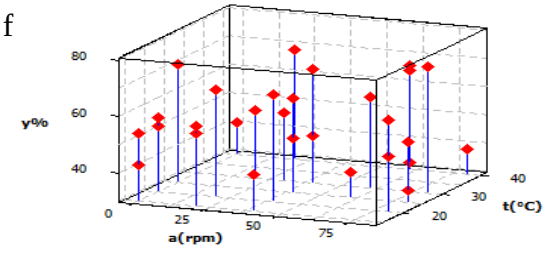

3D Scatter plot of y vs t(°C) vs a(rpm)

Figure 4.30 Scatter plots of decolorization of Acid red 13 using *Thalassospira frigidphilosprofundus*

In the above figure, (a) denote the figure of scatter plot of y% vs c (mg/L) vs p, (b) denote the figure of scatter plot of y% vs c (mg/L) vs t(°C), (c) denote the figure of scatter plot of y% vs c(mg/L) vs a(rpm), (d) denotes the figure of scatter plot of y% vs p vs t(°C), (e) denotes the scatter plot of y% vs p vs a(rpm), (f) denote the scatter plot of y% vs t(°C) vs a(rpm). From the above plots, the majority of the data points tend to rise or fall.

The residual plots of the runs for degradation of D2 using *T. Frigidphilosprofundus* are shown in Fig. 4.31.

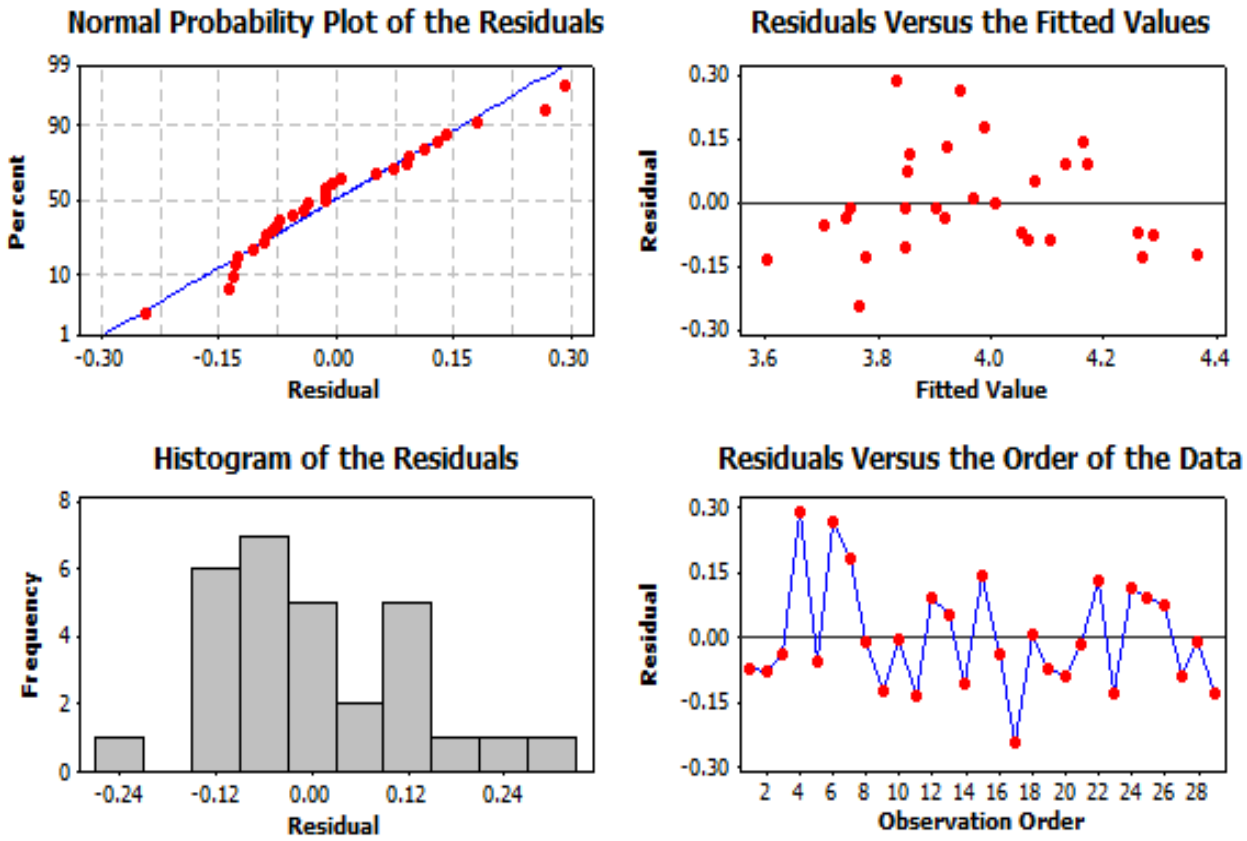

Figure 4.31 Plots showing Residual Plots of lny i.e., normal probability plot of the residuals, residuals versus the order of the data, Histogram of the residuals, Residuals versus the fitted values of decolorization of Acid red 13 solution using *E. burkholder*

The normal Probability plot explains whether the obtained data follows the normality distribution and the obtained data of the experiments form a good fit since the residuals obtained, form nearly a straight line. Histogram of the residuals graph show the number of experiments that correspond to the residual obtained and when the frequency is joined by a straight line, it follows a bell curve with a very less standard deviation, which explains it as a

good fit. The remaining two graphs explain the vertical deviations of the residuals with the corresponding x axes.

4.5 Decolorization of Acid red 13 Using Bacteria *Erwinia chrysanthemi Burkholder*

Table 4.10 shows the observations which were made from the batch experiments of the decolorization of corresponding dye solution D2 using *Thalassospira frigidphilosprofundus* and calculated percentage decolorization.

Table 4.10 Experimental matrix and the % decolorization calculations

					% decolorization	
S.no	c(mg/L)	pH	t(°C)	a(rpm)	In control flask	In microbial flask
1	30	4	15	0.1	13.71	40.44
2	50	6	20	20	7.62	80.28
3	150	10	30	60	16.31	58.81
4	200	12	40	80	10.08	55.68
5	30	6	20	40	13.72	69.83
6	200	10	15	0.1	10.08	59.82
7	30	8	30	40	13.72	70.69
8	150	12	15	20	16.31	48.86
9	50	6	25	0.1	8.29	67.72
10	90	12	20	80	2.25	65.77
11	200	10	15	40	10.08	59.13
12	30	4	30	80	13.72	76.22

13	150	12	40	0.1	16.31	36.65
14	50	6	25	80	14.63	64.28
15	200	8	30	30	10.11	67.31
16	30	12	40	60	13.72	59.53
17	90	12	20	0.1	2.25	55.13
18	150	4	30	40	16.31	63.64
19	50	8	15	20	7.62	55.20
20	30	4	25	60	13.72	43.47
21	200	12	20	0.1	10.07	66.64
22	150	4	25	80	16.31	49.17
23	200	8	30	20	10.07	67.31
24	30	10	20	80	13.72	46.11
25	90	12	25	40	2.25	55.56
26	50	6	15	60	7.62	56.66

4.6.1 Decolorization process

Using the results in Minitab software, the following equation (4.6) was obtained. This equation corresponds to the effect of the independent variables on the dependent variables which is decolorization percentage.

$$y = [\exp(-18.9)] \times c^2 \times p^{13} \times t^9 \times [\exp(c \times \left(0.0036 + (0.00112 \times c) - (0.00328 \times p) + (0.000118 \times p \times t) - (0.000004 \times c \times p)\right)] \times [\exp\left(p \times \left(-3.19 + (0.105 \times p) + (0.00201 \times a) + (0.000114 \times c \times a) + (0.000106 \times t \times a)\right)\right)] \times [\exp\left(t \times \left(-0.593 - (0.00152 \times c) + (0.00504 \times p) + (0.000051 \times c \times a)\right)\right)] \times [\exp(a \times \left(-0.0404 - (0.00123 \times c) + (0.00112 \times t) + (0.000068 \times a)\right)] \quad (4.6)$$

The above equation was obtained with 95.6% of Rsq and 93.6% Rsq (adj). The surface plots and contour plots of the experimental observations corresponding to the modelled equation were obtained from the Minitab software. The surface plots of the runs indicate that the decolorization do not just have a linear relationship or any known curve regressions. They have a lot of local maximums and local minimums. The contour plots indicated many regions which are indicated with respect to their decolorization percentages. Both the plots are shown below.

- The plots shown below in Fig. 4.32, show the relationship between decolorization% (y) and concentration of the sample(c), pH (p) of the sample maintained.

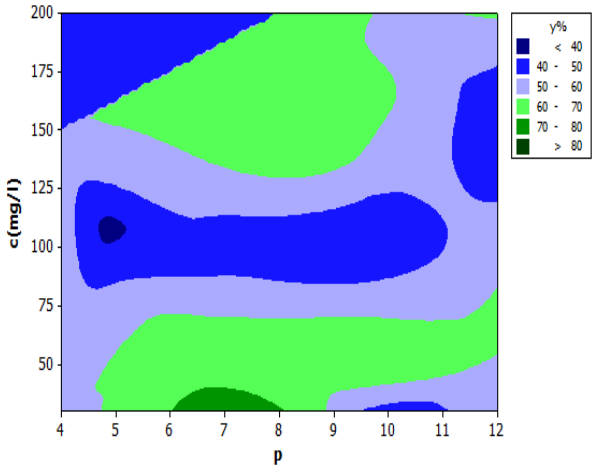

(a) Contour Plot of y vs c(mg/L), p

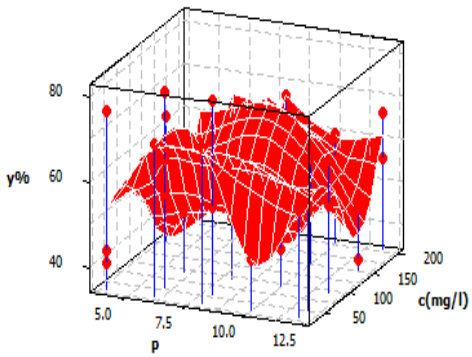

(b) Surface Plot of y vs c(mg/L), p

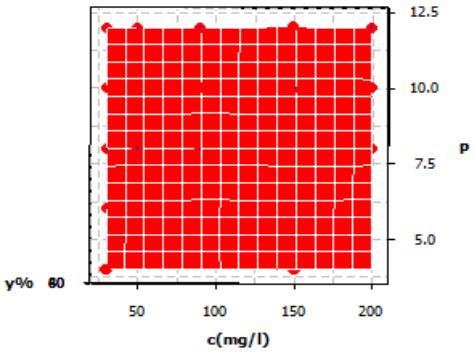

(c) Surface Plot of y vs c(mg/L), p

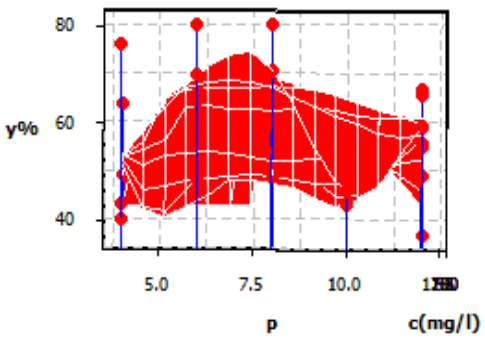

(d) Surface Plot of y vs c(mg/L), p

Figure 4.32 Effect of Concentration and pH on decolorization

Fig. 4.32(a) shows the contour plot that gives us the information that higher amount of decolorization percentage (i.e., 70%-80%) is possible in the region of approximately low concentrations up to 30 (mg/L) concentrations of the sample,6 to 8 pH values. Similar result

was shown in the surface plot (Fig. 4.32(b)), but in a 3D view at 29.166 (mg/L) (from Fig. 4.32(c)) and pH of 7.5 (from Fig. 4.32(d)).

- Surface plot and Contour plots of influence of Temperature of operation and concentration of the synthetic solution on the decolorization percentage are shown in Fig. 4.33.

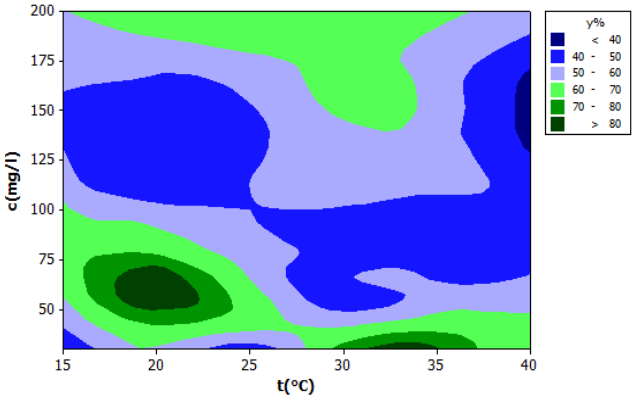

(a) Contour Plot of y vs c(mg/L), t(°C)

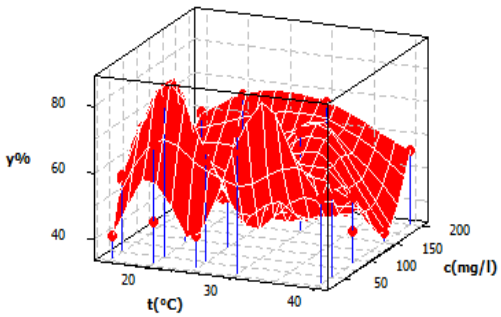

(b) Surface Plot of y vs c(mg/L), t(°C)

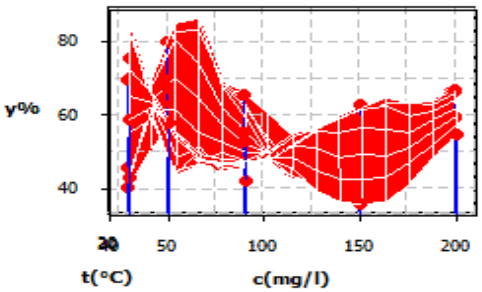

(c) Surface Plot of y vs c(mg/L), t(°C)

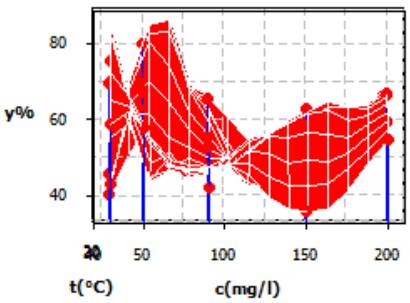

(d) Surface Plot of y vs c(mg/L), t(°C)

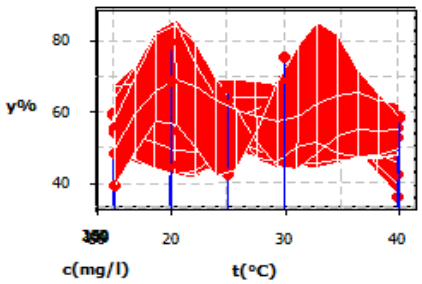

(e) Surface Plot of y vs c(mg/L), t(°C)

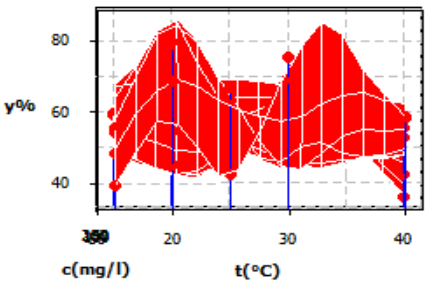

(f) Surface Plot of y vs c(mg/L), t(°C)

Figure 4.33 Effect of Concentration and temperature on decolorization

Fig. 4.33(a) shows the contour plot that gives us the information that maximum amount of decolorization percentage (i.e., greater than 80%) is possible in two regions of approximately 50 (mg/L) to 70 (mg/L) concentration of the sample, 17.5°C to 22.5°C temperature, and concentrations up to 20 (mg/L) concentration of the sample, 31°C to 35°C temperature. Surface plots showed 3D view of the result (from Fig. 4.33(b)) of two regions and it depicted that decolorization (85.909%) was shown at 5 (mg/L), 20°C and 67 (mg/L), 32.8125°C. The concentration values are shown from Fig. 4.33(c), (d) and the temperature values are shown from Fig. 4.33(e), (f).

- Surface plot and Contour plots of influence of agitation of the chamber and concentration of the synthetic solution on the decolorization percentage are shown in Fig. 4.34.

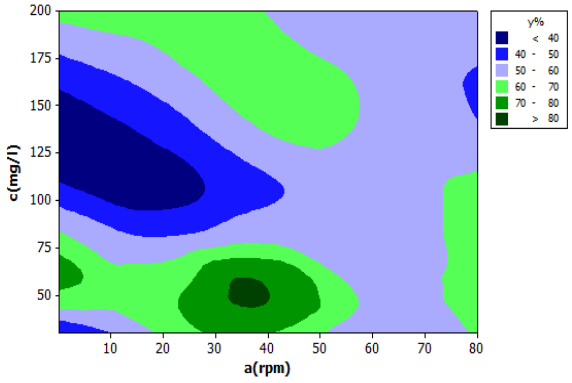

(a) Contour Plot of y vs c(mg/L), a

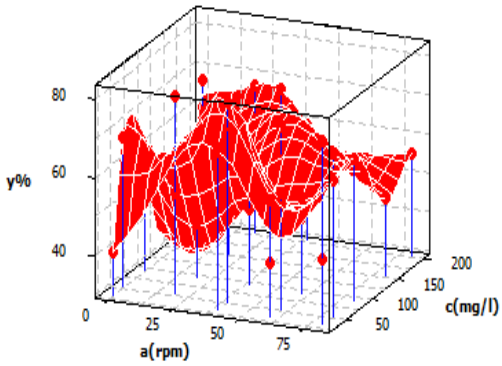

(b) Surface Plot of y vs c(mg/L), a

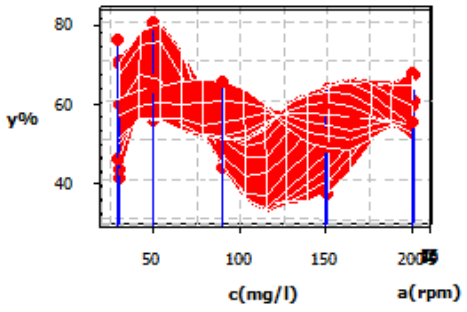

(c) Surface Plot of y vs c(mg/L), a

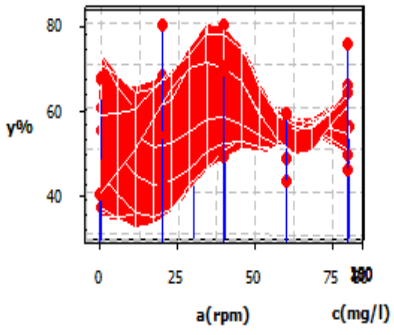

(d) Surface Plot of y vs c(mg/L), a

Figure 4.34 Effect of Concentration and agitation on decolorization

Fig. 4.34(a) explains the contour plot which explains us that the maximum amount of decolorization percentage (i.e., greater than 80%) was possible in the region of 40 (mg/L) to

60 (mg/L) concentrations of the sample, 31 rpm to 40 rpm. Similar result was shown in the surface plot (80%) (from Fig. 4.34(b)), but in a 3D view at position 50 (mg/L). (From Fig. 4.34(c)) and 33.654 rpm (from Fig. 4.34(d)).

- Surface plot and Contour plots of influence of pH of the synthetic solution and the temperature of operation on the decolorization percentage are shown in Fig. 4.35.

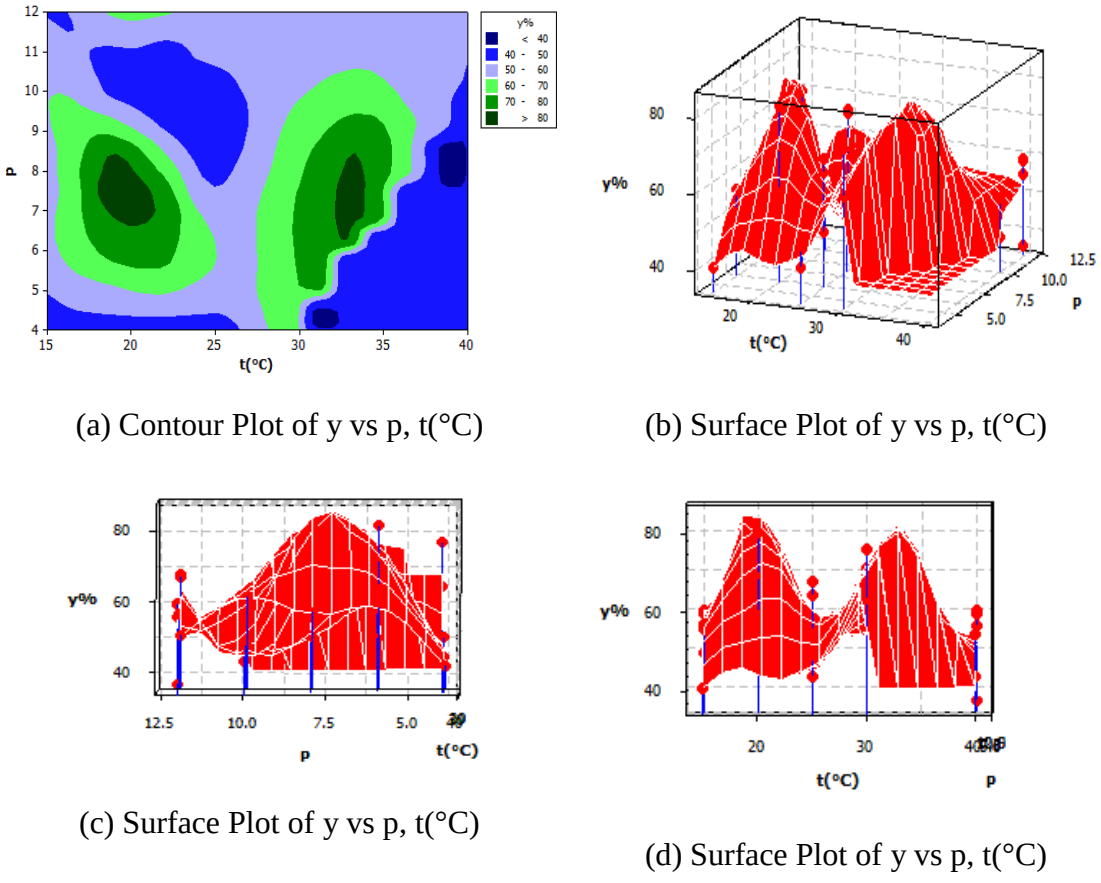

(a) Contour Plot of y vs p, t(°C)

(b) Surface Plot of y vs p, t(°C)

(c) Surface Plot of y vs p, t(°C)

(d) Surface Plot of y vs p, t(°C)

Figure 4.35 Effect of pH and Temperature on decolorization

Fig. 4.35(a) gives the contour plot which shows us that maximum amount of decolorization (i.e., greater than 80%) was possible in two regions of 6.5 to 8.1 pH values ,17.5°C to 22.5°C of temperature, 6 to 8.2 pH values, 32.5°C to 34°C of temperature. Similar results were shown in the surface plot (from Fig. 4.35(b)) but in a 3D view and the decolorization (83.636%) was depicted at 7.5 pH (from Fig. 4.35(c)), 18.235°C (from Fig. 4.35(d)).

- Surface plot and Contour plots of influence of agitation of the chamber and pH of the synthetic solution on the decolorization percentage are shown in Fig. 4.36.

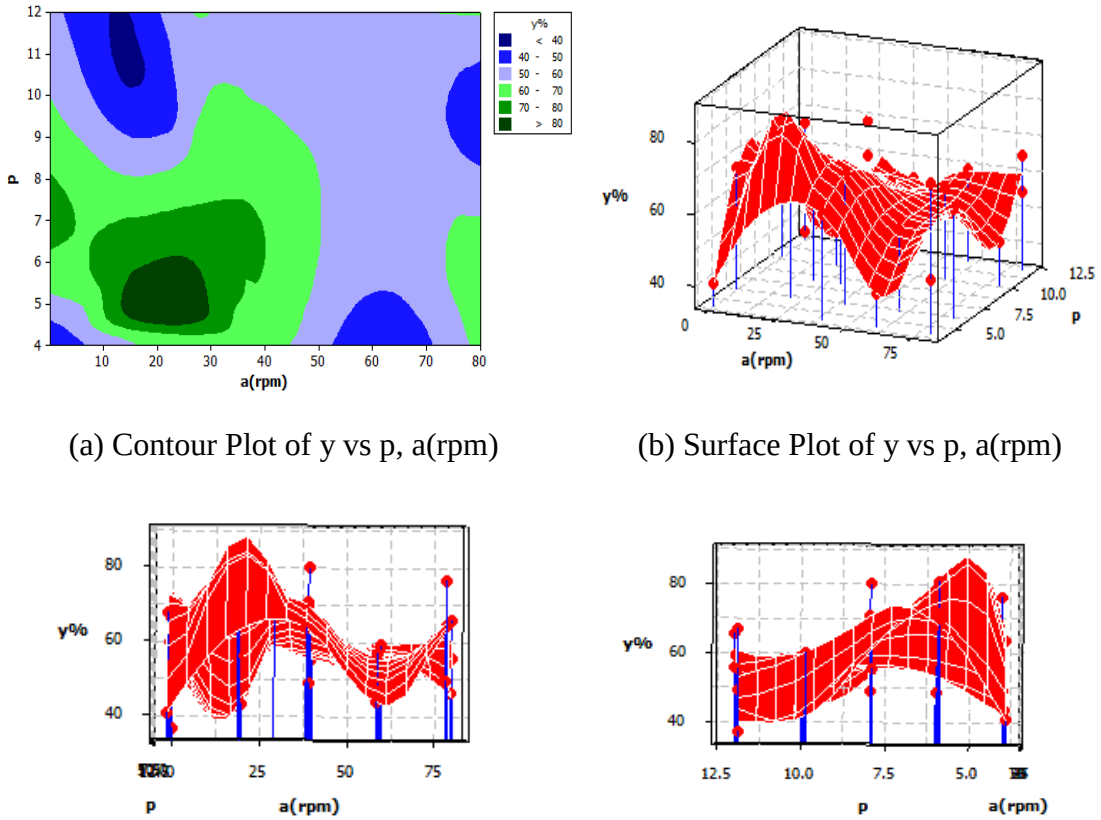

(a) Contour Plot of y vs p, a(rpm)

(b) Surface Plot of y vs p, a(rpm)

(c) Surface Plot of y vs p, a(rpm)

(d) Surface Plot of y vs p, a(rpm)

Figure 4.36 Effect of pH and agitation on decolorization

Fig. 4.36(a) explains the contour plot which shows us that maximum decolorization (i.e., greater than 72%) was possible in the region 4.5 to 6 pH values, 12 rpm to 30 rpm values. Similar result (88.18%) was shown in the surface plot (from Fig. 4.6(b)), but in a 3D view at 5 pH (from Fig. 4.36(c)), 20.84 rpm (Fig. 4.36(d)).

- Surface plot and Contour plots of influence of temperature of operation and agitation of chamber on the decolorization percentage are shown in Fig. 4.37.

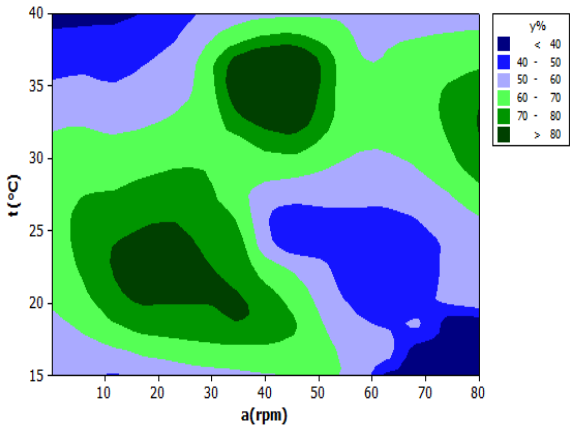

(a) Contour Plot of y vs t(°C), a(rpm)

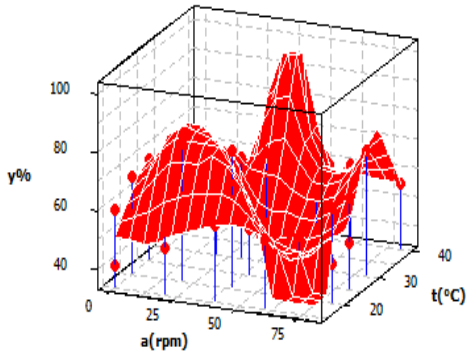

(b) Surface Plot of y vs t(°C), a(rpm)

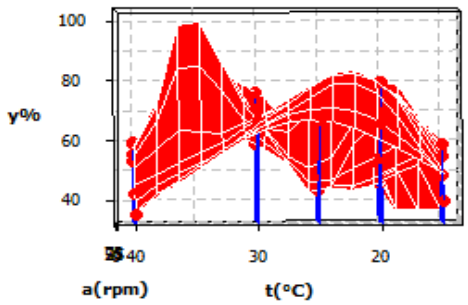

(c) Surface Plot of y vs t(°C), a(rpm)

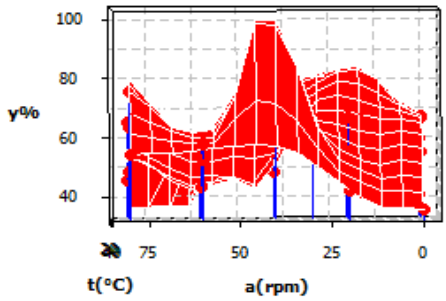

(d) Surface Plot of y vs t(°C), a(rpm)

Figure 4.37 Effect of temperature and agitation on decolorization

Fig. 4.37(a) explains the contour plot which gives us the information that maximum decolorization (i.e., greater than 72%) was possible in three regions of 19°C to 25°C values,10 rpm to 36 rpm values and 31°C to 37.5°C of temperature, 37 rpm to 50 rpm and 31°C to 33°C of temperature, 79 rpm to 80 rpm. Surface plot (from Fig. 4.37(b)) showed 3D view of the result (100%) and it depicted the decolorization among the regions 35.625°C (from Fig. 4.37(c)), 40.625 rpm (from Fig. 4.37(d)).

From the obtained information, it can be deduced that the maximum amount of decolorization can be obtained at the conditions of 58.5 (mg/L) of concentration, pH of 6.25, 33.75°C of temperature, agitation of 31.706 rpm.

ANOVA tables of decolorization of Acid red 13 solution is given in Appendix B. Appendix tables B4, B5 shows the Analysis of variance of decolorization of Acid red 13 using *E. burkholder*, Appendix table B6 shows the Degrees of freedom, seq SS of the individual parameters of decolorization of Acid red 13 using *E. burkholder*. The scatter plots were also obtained as shown in Figure 6. They denote the correlation between the result obtained and the input variables (Barker and Westfall 2022). Here 3D plots were obtained, where the points indicate the percentage decolorization obtained at two particular input variables.

a

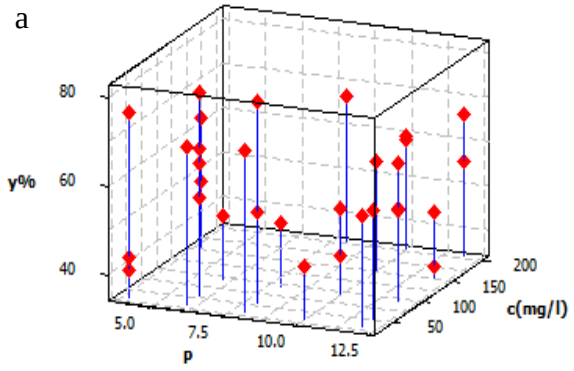

3D Scatter plot of y vs c(mg/L) vs p

b

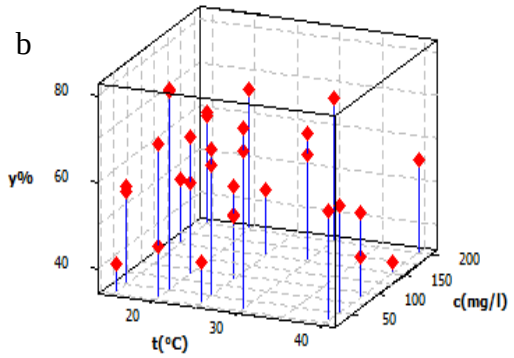

3D Scatter plot of y vs c(mg/L) vs t(°C)

c

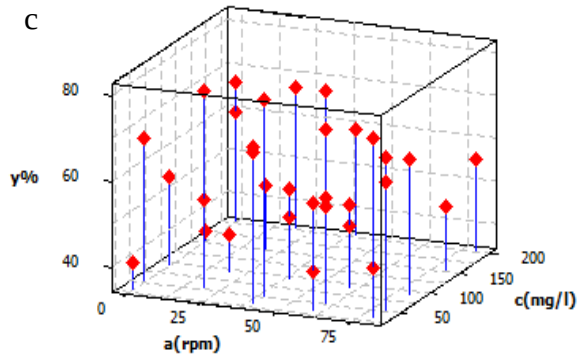

3D Scatter plot of y vs c(mg/L) vs a(rpm)

d

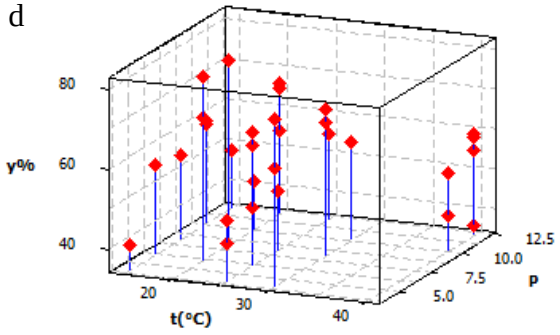

3D Scatter plot of y vs p vs t(°C)

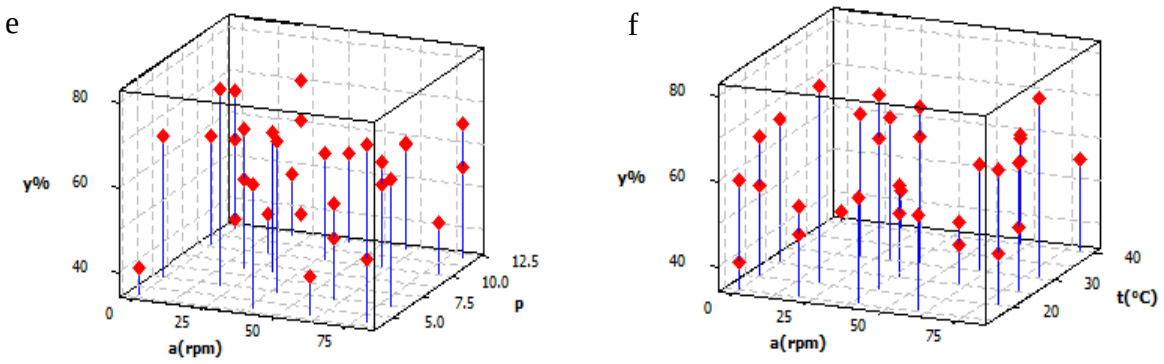

3D Scatter plot of y vs p vs a(rpm) 3D Scatter plot of y vs t(°C) vs a(rpm)

Figure 4.38 Scatter plots of decolorization of Acid red 13 solution using *E. burkholder*

In the above figure, (a) denote the figure of scatter plot of y% vs c (mg/L) vs p, (b) denote the figure of scatter plot of y% vs c (mg/L) vs t(°C), (c) denote the figure of scatter plot of y% vs c(mg/L) vs a(rpm), (d) denotes the figure of scatter plot of y% vs p vs t(°C), (e) denotes the scatter plot of y% vs p vs a(rpm), (f) denote the scatter plot of y% vs t(°C) vs a(rpm). From the above plots, the majority of the data points tend to rise or fall.

The residual plots of the runs for degradation of D2 using *E. burkholder* are shown in Fig. 4.39

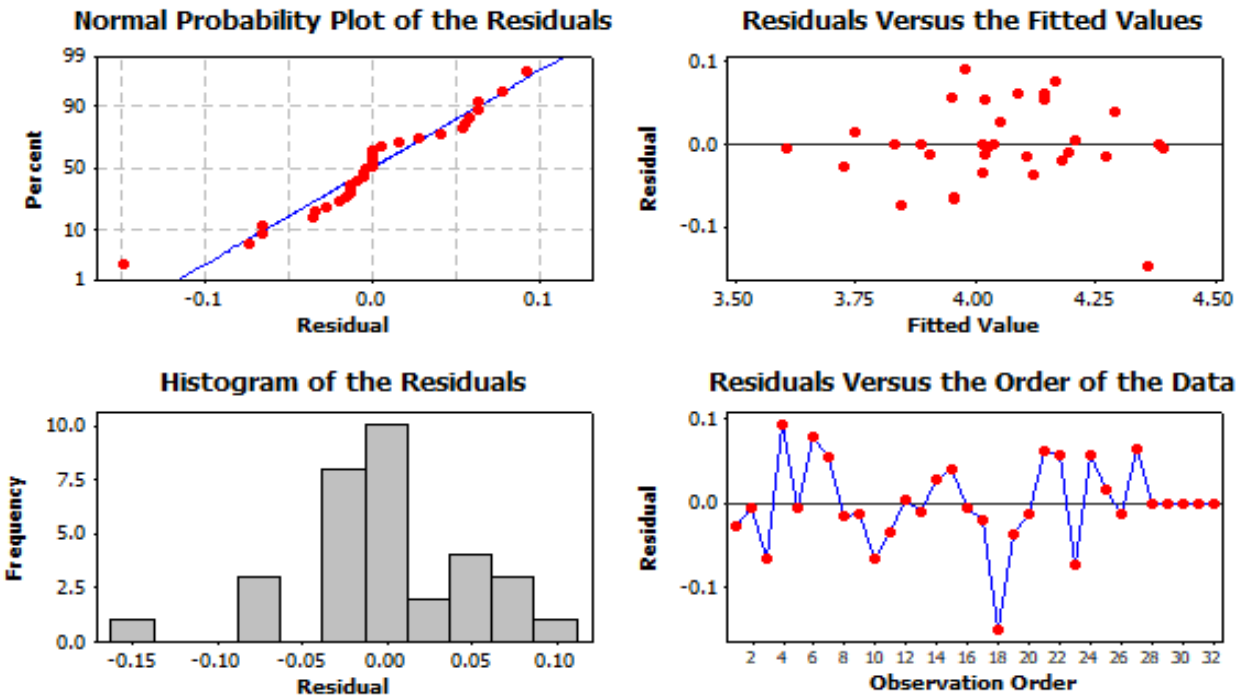

Figure 4.39 Plots showing Residual Plots for lny i.e., Normal probability plot of the residuals, residuals versus the order of the data, Histogram of the residuals, Residuals versus the fitted values of decolorization of Acid red 13 solution using *E. burkholder*

The normal Probability plot explains whether the obtained data follows the normality distribution and the obtained data of the experiments form a good fit since the residuals obtained, form nearly a straight line. Histogram of the residuals graph show the number of experiments that corresponding to the residual obtained and when the frequency is joined by a straight line, it follows a bell curve with a very less standard deviation, which explains it as a good fit. The remaining two graphs explain the vertical deviations of the residuals with the corresponding x axes.

4.7 Decolorization of Acid red 13 Using Yeast *Pichia pastoris*

The experiments were performed in the conditions that are mentioned in the below observation table. The percentage decolorization is calculated and is mentioned in the Table 4.11 shown below.

Table 4.11 Experimental matrix and percetage decolorization calculations

S.no	Model Parameter using CCD				% Decolorization determined by performing Experiment	
	Concentration(c) (mg/L)	pH (p)	Inoculum dosage(C) (%v)	Methanol(D) (ml)	In Control flask	In microbial flask
1	184.09	7	10	10	0.64	61.03
2	15.91	7	10	0	10.81	82.71
3	150	10	5	5	7.97	86.28
4	184.09	7	10	0	0.64	45.59
5	50	4	5	0	9.59	85.32
6	100	7	10	10	8.22	36.17
7	50	4	5	5	9.59	86.18
8	100	1.95	10	0	8.22	61.06

9	15.91	7	10	10	10.81	87.13
10	100	7	10	10	8.22	36.17
11	100	7	18.4	18.4	8.22	95.43
12	100	7	10	0	8.22	69.89
13	100	7	10	10	8.22	36.17
14	150	4	15	0	7.97	52.45
15	100	1.95	10	10	8.22	66.04
16	100	7	1.5	0	8.22	56.36
17	50	4	15	15	9.59	90.76
18	100	7	1.5	1.5	8.22	41.72
19	100	7	10	0	8.22	69.89
20	150	10	5	0	7.97	85.27
21	50	10	5	5	9.59	75.28
22	150	4	5	0	7.97	29.47
23	50	10	15	0	9.59	76.39
24	100	7	18.4	0	8.22	68.32
25	150	4	15	15	7.97	47.29
26	100	7	10	0	8.22	69.89
27	50	10	15	15	9.59	79.18
28	100	7	10	0	8.22	69.89
29	50	4	15	0	9.59	77.71
30	150	4	15	0	7.97	52.45

31	150	10	15	15	7.97	84.42
32	150	4	15	0	7.97	52.45
33	150	10	15	0	7.97	87.55
34	100	7	10	0	8.22	69.89
35	100	7	10	0	8.22	69.89
36	100	12.04	10	0	8.22	81.62
37	50	10	5	0	9.59	68.92
38	150	4	5	5	7.97	60.81
39	150	4	15	0	7.97	52.45
40	100	12.04	10	10	8.22	87.99

4.7.1 Response surface methodology

To fit the response and calculate the percentage decolorization, a regression analysis was done using the results. The model equations (4.7) and (4.5) were obtained from Design expert 7 software.

When the content of methanol added to the culture is low i.e., the volume added is 0 ml,

$$y = 181.74 - 1.13 \times c - 16.4 \times p - 2.4 \times C + 0.08 \times cp + 0.000385 \times cC + 0.02 \times pC + 0.002 \times c^2 + 0.74 \times p^2 + 0.14 \times C^2 \quad (4.7)$$

When the content of methanol added to the culture is high i.e., its volume is equal to the volume of the inoculum added,

$$y = 170.15 - 1.1 \times c - 16.4 \times p - 1.84 \times C + 0.08 \times cp + 0.0004 \times cC + 0.022 \times pC + 0.002 \times c^2 + 0.74 \times p^2 + 0.14 \times C^2 \quad (4.8)$$

Table 4.12 ANOVA for decolorization of Acid red 13 using P. pastoris

	Sum of Squares	Degreed of Freedom	Mean Square	F-value	p-value
Model.	8011.07	12	667.59	4.41	0.0007
c	1653.86	1	1653.86	10.92	0.0027
p	1250.91	1	1250.91	8.26	0.0078
C	605.89	1	605.89	4	0.0557
D	98.28	1	98.28	0.65	0.4276
cp	2344.5	1	2344.5	15.48	0.0005
c*C	0.15	1	0.15	0.000978	0.9753
c*D	13.96	1	13.96	0.092	0.7637
p*C	1.8	1	1.8	0.012	0.9141
C*D	53.41	1	53.41	0.35	0.5576
c^2	685.94	1	685.94	4.53	0.0426
p^2	1280.93	1	1280.93	8.46	0.0072
C^2	370.67	1	370.67	2.45	0.1294
Residual	4089.7	27	151.47		
Lack of fit	3692.14	17	217.18	5.46	0.0047
Pure error	397.56	10	39.76		
Total	12100.76	39			

From ANOVA table shown as Table 4.12, we can observe that the linear terms of the equation along with the squares of the linear terms and their interaction terms were found significant except AD and C^2. The Model F value of 4.41 suggests that the model is significant. There is only a 0.07% probability of this high "Model F-Value" could happen because of noise. The

model had an R^2 value of 96.2% which explains that the experimental results were found to be agreeing satisfactorily with the model results. The optimum values of the degradation reaction of the dye were found out and they are, A of 50.03 mg/L, B of 4, C of 15 %v and D of 15 ml. The experimental validation yielded decolorizing percentage of 85. The graphical representation of the model is shown as the surface plots and the contour plots from Fig. 4.40. The plots were obtained at the hold value of low methanol content added along with other hold value as mentioned in the figure.

The experimental validation yielded decolorizing percentage of 90.4.

The residual plots of the runs for decolorization of Acid red 13 using *P. pastoris* are shown in Fig. 4.41.

Figure 4.40 (a) Contour plot of B vs A (b) Surface plot of B vs A (c) Contour plot of C vs B (d) Surface plot of C vs B (e) Contour plot of C vs A (f) Surface plot of C vs A

a

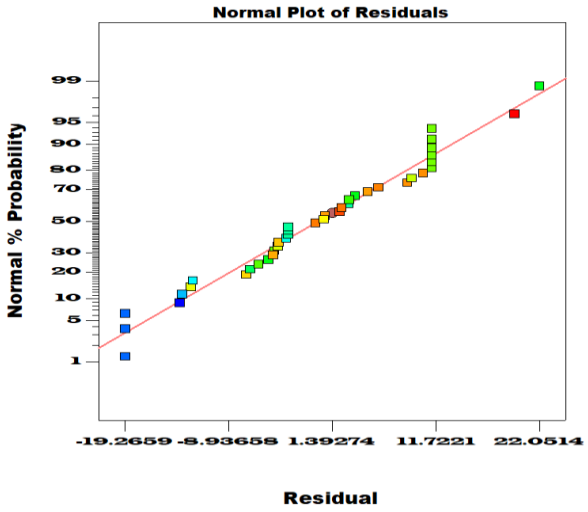

b

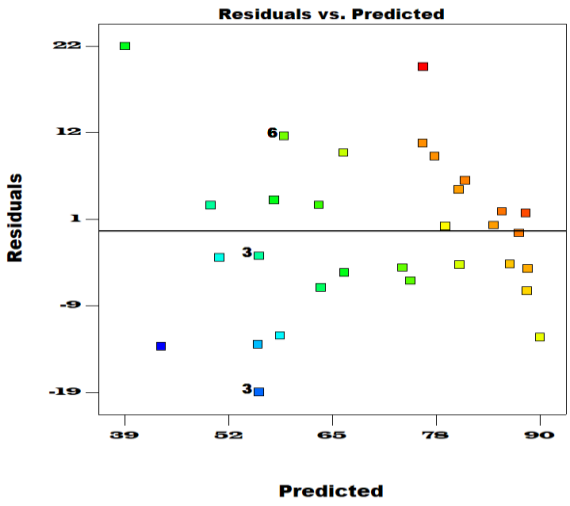

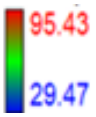

(a) Hold value: Inoculum Dosage (%v)=10 (b)

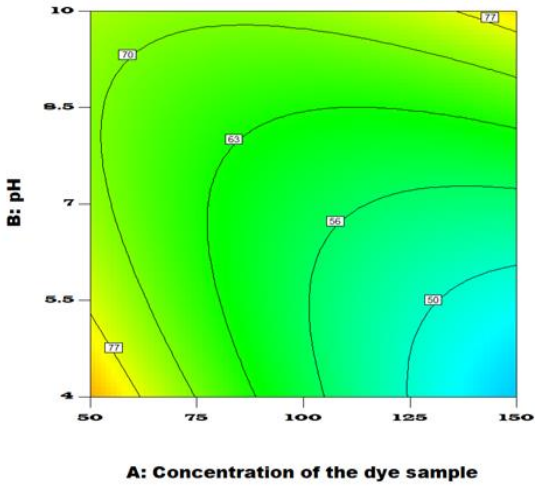

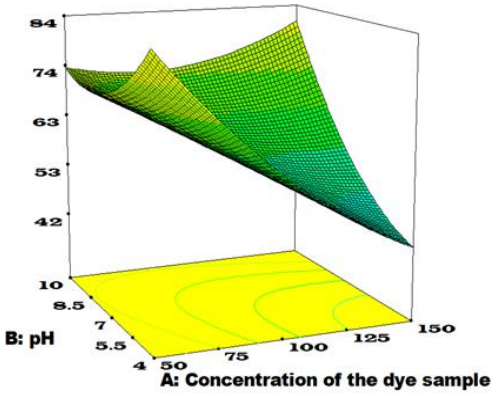

(c) Hold value: Concentration of the dye sample (mg/L)=100 (d)

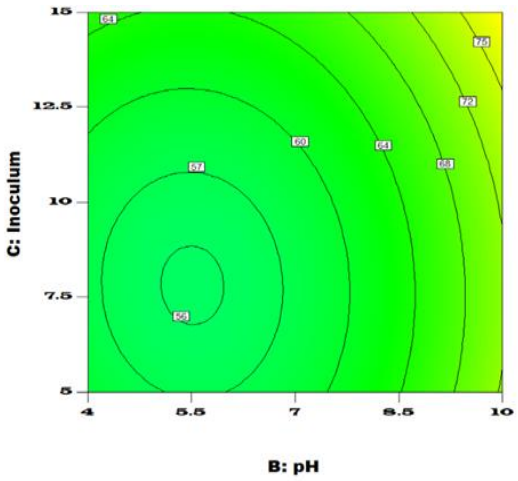

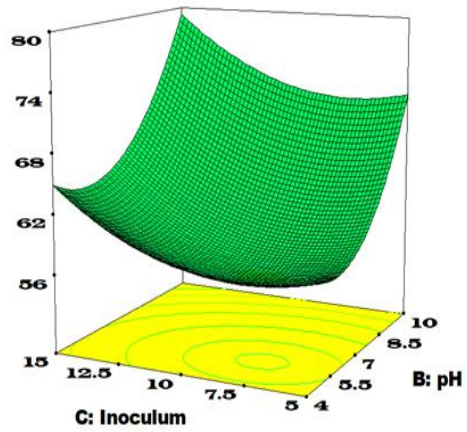

(e) (f)

Hold value: pH=7

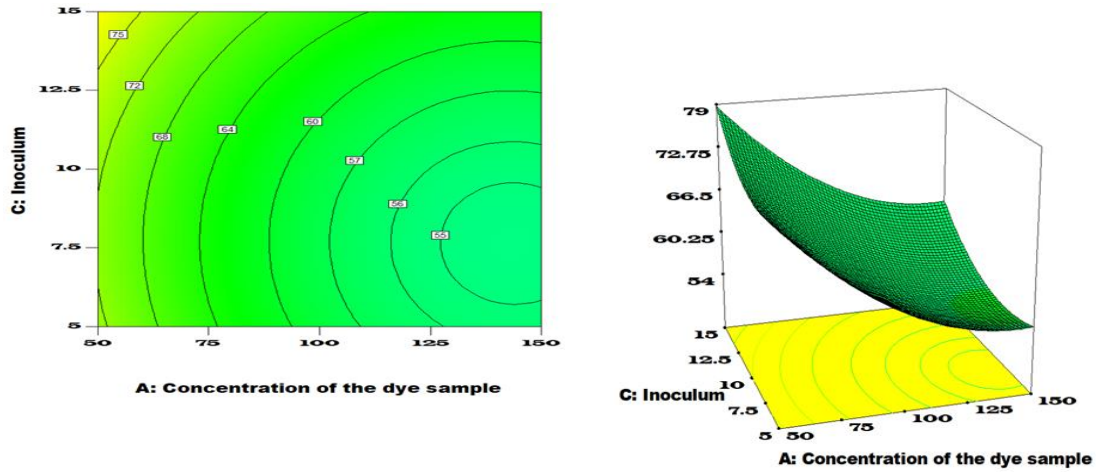

c d

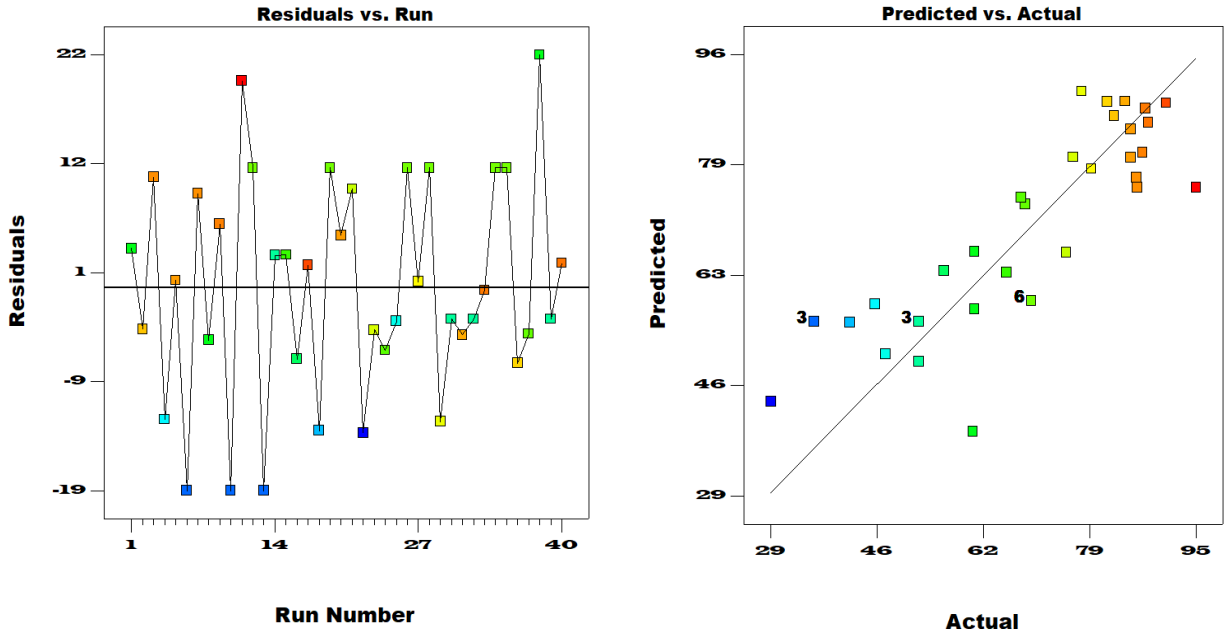

Figure 4.41 Residual plots of decolorization of Acid red 13 solution using *P. pastoris* (a) Normal Plot of residuals (Normal % Probability vs Residuals) (b) Residuals vs Predicted (c) Residuals vs Run (d) Predicted vs Actual

The optimum values of the degradation reaction of the dye were found out (shown as Fig. 4.42) and are c of 50.01 mg/L, p of 4, C of 15 %v.

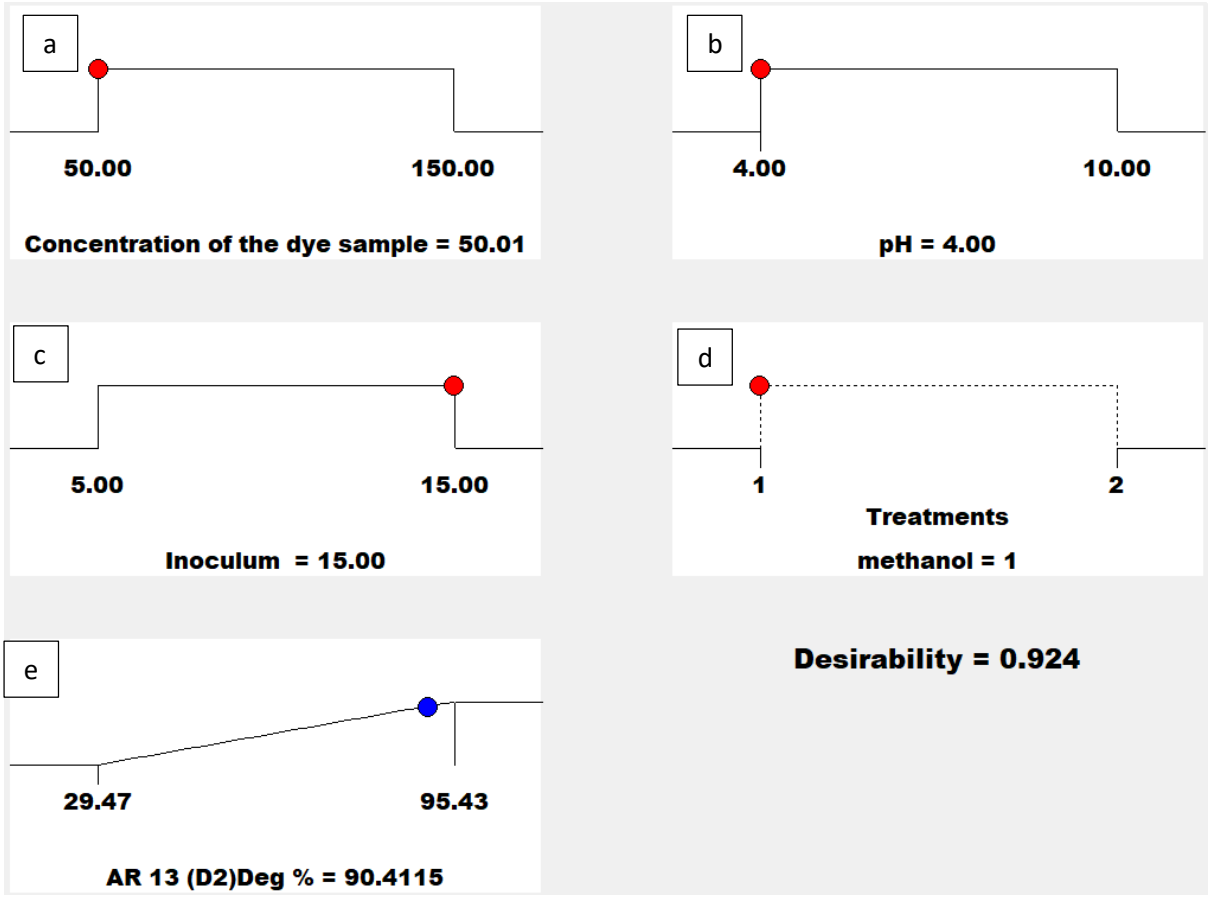

Figure 4.42 For Acid Red 13, Optimal values required for (a) concentration of the dye sample to take (b) pH (c) dosage of inoculum needed (d) Methanol required (e) Decolorization of dye obtained at given optimal conditions

4.7.2 Biodegradation analysis

FTIR was used to analyse samples before and after decolorization and FTIR analysis is shown as Fig. 4.43.

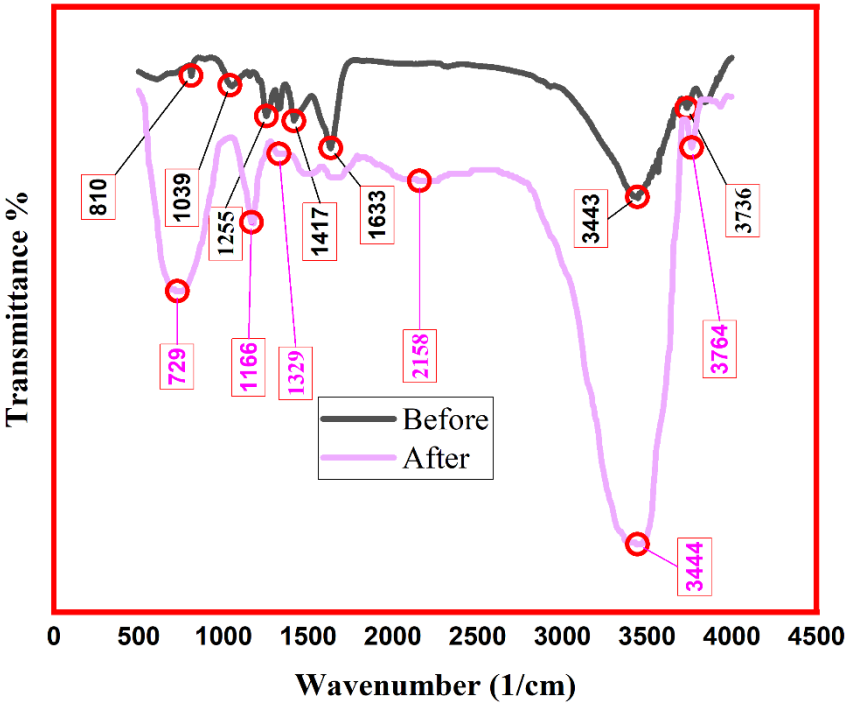

In Figure 4.43 FTIR spectrum of decolorization of Acid red 13 solution using *P. pastoris*: before and after microbial degradation

Before decolorization in Fig. 4.23, 1326 cm^{-1} for the Methyne CH bend and 810 cm^{-1} for the para disubstituted aromatic ring and 1039 cm^{-1} for primary amine i.e., CN stretch and 1255 cm^{-1} for aromatic primary amine CN stretch and 1417 cm^{-1} for vinyl CH and 1633 cm^{-1} for the presence of azo bond, the wavenumber 2929 cm^{-1} corresponded to the presence of methyl CH asymmetric bonds and peak at 3443 cm^{-1} with broad peak corresponding to OH group. The range from 3443-3736 cm^{-1} has a lot of disturbances as small peaks which all correspond to the alcoholic group along with peak at 3840 cm^{-1} may correspond to ONa group. Whereas after decolorization, the peak at 729 cm^{-1} may correspond to the new bond Thioether (CH_3-S-) and 1166 cm^{-1} for primary amine i.e., CN stretch and 1329 cm^{-1} for phenol and a small peak at 2158 cm^{-1} may correspond to the formation of new bond which might be thiocyanate ion and peak at 3444 cm^{-1} with broad peak corresponding to OH group and 3764 cm^{-1} with medium sharp peak corresponds to OH. So, it might be ONa group. There is no peak for azo bond for the after decolorization curve. Hence the azo bond is completely reduced after decolorization along with the formation of some new bonds.

4.7.3 Experimental Validation

The regression models were used to compare the experimentally validated optimal values of both the dyes. The variation in the experimental and model values was less than 10% which can be considered to be acceptable. Table regarding the depiction of error of degradation is briefly shown. In Table 4.13.

Table 4.13 Error between optimized model and experimental values

					% decolorization		
Dye	Concentration of Dye solution (mg/L)	pH	Inoculum Dosage (%v)	Methanol (ml)	model value	Expt. value	error %
Acid red 13	50	4	15	0	90.4	85.0	6.0

4.7.4 Toxicity studies

Dyes decolorized by microbes when compared to those of seedlings treated with water, were substantially higher than the seedlings treated with the dye simulated water. Many researchers like (Jadhav et al., 2011) have suggested using bioassays such as phytotoxicity to consider the hazardous impacts of dyes and their treated samples on plants. Furthermore, seedlings grown with dye and effluents had shorter plumule and radicle lengths than seeds grown with pure water. The dyes were harmful to these plants, but the metabolites generated after microbial degradation was less harmful, indicating that the dyes were detoxified by *Pichia Pastoris*. These outcomes mention the significance of yeast for bioremediation of dye as decolorization and detoxification. Biodegradation results in the development of simpler, harmless chemicals. With the formation of reasonably mild toxic sludge, this procedure of biodegradation is more cost-effective (Krishnan et al., 2017).

After 48 hours, the decolorization rate of dyes decolorized by *Pichia pastoris* reached approximately 90%. Phytotoxicity Table 4.14 show that both the dyes have different biological characteristics of the considered agricultural seeds when compared to water-treated seedlings.

Table 4.14 Phytotoxicity of Acid red 13 solution, their metabolites formed after degradation by microbe

The tabled values taken are mean of 10 seeds in 3 sets SEM (±). Spinacia oleracea seeds grown in Acid red 13 are not dissimilar from the seeds grown in pure water at *P<0.05, **P<0.001.

		Germination %	plumule(cm)	Radical(cm)
Spinacia Oleracea	Distilled water	100	2.56±0.1	1.22±0.3
	Dye	20	0.25*±0.18	0.25**±0.17
	Metabolites	90	1.86*±0.23	1.47±0.25
Capsicum Frutescens	Distilled water	100	2.4±0.06	3.45±0.34
	Dye	20	$0.46^{@}$±0.3	$0.22^{@@}$±0.15
	Metabolites	80	$1.32^{@@}$±0.06	$0.84^{@@}$±0.24
Trigonella Foenum	Distilled water	100	3.22±0.2	7.46±0.73
	Dye	30	$0.92^{\#}$±0.5	$1.01^{\#\#}$±0.5
	Metabolites	90	$4.35^{\#}$±0.6	$1.47^{\#\#}$±0.25

Capsicum frutescens kernels grown in Acid Red 13, as well as metabolites of the treated water are not dissimilar from those grown in pure water at @P<0.05 and @@P<0.001. Trigonella foenum seeds grown in Acid red 13, as well as metabolites of the treated water are not dissimilar from those grown in pure water at #P<0.05 and ##P<0.001 using 1-way ANOVA with Tukey Kramer analysis.

Decolorization comparisons

In the following studies, the decolorizing efficiencies of both bacteria on biodegradation are compared along with the comparison of decolorization rates of bacteria to yeast.

4.8 Comparison Between Bacterial Decolorization

In the Fig. 4.44 shown below, when the bacterial decolorizations of D1 were compared in a Box-Whisker plots and the balance picture showing the average decolorization, we can clearly see that, NM1 has a better impact in decolorization when compared to the decolorization with NM2. It is since, the enzyme β-galactosidase produced NM1 cleaves the bond to produce glucose and energy (Saqib et al., 2017) hence reduces the activation energy required for the reaction to take place.

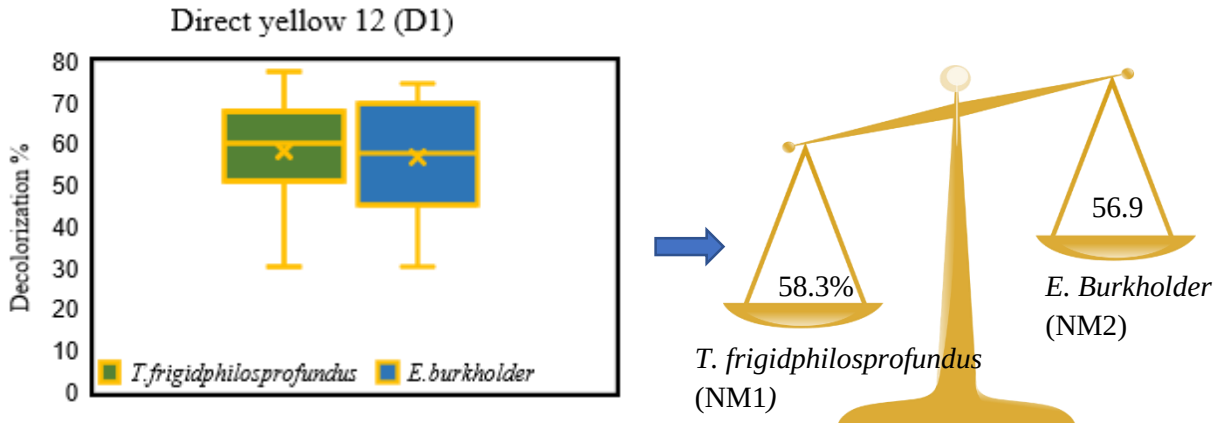

Figure 4.44 Comparison of decolorizing efficiencies of both the bacteria on Direct yellow 12

In the Fig. 4.45 shown below, when the bacterial decolorizations of D2 were compared in a Box-Whisker plots and the balance picture showing the average decolorization, we can clearly see that, NM2 has a better impact in decolorization when compared to the decolorization with NM1. A possible explanation is that, NM1 is an aerobic bacterium whereas NM2 is facultatively anaerobic (Kaneshiro et al., 2008) and the results indicate that degradation of the dye Direct yellow 12 takes place at a higher rate with an aerobic microbe when compared to the facultatively anaerobic microbe. A possible explanation for it could be that NM2 thrives mostly in the temperature range of 27°C and 30°C and many experiments were done out of this range. Moreover, the anaerobes cleave the azo bond in forming the aromatic amines whereas cleaving by aerobes is less when compared (Van Der Zee & Villaverde, 2005).

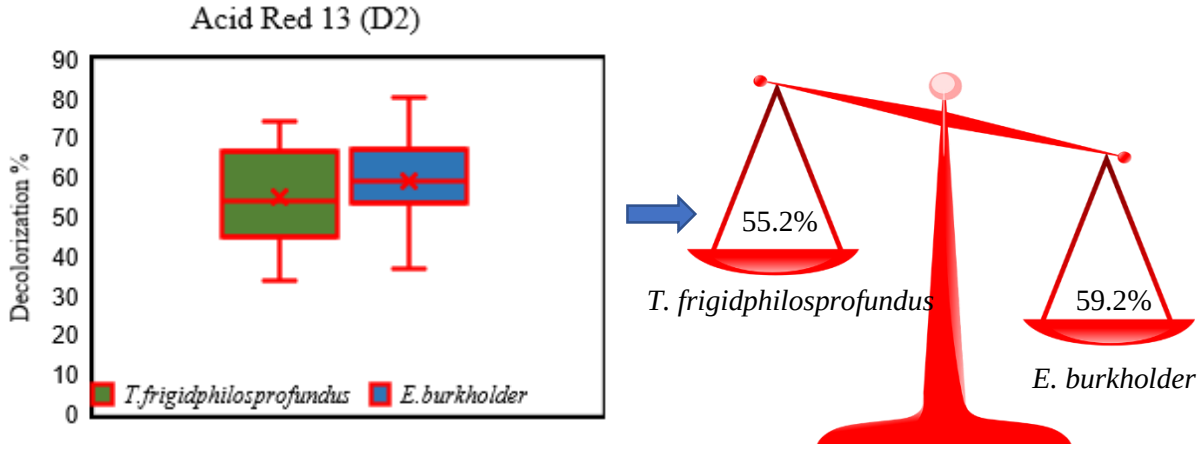

Figure 4.45 Comparison of decolorizing efficiencies of both the bacteria on Acid red 13

4.7 Decolorization comparison between bacteria and yeast

Now, when the decolouration rates of bacteria and yeast are compared (using percentage change in COD values), yeast has more fruitful percentage change than with the bacteria.

For Biodegradation of Direct yellow 12, Table 4.15 shows the values of COD and BOD of D1 before decolorization using microbes and after decolorization. In the Fig. 4.46 shown below, and from the values of Table 4.15, the biodegradation by yeast is higher when compared with that of bacteria.

Table 4.15 COD , BOD value of microbial decolorization of Direct yellow12

Microbe	Initial		Final	
	COD	BOD	COD	BOD
T. Frigidphilosprofundus	621	448	117.99	169.11
E. Burkholder	621	448	135.71	195.57

P. pastoris	621	448	92.11	121.47

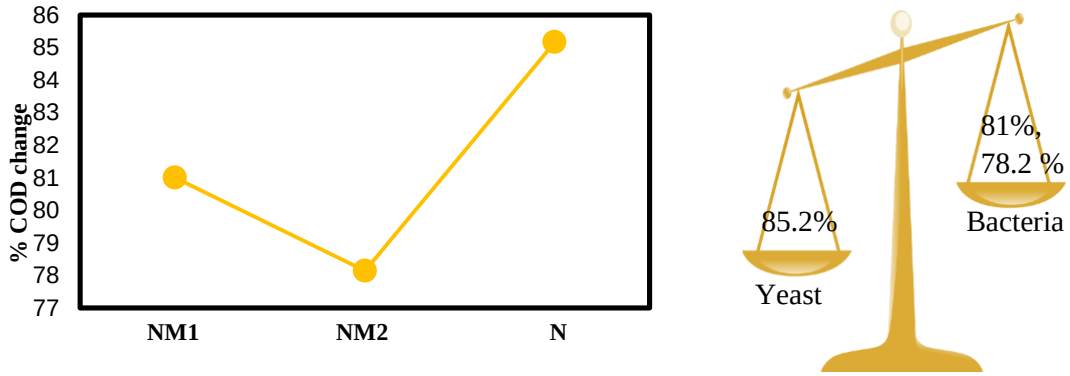

Figure 4.46 Comparison of %COD value changes of bacteria and yeast on Direct yellow 12

For biodegradation of Acid red 13, Table 4.16 shows the values of COD and BOD of D1 before decolorization using microbes and after decolorization.

Table 4.16 COD , BOD value of microbial decolorization of Acid red 13

	Initial		**Final**	
Microbe	COD	BOD	COD	BOD
T. Frigidphilosprofundus	272	241.9	84.41	98.71
E. Burkholder	272	241.9	72.1	81.54
P. pastoris	272	241.9	52.2	58.14

In the Fig. 4.47 shown below, from the values of table 8, the biodegradation by yeast is higher when compared with that of bacteria.

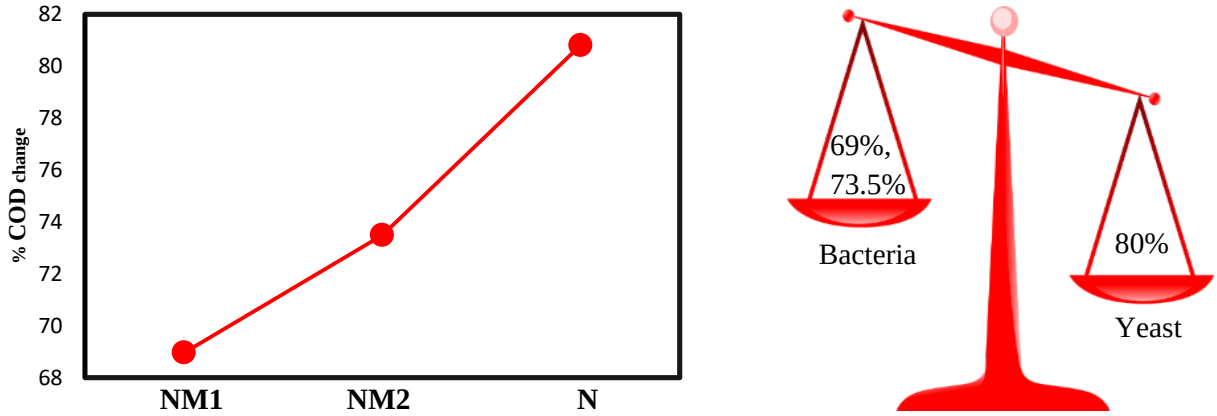

Figure 4.47 Comparison of %COD value changes of bacteria and yeast on Acid red 13

4.9 Kinetics of Bacterial Decolorization

4.9.1 For Direct yellow 12

The Kinetics of Biodegradation followed Hanes Woolf Plot, whose equation is stated below as equation (4.9)

$$\frac{S}{V} = \frac{K_m}{V_m} + \frac{1}{V_m} S \qquad (4.9)$$

The kinetic values of degradation by NM1 are shown in the Table 4.17 given below

Table 4.17 Kinetic constants for the experimental studies of microbial decolorization of D1

	D1	
	V_m (mg/L.h)	**K_m (mg/L)**
T. frigidphilosprofundus	1.72	28.05
E. burkholder	1.59	26.33

4.9.2 For Acid red 13

The kinetics of Biodegradation followed Eadie Hofstee plot, whose equation is stated below

$$V/S = V/K_m + V_m/K_m \quad (4.10)$$

The kinetic values of degradation by NM1 are shown in the Table 4.18 given below

Table 4.18 Kinetic constants for the experimental studies of microbial decolorization of D2

	D2	
	V_m (mg/L.h)	**K_m (mg/L)**
T. frigidphilosprofundus	1.308	20.204
E. burkholder	1.801	25.35

4.10 Kinetics of Yeast Decolorization

A double-reciprocal plot gives good estimates on V_m, but not necessarily on K_m.

- ✓ Eadie–Hofstee plots can be subject to large errors since both coordinates contain V, but there is less bias on points at low [S].
- ✓ Hanes Woolf plot is used to determine V_m more accurately

Hence The final constants were calculated by using these plots and tabled below as Table 4.19

Table 4.19 Kinetic constants for the experimental studies of yeast decolorization of Direct yellow 12 and Acid red 13

	V_m (mg/L.h)	**K_m (mg/L)**
For Direct yellow 12	1.78	57.14
For Acid red 13	0.83	3.98

Immobilization of Activated Carbon

The activated carbon that is fabricated is immobilized with *P. pastoris* and then the decolorization process is improved by using this immobilized carrier particles in the bioreactors. The methods of fabrication and immobilization processes were explained in Material and Methods chapter.

Decolorization experiments in Reactors

From the results of free cell mediated approach, it was clearly evident that among bacterial decolorization and decolorization using yeasts, the latter has given the more fruitful results when compared with the former. Henceforth, the biodegradation studies in the reactors were done using the yeast *P. pastoris* at about closer to same conditions (concentration of dye in the solution and pH maintained) of the optimum decolorization obtained in free cell mediated approach.

Approach 2

An approach using bioreactors

4.11 Batch Reactor Tank Experiments

Experiments were done for the decolorization of the synthetic solutions made of Direct yellow 12 (D1) and Acid red 13 (D2). Immobilized activated carbon was used for adsorption-degradation experiments in the Batch reactor tank. For D1 biodegradation experiments c of 200 mg/L, Inoculum dosage of 20 mg/L, pH of 6, and temperature were maintained at 28°C is shown as Fig. 4.48 and for D2 biodegradation experiments, c of 50 mg/L, inoculum dosage of 20 mg/L, pH of 6, and temperature were maintained at 28°C it is shown in Fig. 4.49. Following images show the decolorization timeline in the reactor (BRT).

(a) At t=0 h (b) At t=48 h

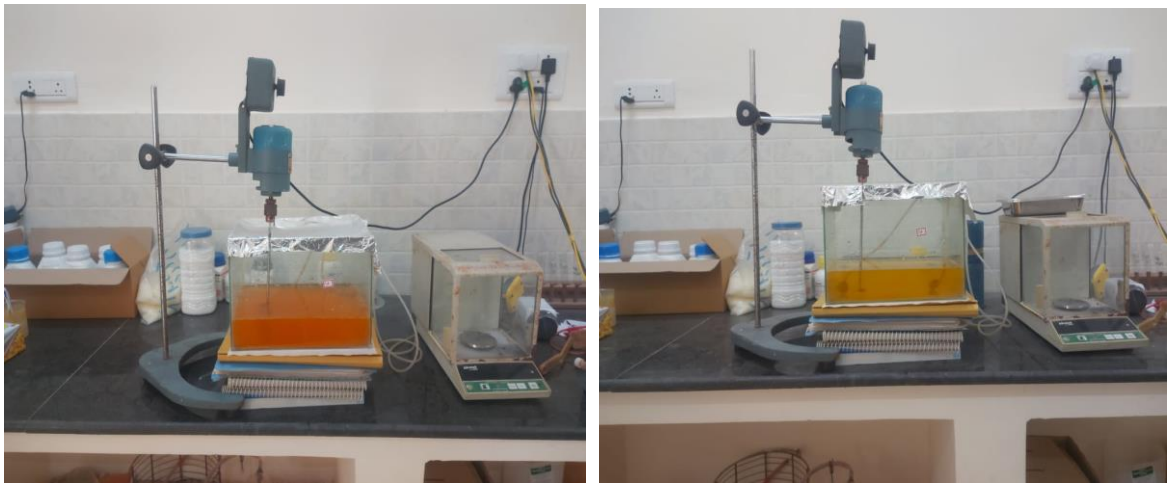

Figure 4.48 Decolorization of Direct yellow 12 in a BRT

(a) At t=0 h (b) At t=48 h

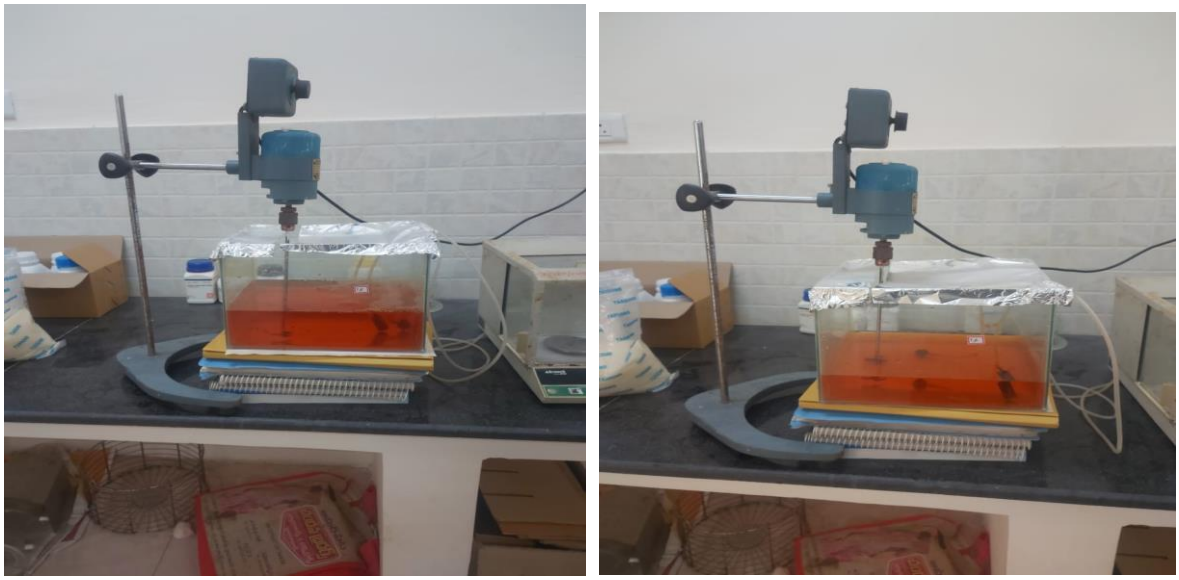

Figure 4.49 Decolorization of Acid red 13 in a BRT

4.12 Fluidized Bed Bioreactor Experiments

Experiments were done for the decolorization of the synthetic solutions made of D1 and D2. Immobilized activated carbon was used for adsorption-degradation experiments in the Fluidized Bed Bioreactor (FBBR). Following figure shows a run of D1 in a Fluidized Bed Bioreactor. Fig. 4.50 shown below displays the FBBR that is used for the biodegradation experiments

Figure 4.50 Fluidized bed Bioreactor used for biodegradation experiments

Following images show the decolorization timeline in the reactor. For D1 biodegradation experiments c of 200 mg/L, Inoculum dosage of 20 mg/L, pH of 6, and temperature were maintained at 28°C is shown as Fig. 4.51 and for D2 biodegradation experiments, c of 50 mg/L, inoculum dosage of 20 mg/L, pH of 6, and temperature were maintained at 28°C it is shown in Fig. 4.52.

(a) At t=0 h

(b) At t=48 h

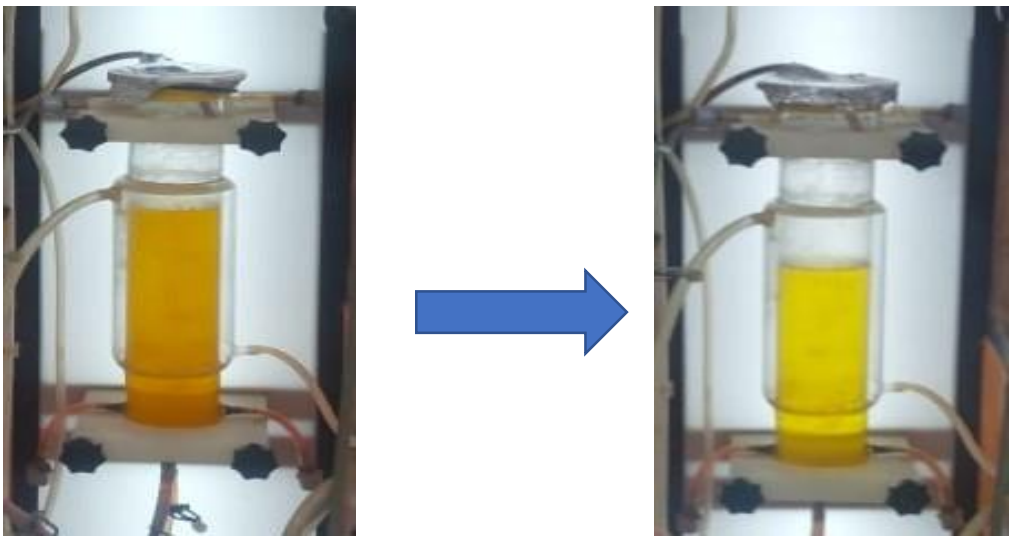

Figure 4.51 Decolorization of Direct yellow 12 in a FBBR

(a) At t=0 h

(b) At t=48 h

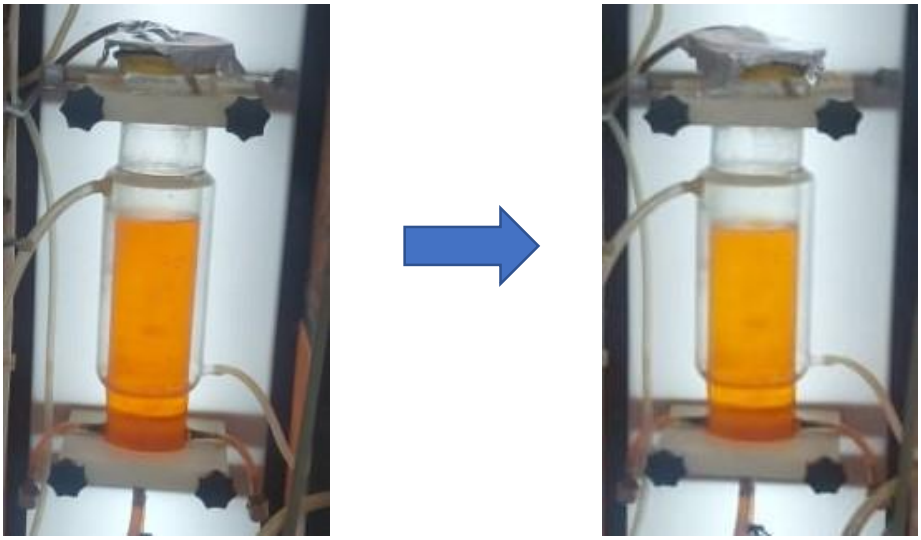

Figure 4.52 Decolorization of Acid red 13 in FBBR

4.13 Comparison of Decolorization Rates in BRT with FBBR

4.13.1 For Decolorization of Direct yellow 12 in Bioreactors

For Direct Yellow 12 solution, after performing experimental studies, the results were tabled as below as Table 4.20.

Table 4.20 Experimental studies of decolorization of D1 in both reactors

Adsorbent studies (C=150 mg/L, pH=7, T=28°C)						
Dosage		10 mg/L	20 mg/L	30 mg/L	40 mg/L	50 mg/L
y (% decolorization)	FBBR	87.61	85.88	91.89	89	91.43
	BRT	76.27	54.28	78.35	84.26	80.09
Concentration studies (pH=7, T=28°C, dosage=30 mg/L)						
Concentration		100 mg/L	125 mg/L	150 mg/L	175 mg/L	200 mg/L
y (% decolorization)	FBBR	59.672	81.044	89.157	83.211	74.646
	BRT	72.623	82.388	82.812	81.121	66.509
pH studies (C=150 mg/L, T=28°C, dosage=30 mg/L)						
pH		5	6	7	8	9

y (% decolorization)	FBBR	77.13068	70.17045	92.1875	77.69	9.86
	BRT	71.733	68.04	77.13	66.05	78.977

The following graphs shown as Fig. 4.53 were obtained for the respective studies.

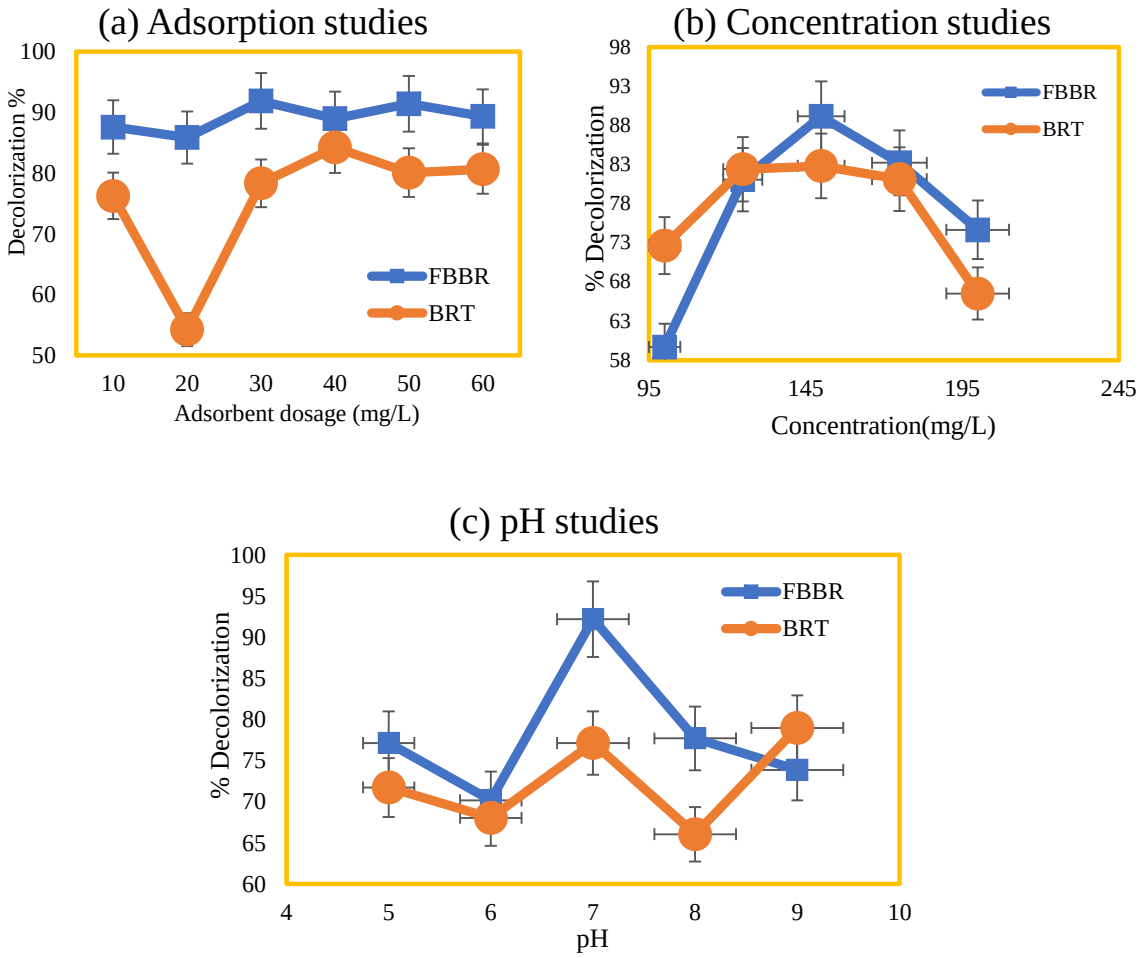

Figure 4.53 Comparison of decolorization rates in Batch reactor tank with FBBR for Direct yellow 12

4.13.2 For Decolorization of Acid red 13 in Bioreactors

For Acid Red 13 solution, after performing experimental studies, the following results were obtained and shown as Table 4.21.

Table 4.21 Experimental studies of decolorization of D2 in both reactors

Adsorbent studies (C=50 mg/L, pH=7, T=28°C)						
Dosage		10 mg/L	20 mg/L	30 mg/L	40 mg/L	50 mg/L
y (% decolorization)	FBBR	60.515	59.461	74.985	81.89	55.18
	BRT	58.55	59.84	70.06	67.81	56.06
Concentration studies (pH=7, T=28°C, dosage=40 mg/L)						
Concentration		30 mg/L	50 mg/L	70 mg/L	90 mg/L	110 mg/L
y (% decolorization)	FBBR	89.51	84.51	78.15	79.64	72.76
	BRT	72.79	74.95	74.17	53.008	24.85
pH studies (C=50 mg/L, T=28°C, dosage=40 mg/L)						
pH		5	6	7	8	9
y (% decolorization)	FBBR	62.03	67.13	73.46	43.23	53.95
	BRT	69.42	53.602	45.52	20.21	17.39

The following graphs shown as Fig. 4.54 were obtained for the respective studies.

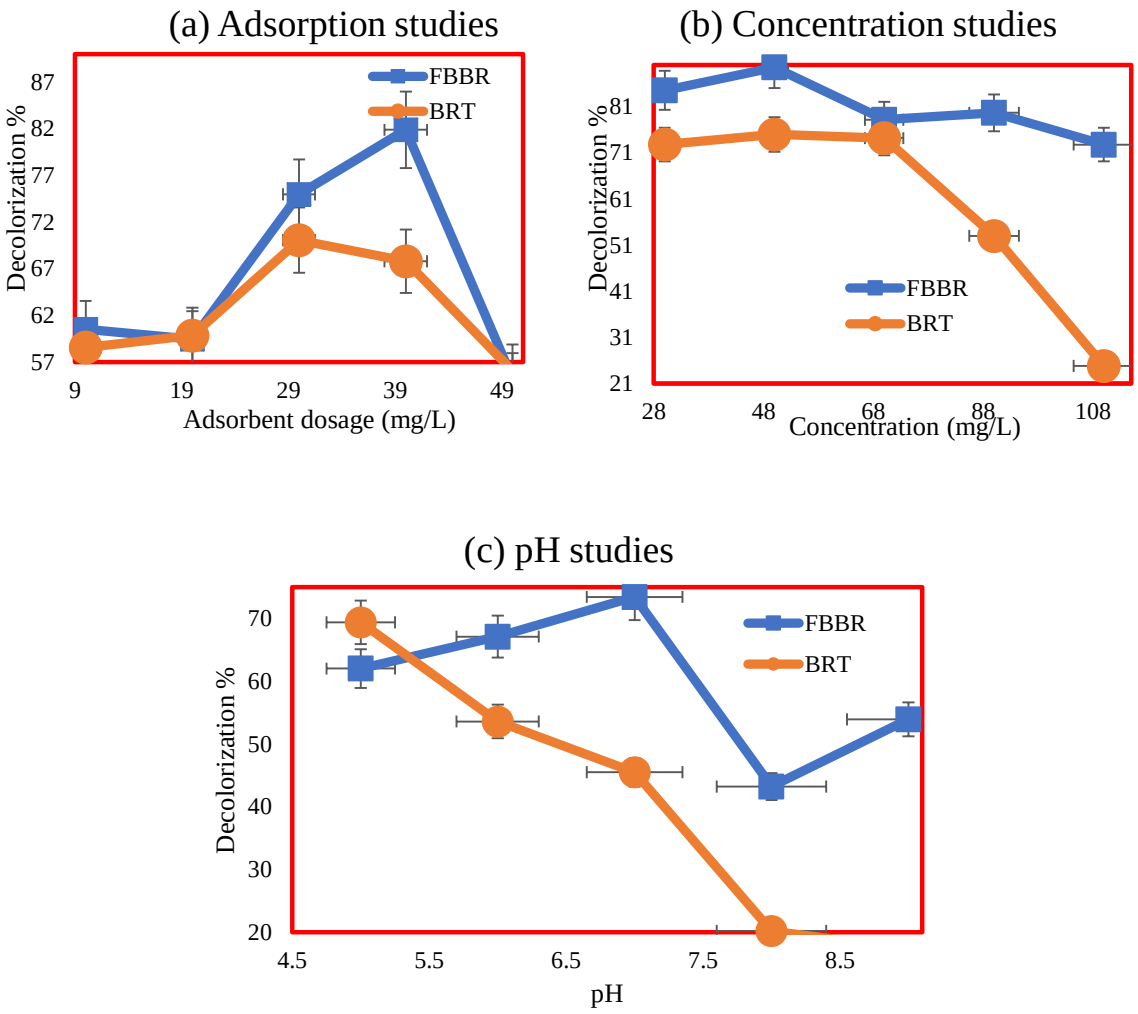

Figure 4.54 Comparison of decolorization rates in Batch reactor tank with FBBR for Acid red 13

- For Direct yellow 12, 73% and 90% respectively are obtained for BRT and FBBR at the conditions of C=150 mg/L, pH=7, T=28°C, adsorbent dosage of 30mg/L.
- For Acid red 13, 75% and 89.5% respectively are obtained for BRT and FBBR at the conditions of C=50 mg/L, pH=7, T=28°C, adsorbent dosage of 40 mg/L.

4.14 Toxicity studies

The discharge of untreated or insufficiently treated industrial effluent is the primary cause of contamination of ocean and river water quality. Hence the biological method of decolorization is employed in this study. Many studies have suggested using bioassays such as phytotoxicity to consider the hazardous impact of dyes and their treated samples on plants (Jadhav et al., 2011). Furthermore, seedlings grown with dye and effluents had shorter gemule and radicle

lengths than seeds grown with pure water. The dye was harmful to these plants, but the metabolites generated after microbial degradation was less harmful, indicating that the dyes were detoxified by *Pichia pastoris*. These outcomes mention the significance of yeast for bioremediation of dye as decolorization and detoxification. Biodegradation results in simpler and harmless chemicals as by-products. With the formation of reasonably mild toxic sludge, biodegradation is considered to be a cost-effective one.

Both the dyes and their metabolites are assessed for toxicity by conducting phytotoxicity experiments on the agricultural seeds, (i) *Spinacia oleracea* (ii) *Capsicum frutescens* (iii) *Trigonella foenum*. Each crop's ten seeds were planted independently in a plastic vessel with 50 g clean and oven dry sand. The toxicity test was carried out by spraying 5 ml of Dye solutions and their metabolites daily for 14 days at 28°C. For comparison, distilled water was sprayed on the plant seed samples under similar conditions. Germination (%), length of gemule, length of the roots were noted after 14 days. Toxicity studies of the metabolites of D1 biodegradation from FBBR were done and the results are shown in Table 4.22. Dye decolorized by microbes when compared to those of seedlings treated with water, were substantially higher than the seedlings treated with the dye simulated wastewater.

Table 4.22 Phytotoxicity studies for decolorization of direct yellow 12 *using P.pastoris*

The values in Table obtained are the mean of 10 seeds in 3 sets Standard error of the mean (SEM) (±). Spinacia oleracea seeds grown in Direct yellow 12 are dissimilar from the seeds grown in pure water at *P<0.05, **P<0.05. Capsicum frutescens kernels grown in Direct yellow 12, as well as metabolites of the treated water are dissimilar from those grown in pure water at @P<0.005. Trigonella foenum seeds grown in Direct yellow 12, as well as metabolites of the treated water, are dissimilar from those grown in pure water at #P<0.05 and ##P<0.005 using1-way ANOVA with Tukey Kramer analysis.

Toxicity studies for Direct yellow 12		Germination (%)	Gemule (cm)	Radical (cm)
Spinacia Oleracea	Distilled water	100	2.58±0.08	1.3±0.09
	Dye	30	0.3*±0.17	0.13*±0.08
	Metabolites	90	2.3##±0.27	1.16##±0.16
Capsicum Frutescens	Distilled water	100	2.4±0.06	3.33±0.35
	Dye	40	0.28*±0.13	0.37*±0.16
	Metabolites	80	1.87#±0.32	$2.52^{\#}$±0.52
Trigonella Foenum	Distilled water	100	3.13±0.15	7.46±0.73
	Dye	40	0.25*±0.13	0.47*±0.2
	Metabolites	80	2.72#±0.32	6.56##±0.96

Chapter 5

Mechanisms

Chapter 5

5. Mechanisms

The mechanisms of decolorizations of dyes by the action of *P. pastoris* in FBBR were obtained.

5.1 Adsorption Parameters

The processes' adsorption parameters were obtained from the below given isotherms Langmuir isotherm

- ✓ Freundlich isotherm
- ✓ Temkin isotherm

For each isotherm, the plots were drawn and results were tabulated.

5.1.1 Langmuir Isotherm

The following equation gives the Langmuir equation (equation (4.11))

$$C_e/\, q_e \;=\; 1/\, q_m K_L \;+\; C_e \,/\, q_m \qquad (4.11)$$

Langmuir plots shown as Fig. 5.1were obtained for Direct yellow 12 as Fig. 5.1(a) and for Acid red 13 as Fig. 5.1(b)

(a) Direct Yellow 12 (b) Acid Red 13

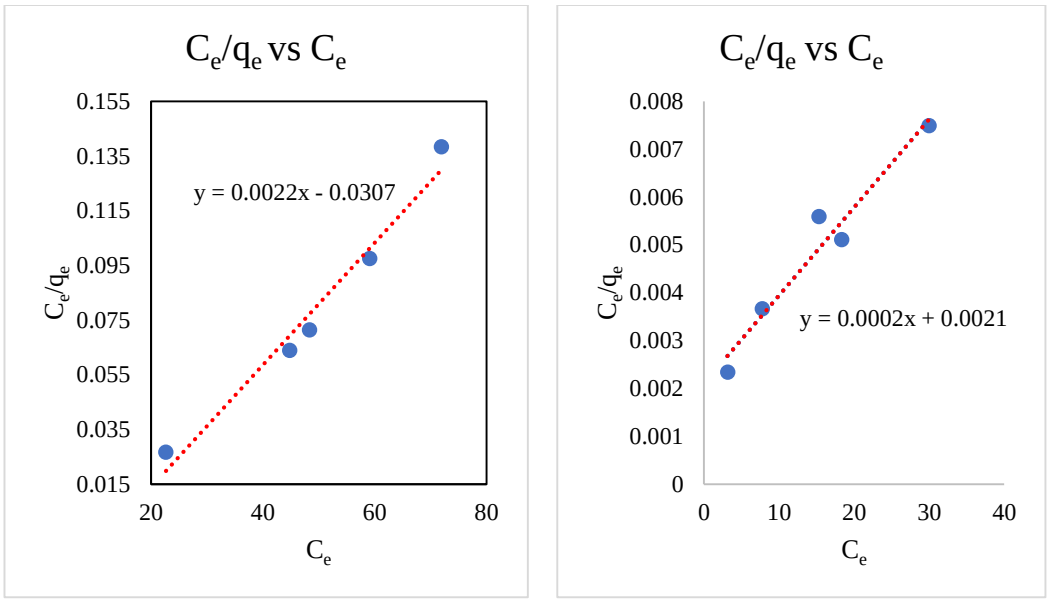

Figure 5.1 Langmuir plots

5.1.2 Freundlich Isotherm

The following equation gives the Freundlich equation (equation (4.12))

$$q_e = k_f C_e^n \qquad (4.12)$$

Freundlich plots shown as Fig. 5.2 were obtained for Direct yellow 12 as Fig. 5.2(a) and Acid red 13 as Fig. 5.2(b)

(a) Direct Yellow 12 (b) Acid Red 13

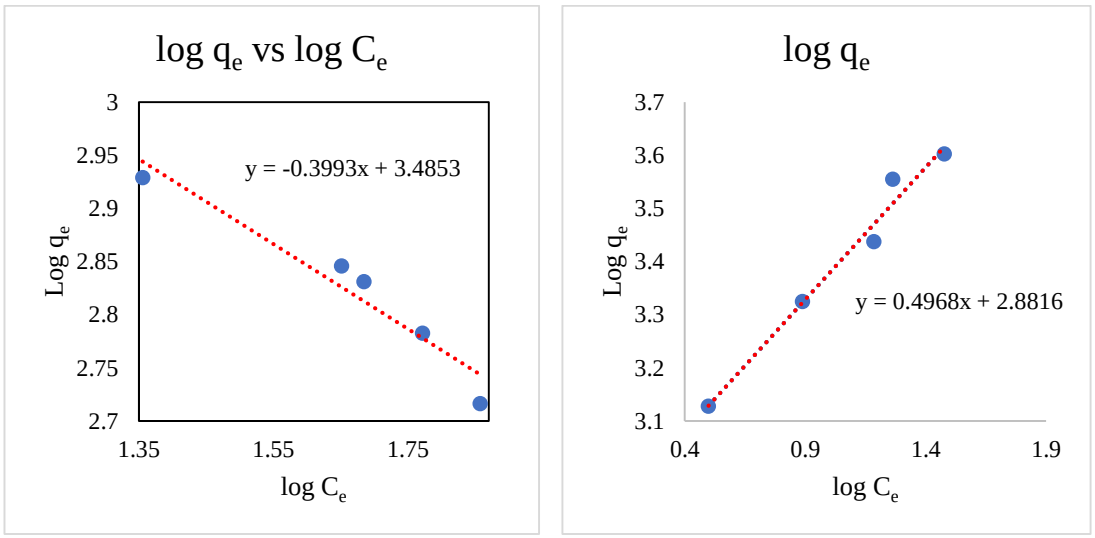

Figure 5.2 Freundlich plots

5.1.3 Temkin Equation.

The following equation gives the Temkin equation (equation (4.13))

$$q_e = B \ln C_e + B \ln A \quad (4.13)$$

Temkin plots shown as Fig. 5.3 were obtained for Direct yellow 12 as Fig. 5.3(a) and Acid red 13 as Fig. 5.3(b)

(a) Direct Yellow 12 (b) Acid Red 13

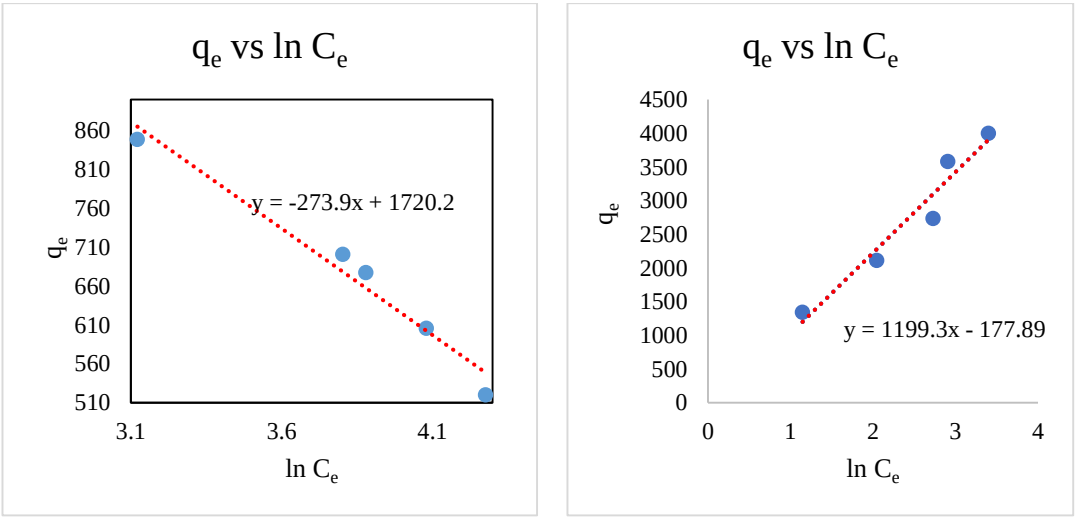

Figure 5.3 Temkin plots

The various adsorption constants were obtained from the above plots and are tabled as Table 5.1

Table 5.1 Adsorption constants using Languir, Freundlich, Temkin plots

	Langmuir			Freundlich			Temkin			
	q_M	K_L	R^2	n	K_f	R^2	B	A	K_T	R^2
Direct yellow 12 (D1)	454.545	0.0716	0.97	-2.5	30.5703	0.92	-273.9	0.0018	17.202	0.96
Acid red 13 (D2)	5000	0.095	0.9517	0.4968	761.37	0.9771	1199.3	0.8624	177.89	0.94

The following points can be discussed based on the table.

- ✓ For D1 biodegradation, R^2 of Langmuir plot is higher and is closer to 1 than other plots. Hence it best describes the uptake of D1 which implies that unimolecular adsorption is taking place whereas in D2 biodegradation, R^2 value of Freundlich plot is higher and is closer to 1 than other plots. Hence it best describes the uptake of D2
- ✓ The value of B from Temkin plot of D1 biodegradation has negative value. It means that the process is endothermic. Whereas, B value from Temkin plot has positive value. It means that the process is exothermic.
- ✓ A's value describes the attraction of sorbent material for dye and it is high for D2 rather than D1.

5.2 Pseudo Kinetics

Pseudo Kinetics of the biodegradation reactions were calculated from Pseudo 1st order, Pseudo 2nd order and Bangham kinetics for proposing the mehanisms.

5.2.1 Pseudo 1st Order

To study the Kinetics of the biodegradation reactions pseudo first-order, pseudo second-order, and Bangham equations were used. Pseudo first-order equation (4.14) is given below.

$$\log(q_e - q_t) = \log q_e - \frac{K_1}{2.303} t \qquad (4.14)$$

If the curve of $\log(q_e - q_t)$ versus t is a line, it can be said that pseudo first order can be applied in the finding the kinetics and it is obtained to be similar and is shown as Fig. 5.4. q_e and k_1 can be determined from the intercept and slope of the plot, respectively. Pseudo 1st order plot for D1 biodegradation is shown as Fig. 5.4(a) and for D2 is shown as Fig. 5.4(b).

(a) Direct yellow 12 (b) Acid red 13

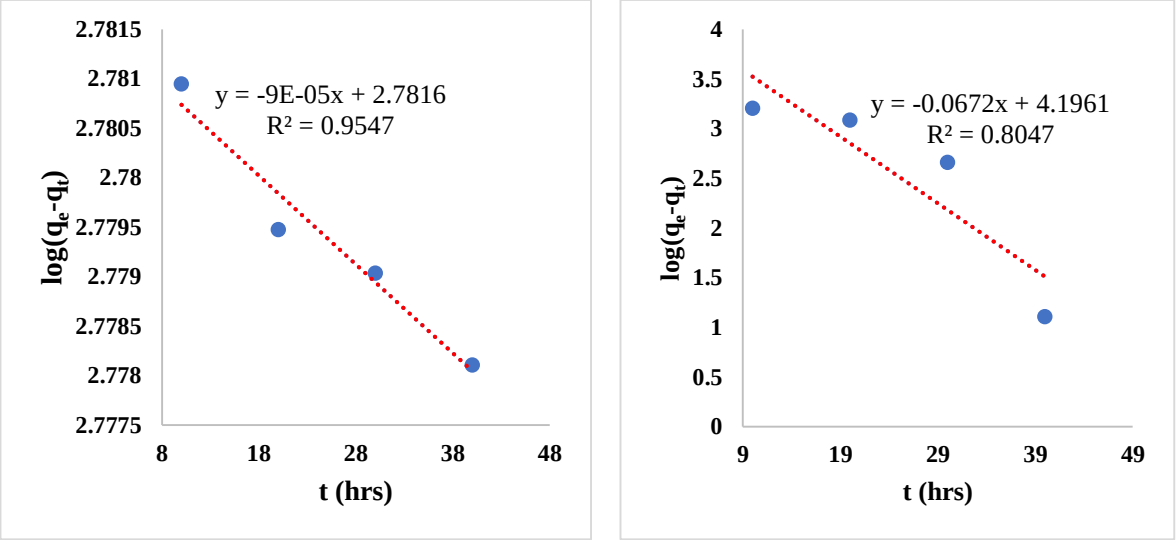

Figure 5.4 Pseudo 1st order plots

5.2.2 Pseudo 2nd Order

The pseudo-second order kinetics equation (4.15) is shown as below

$$\frac{t}{q_t} = \frac{1}{K_2 q_e^2} + \frac{1}{q_e} t \qquad (4.15)$$

The initial adsorption rate, h given below as equation (4.16)

$$h = k_2 q_e^2 \qquad (4.16)$$

If the curve of $\log(q_e - q_t)$ versus t is a line, it can be said that pseudo second order can be applied in the finding the kinetics. Pseudo 2nd order plot are obtained and is shown as Fig. 5.5. q_e, k_2 can be determined from the slope and intercept of the plot, respectively which are found from the following plots Fig. 5.5(a) and Fig. 5.5(b).

(a) Direct Yellow 12 (b) Acid Red 13

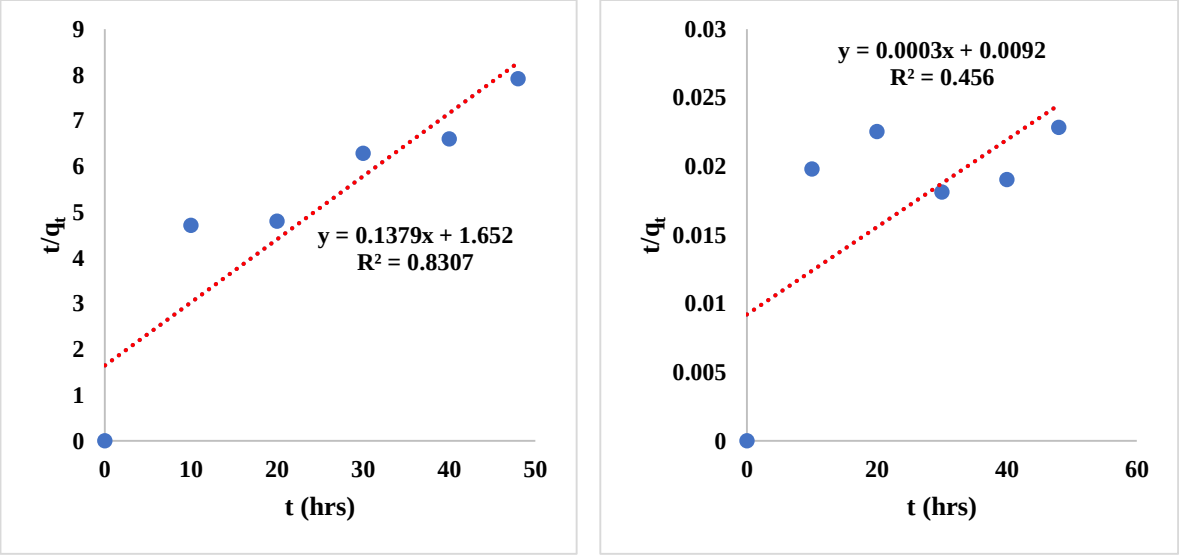

Figure 5.5 Pseudo 2nd order plots

The rationality of the kinetic models is known from the value of R^2 given. In the graphs that were obtained from the results of the experimental observations, D2 biodegradation is following pseudo second order kinetics to a very less extent when compared with D1 biodegradation since it is not closer to a straight line

For D2, the pseudo 1st order kinetic equation has the best fit to the experimental data compared with other kinetic adsorption models, since the calculated q_e is very near to the experimental q_e and its R^2 is higher than that of pseudo 2nd order model.

5.2.3 Bangham Kinetics

The data obtained can also be used to know whether the reaction taking place is a pore diffusion i.e., simple diffusion or facilitated diffusion using Bangham kinetics expression shown as below.

$$loglog\frac{C_0}{C_0 - q_t m} = log\frac{K_B m}{2.303v} + \alpha log t \qquad (4.17)$$

The plot for D1 biodegradation is obtained and shown as Fig. 5.6(a) whereas for Acid Red degradation, Bangham kinetics were not getting correlated.

(a) Direct Yellow 12	Acid Red13
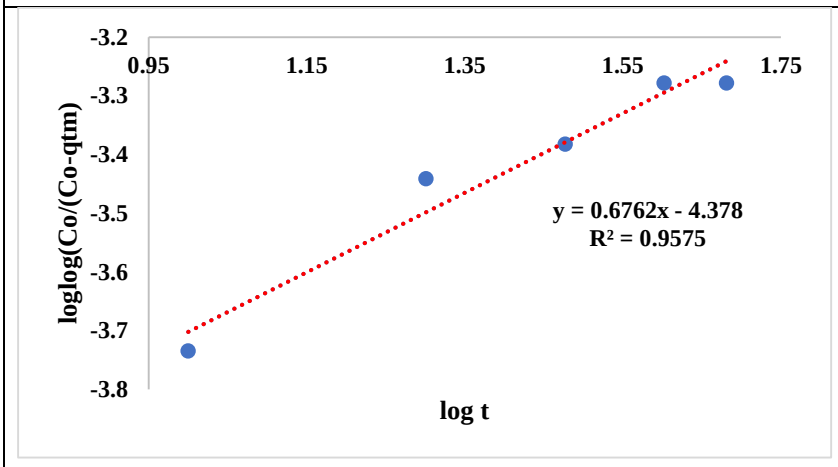	Not getting correlated

Figure 5.6 Bangham kinetic plots

For decolorization of direct yellow 12, the experimental data are getting correlated with R^2 above 95% which is not the case with Acid red 13 decolorization. Hence the reaction with Acid red 13 decolorization is limited with pore diffusion and this situation represents that the diffusion into pores of the sorbent cannot be said as the lone rate-controlling phase.

Table 5.2 provide pseudo 1st order constants k_1, pseudo 2nd order constants k_2, h, $q_{e,cal}$, $q_{e,exp}$ for direct yellow 12 decolorization.

5.3 Pseudo Constants

5.3.1 For Decolorization of Direct yellow 12 using *P. pastoris*

Table 5.2 Pseudo 1st , 2nd and Bangham kinetic constants of D1 biodegradation

Conc (mg/L)	$q_{e,exp}$	Pseudo First-Order			Pseudo second-Order				Bangham Equation		
		$q_{e,cal}$	K_1 (L/hr)	R^2	$q_{e,cal}$	K_2	R^2	h	K_B (L/g)	α	R^2
150	606	604.7	0.0002	0.95	7.25	0.012	0.83	0.604	0.006	0.68	0.957

From the above table, correlation from the pseudo 1st order model has R^2>0.95. Moreover, the q_e value from the pseudo 1st model is similar with the experimental q_e value. Hence, it can be said that the rate-limiting step may be chemisorption or covalent forces i.e., exchange of

electrons between them. Hence the following two mechanisms can be proposed for its decolorization reaction.

5.3.1.1 Mechanism 1(a)

According to the below mechanism for direct yellow 12, both yeast and the dye substrate react as if they are the two individual reactants both participating the reaction proportionately with the high amount of activated carbon (adsorbent concentration). Hence pseudo 2nd order is followed and the mechanism of the reaction is shown as below Fig. 5.7

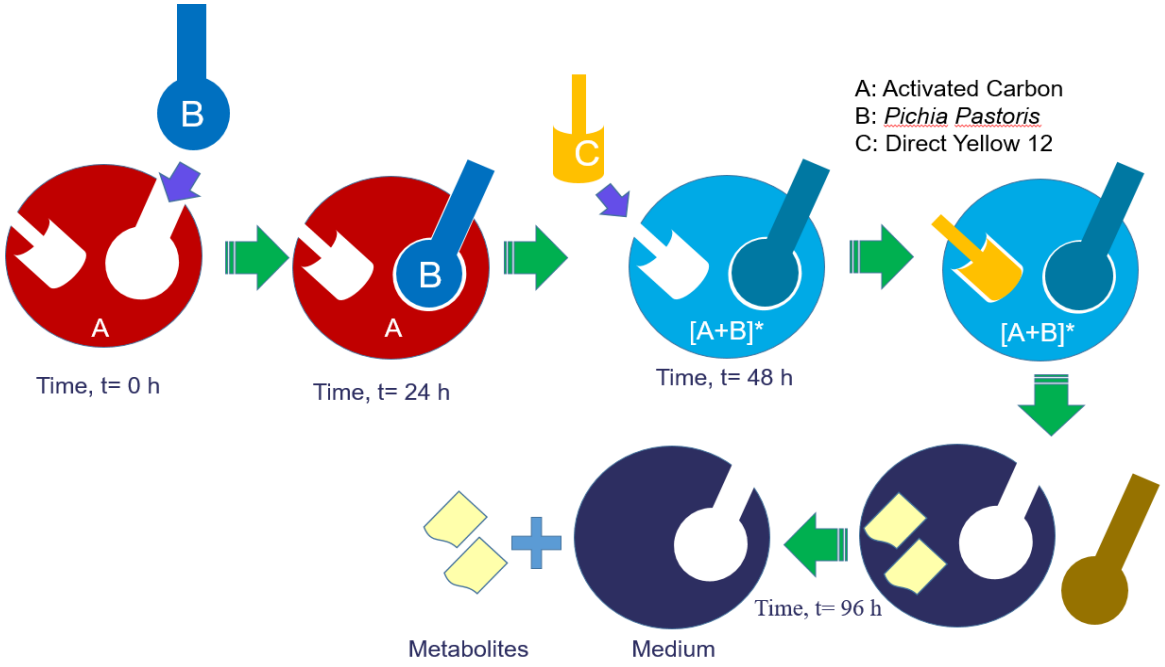

Figure 5.7 Mechanism 1(a) for the biodegradation of Direct yellow 12

5.3.1.2 Mechanism 1(b)

It was possible that adsorbent along with the inoculum dosage is in high quantity and dye substrate concentration are is in limited quantity. Hence pseudo 1st order is followed since only one reactant is virtually involved and and the mechanism of the reaction is shown as below Fig. 5.8.

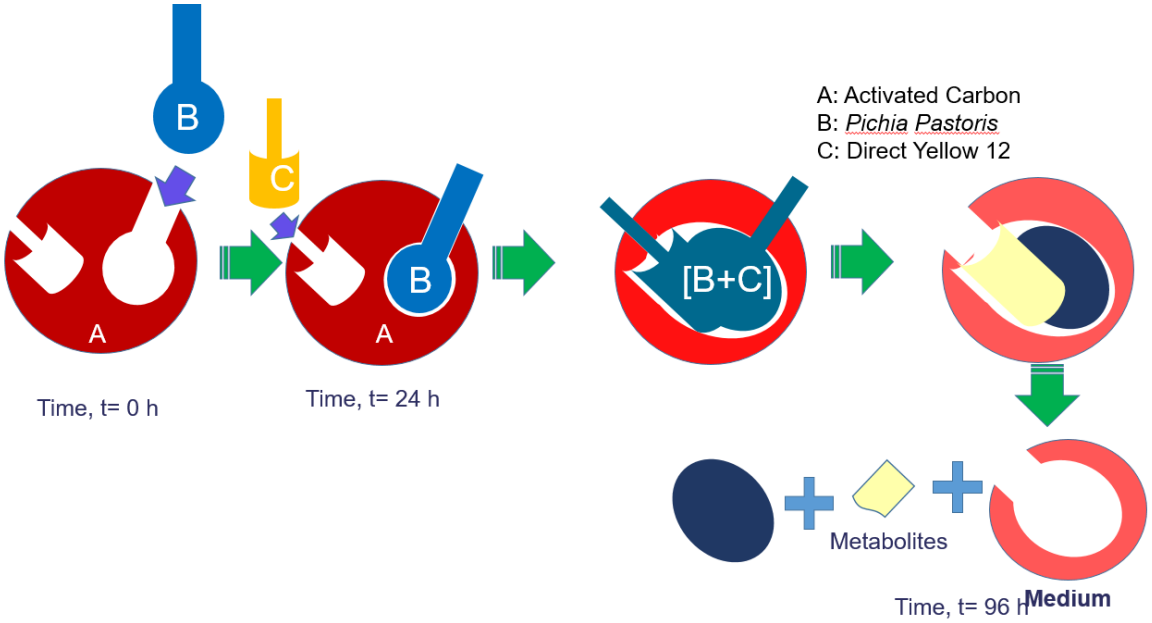

Figure 5.8 Mechanism 1(b) for the biodegradation of Direct yellow 12

5.3.2 For Decolorization of Acid red 13 using *P. pastoris*

Table 5.3 provide pseudo 1st order constants k_1, pseudo 2nd order constants k_2, h, $q_{e,cal}$, $q_{e,exp}$ for D2.

Table 5.3 Pseudo 1st , 2nd and Bangham kinetic constants of Acid red 13 biodegradation

Conc (mg/L)	$q_{e,exp}$	Pseudo 1st Order			Pseudo 2nd Order				Bangham Equation		
		$q_{e,cal}$	K_1 (L/hr)	R^2	$q_{e,cal}$	K_2 (g/mg.hr)	R^2	h (mg/g.h)	K_B (L/g)	α	R^2
50	2112.8	1570.7	0.155	0.805	3333.3	0.0000085	0.45	94.34	NA	NA	NA

From the above table, correlation coefficients calculated from the pseudo First-order model has R^2 higher than that of pseudo 2nd order model. Moreover, Bangham equation is also not getting correlated. Hence pore diffusion might be the only rate limiting phase.

Hence the following mechanism 3 might be followed for the biodegradation reaction.

5.3.2.1 Mechanism 3

In the below mechanism for acid red 13, it was possible that adsorbent with the inoculum dosage is in high quantity and the dye substrate concentration is reacting in limited quantity. Hence Pseudo 1st order is followed where only one reactant i.e., dye substrate is virtually involved and the mechanism proposed for the biodegradation of Acid red 13 is shown as Fig. 5.9.

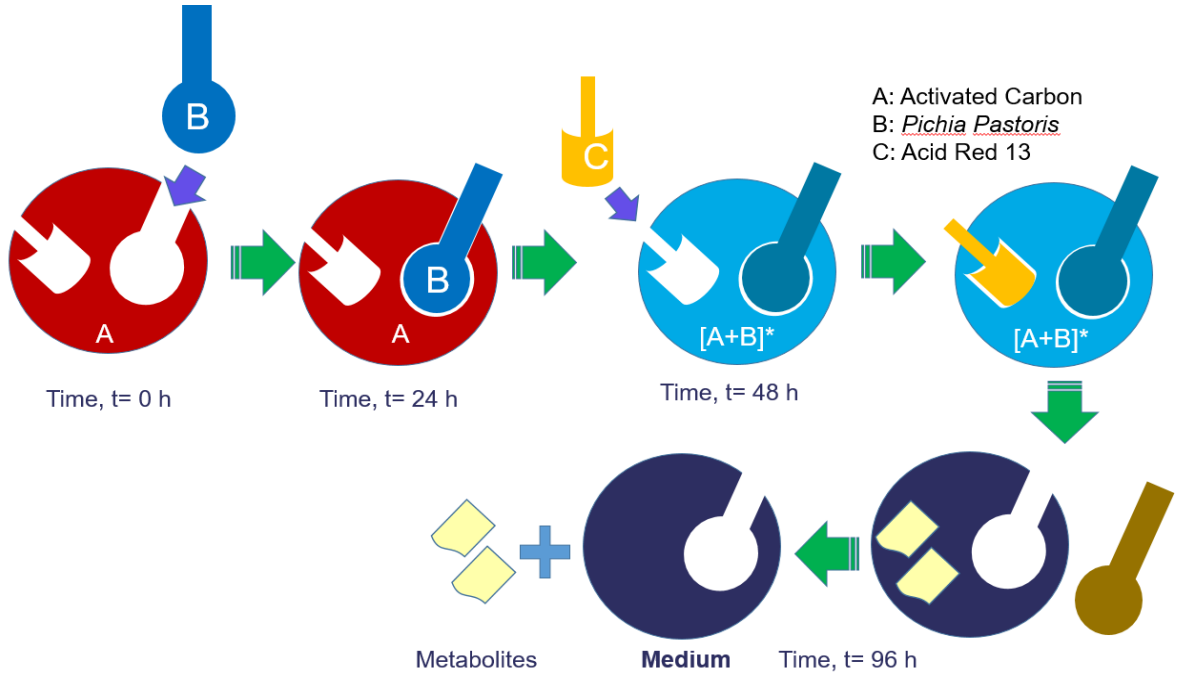

Figure 5.9 Mechanism 2 for the biodegradation of Acid red 13

Chapter 6

Conclusions and Future work

Chapter 6

6. Conclusions and Future work

6.1 Conclusions

Here, the thesis's culminating insights have been mentioned as few major parts that contribute to the research field while highlighting the potential for additional investigation.

Azo dyes are the most prevalent and significant class of commercial dyes used in the textile industry, making up between 60 and 70 percent of all the textile dyes produced. The studies were performed in order to provide sustainable, ecofriendly biodegradation of Direct Yellow 12 and the Acid Red 13, since there are no available studies of the biodegradation of the aforementioned dyes. The bacterial cultures *Thalassospira frigidphilosprofundus* and *Erwinia chrysanthemi burkholder* were used in the bacterial decolorization whereas Yeast culture *Pichia pastoris* was used in the biodegradation.

6.1.1 Significant Findings

6.1.1.1 Batch Findings

- For Direct yellow 12

1) Using *Thalassospira frigidphilosprofundus*, decolorization greater than 80% was obtained at the conditions of 90 mg/L of concentration, pH of 7.2, 26^{o}C of temperature, agitation of 40 rpm.

2) Using *Erwinia chrysanthemi burkholder*, decolorization greater than 80% was obtained at the conditions of 90 mg/L of concentration, pH of 6.5, 22°C of temperature, agitation of 50 rpm.

3) *T. frigidphilosprofundus* has higher efficiency in decolorizing than *E. burkholder*

4) Using *Pichia pastoris*, decolorization percentage of 89.2 was obtained at the conditions of 149.52 mg/L of concentration, pH of 9.94, 14.97% v/v inoculum dosage, 14.97 ml of methanol addition which can provide a desirability of 1.

- For Acid red 13

1) Using *Thalassospira frigidphilosprofundus*, decolorization greater than 72% was obtained at the conditions of 55-70 mg/L of concentration, pH of 5.5-6.5, 17.5-21^{o}C of temperature, agitation of 72-80 rpm.

2) Using *Erwinia chrysanthemi burkholder*, decolorization greater than 80% was obtained at the conditions of 50 mg/L of concentration, pH of 6-8.2, 17.5-35.6°C of temperature, agitation of 40.6 rpm. *E. Burkholder* has higher efficiency in decolorizing than *T. frigidphilosprofundus*

3) Using *Pichia pastoris*, decolorization percentage of 90.8 was obtained at the conditions of 50.01 mg/L of concentration, pH of 4, 15% v/v inoculum dosage, 15 ml of methanol addition which can provide a desirability of 0.924

6.1.1.2 Bioreactor Findings

- ❖ The decolorizing capacity of Yeast is higher than that of bacteria since percentage change in COD for decolorized metabolites of both dyes Direct yellow 12 and Acid red 13 using yeasts is higher than that with the bacteria.
- ❖ Based on percentage COD change, the action of *P. pastoris* is higher in decolorizing Direct yellow 12 than Acid red 13.
- ❖ Percentage Decolorization in Batch reactor tank is lower when compared to that with Fluidized bed Bioreactor. For Direct yellow 12, 83% and 90% are obtained at the conditions of C=150 mg/L, pH=7, T=28°C, Adsorbent dosage of 30mg/L. For Acid Red 13, 75% and 89.5% are obtained at the conditions of C=50 mg/L, pH=7, T=28°C, Adsorbent dosage of 40 mg/L.

6.2 Scope for Future Work

The conclusions of this current work suggest the following recommendations of future work. The following scope gives an idea to

- ✓ Adsorbent can be further modified by attaching various functional groups such as amino groups, hydroxyl groups that can enhance the adsorption efficiency.
- ✓ Microbe can be immobilized on various types of adsorbents (subjected to availability, cost of usage and reproducibility).
- ✓ Detailed study of RTD in Fluidized bed bioreactor and Batch reactor tank can be done using experiments and CFD.
- ✓ Modelling of the process for the bioreactor can be done.

Appendix A

Table A1 Analysis of variance of decolorization of Direct yellow 12 using *T. frigidphilosprofundus*

Predictor	Coef	SE Coef	T	P
Constant	1.590	7.784	0.2	0.843
C	-0.02143	0.02626	-0.82	0.438
P	1.902	1.115	1.71	0.126
T	0.1406	0.4290	0.33	0.752
A	0.00693	0.03137	0.22	0.831
C^2	0.00002428	0.00005983	0.41	0.695
P^2	-0.06154	0.03372	-1.82	0.105
T^2	-0.002051	0.003988	-0.51	0.621
A^2	-0.0001844	0.0001195	-1.54	0.161
C*P	-0.000606	0.0017	-0.36	0.731
C*T	0.0001995	0.0007274	0.27	0.791
C*A	0.0008902	0.0006026	1.48	0.178
P*T	-0.011587	0.009270	-1.25	0.247
P*A	-0.002767	0.003992	-0.69	0.508
T*A	0.000303	0.001509	0.2	0.846
C*P*T	0.00003969	0.00007515	0.53	0.612
C*P*A	-0.00006438	0.00005596	-1.15	0.283
C*T*A	-0.00003346	0.00002466	-1.36	0.212

P*T*A	0.0001752	0.000167	1.05	0.325
C*P*T*A	0.00000201	0.00000218	0.92	0.385
lnC*C	0.4407	0.4098	1.08	0.314
lnP*P	-2.637	1.918	-1.37	0.206
lnT*T	-0.087	2.512	-0.03	0.973
lnA*A	-0.0465	0.02731	-1.7	0.127

Table A2 Analysis of variance of decolorization of Direct yellow 12 using *T. frigidphilosprofundus*

Source	DF	SS	MS	F	P
Regression	23	2.1362	0.09272	5.14	0.011
Residual Error	8	0.1443	0.01804		
Total	31	2.27692			

Table A3 Degrees of freedom, seq SS of the individual parameters of decolorization of Direct yellow 12 using *T. frigidphilosprofundus*

Source	DF	Seq SS
C	1	0.41906
P	1	0.16629
T	1	0.01827
A	1	0.00876
C*C	1	0.00617
P*P	1	0.24279
T*T	1	0.11249
A*A	1	0.01355

C*P	1	0.05196
C*T	1	0.01346
C*A	1	0.04361
P*T	1	0.24424
P*A	1	0.02926
T*A	1	0.48118
C*P*T	1	0.00015
C*P*A	1	0.00037
C*T*A	1	0.01741
P*T*A	1	0.12207
C*P*T*A	1	0.00754
lnC*C	1	0.01094
lnP*P	1	0.07051
lnT*T	1	0.00027
lnA*A	1	0.05229

Table A4 Analysis of variance of decolorization of Direct yellow 12 using *E. burkholder*

Predictor	**Coef**	**SE Coef**	**T**	**P**
Constant	-6.566	2.702	-2.43	0.035
C	-0.05298	0.02135	-2.48	0.032
P	2.1114	0.8620	2.45	0.034
T	-0.19561	0.03563	-5.49	0
C*C	0.00018202	0.00005451	3.34	0.007
P*P	-0.06524	0.02713	-2.41	0.037
A*A	-0.00021591	0.00004634	-4.66	0.001
C*A	-0.0006642	0.0004034	-1.65	0.131
T*A	0.000739	0.0002693	2.74	0.021
C*P*T	0.00011175	0.00005067	2.21	0.052
C*P*A	0.00006193	0.00003469	1.79	0.105
C*T*A	0.00003268	0.00001754	1.86	0.092
C*P*T*A	0.00000308	0.00000147	-2.1	0.062
lnP*P	55734	16318	3.42	0.007
lnA*A	-55741	16318	-3.42	0.007
lnC*P	-111479	32637	-3.42	0.007
lnC*A	111482	32637	3.42	0.007
lnP*T	3.63660	0.902	4.03	0.002
C*P	-0.002161	0.00129	-1.68	0.125
C*T	-0.0009632	0.000605	-1.59	0.142

Table A5 Analysis of variance of decolorization of Direct yellow 12 using *E. burkholder*

Source	**DF**	**SS**	**MS**	**F**	**P**
Regression	19	1.69283	0.0891	6.13	0.003
Residual error	10	0.14546	0.01455		
Total	29	1.83829			

Table A6 Degrees of freedom, seq SS of the individual parameters of decolorization of Direct yellow 12 using *E. burkholder*

Source	**DF**	**Seq SS**
C	1	0.29429
P	1	0.24018
T	1	0.01176
C*C	1	0.03126
P*P	1	0.07726
A*A	1	0.15140
C*A	1	0.00236
T*A	1	0.28333
C*P*T	1	0.00729
C*P*A	1	0.13496
C*T*A	1	0.00935
C*P*T*A	1	0.02821
lnP*P	1	0.00392

lnA*A	1	0.02534
lnC*P	1	0.11185
lnC*A	1	0.02662
lnP*T	1	0.21249
C*P	1	0.00409
C*T	1	0.03687

Appendix B

Table B1 Analysis of variance of decolorization of Acid red 13 using *T. frigidphilosprofundus*

Source	DF	SS	MS	F	P
Regression	16	1.06445	0.06653	1.81	0.152
Residual error	12	0.44151	0.03679		
Total	28	1.50595			

Table B2 Analysis of variance of individual coefficients of decolorization of Acid red 13 using *T. frigidphilosprofundus*

Predictor	Coef	SE Ceof	T	P
Constant	-1.184	2.457	-0.48	0.638
c	0.020579	0.007007	2.94	0.012
p	-1.1978	0.4044	-2.96	0.012
t	-0.19116	0.08465	-2.26	0.043
a	-0.10702	0.03477	-3.08	0.01

p*p	0.03757	0.01185	3.17	0.008
a*a	0.0002942	0.0001385	2.12	0.055
c*p	-0.0008380	0.0003889	-2.16	0.052
c*t	-0.0004037	0.0001471	-2.74	0.018
p*t	0.010377	0.005365	1.93	0.077
p*a	0.006427	0.00263	2.44	0.031
t*a	0.002551	0.001191	2.14	0.054
p*t*a	-0.0002796	0.0001161	-2.41	0.033
c*p*t*a	0.00000029	0.00000013	2.27	0.042
lnc*c	-0.4199	0.1517	-2.77	0.017
lnc*a	0.18855	0.06906	2.73	0.018
lnp*t	3.418	1.129	3.03	0.011

Table B3 Degrees of freedom, seq SS of the individual parameters of decolorization of Acid red 13 using *T. frigidphilosprofundus*

Source	DF	Seq SS
c	1	0.29429
p	1	0.24018
t	1	0.01176
c*c	1	0.03126
p*p	1	0.07726
a*a	1	0.15140
c*a	1	0.00236

t*a	1	0.28333
c*p*t	1	0.00729
c*p*a	1	0.13496
c*t*a	1	0.00935
c*p*t*a	1	0.02821
lnp*p	1	0.00392
lna*a	1	0.02534
lnc*p	1	0.11185
lnc*a	1	0.02662
lnp*t	1	0.21249
c*p	1	0.00409
c*t	1	0.03687

Table B4 Analysis of Variance of decolorization of Acid red 13 using E. burkholder

Source	DF	SS	MS	F	P
Regression	28	1.09924	0.03926	1.56	0.405
Residual error	3	0.0755	0.02517		
Total	31	1.17475			

Table B5 Analysis of Variance of individual parameters of decolorization of Acid red 13 using *E. burkholder*

Predictor	Coef	SE Coef	T	P
Constant	-18.88	12.62	-1.5	0.232
c	0.00361	0.03771	0.1	0.93
p	-3.19	1.855	-1.72	0.184
t	-0.5933	0.6747	-0.88	0.444
a	-0.04043	0.04429	-0.91	0.429
c*c	0.00011234	0.00008853	1.27	0.294
p*p	0.10475	0.05578	1.88	0.157
t*t	0.005042	0.006539	0.77	0.497
a*a	0.0000682	0.0002034	0.34	0.76
c*p	-0.003284	0.002433	-1.35	0.27
c*t	-0.001519	0.001079	-1.41	0.254
c*a	-0.001226	0.0009327	-1.31	0.28
p*t	0.00003	0.01309	0	0.999
p*a	0.002009	0.006	0.33	0.76
t*a	0.001123	0.002216	0.51	0.647
c*p*t	0.0001182	0.0001067	1.11	0.349
c*p*a	0.00011364	0.00008929	1.27	0.293
c*t*a	0.00005078	0.00003814	1.33	0.275

p*t*a	-0.0001057	0.0002483	-0.43	0.699
c*p*t*a	-0.00000439	0.00000345	-1.27	0.292
lnc*c	-10037	7477	-1.34	0.272
lnp*p	17423	50081	0.35	0.751
lnt*t	-13250	40966	-0.32	0.768
lna*a	-51750	50842	-1.02	0.384
lnc*p	-72383	71743	-1.01	0.387
lnc*t	-5962	32602	-0.18	0.867
lnc*a	98421	63107	1.56	0.217
lnp*t	32471	86115	0.38	0.731
lnp*a	5079	49672	0.1	0.925

Table B6 Degrees of freedom, seq SS of the individual parameters of decolorization of Acid red 13 using *E. burkholder*

Source	DF	Seq SS
c	1	0.00121
p	1	0.01592
t	1	0.01121
a	1	0.01264
c*c	1	0.09331
p*p	1	0.07371
t*t	1	0.15756

a*a	1	0.01893
c*p	1	0.00365
c*t	1	0.02105
c*a	1	0.0178
p*a	1	0.00549
t*a	1	0.04305
c*p*t	1	0.00051
c*p*a	1	0.02456
c*t*a	1	0.00056
p*t*a	1	0.03211
c*p*t*a	1	0.00695
lnc*c	1	0.1482
lnp*p	1	0.12323
lnt*t	1	0.0021
lna*a	1	0.00006
lnc*p	1	0.07885
lnc*t	1	0.01866
lnc*a	1	0.15439
lnp*t	1	0.00419
lnp*a	1	0.00026

Works of Tables B1, B2, B3, B4, B5, B6 are published in (Mukkera et al., 2023)

Chapter 7

7. References

Adnan, L. A., Sathishkumar, P., Mohd Yusoff, A. R., & Hadibarata, T. (2015). Metabolites characterisation of laccase mediated Reactive Black 5 biodegradation by fast growing ascomycete fungus Trichoderma atroviride F03. *International Biodeterioration and Biodegradation*, *104*, 274–282. https://doi.org/10.1016/j.ibiod.2015.05.019

Ajaz, M., Rehman, A., Khan, Z., Nisar, M. A., & Hussain, S. (2019). Degradation of azo dyes by Alcaligenes aquatilis 3c and its potential use in the wastewater treatment. *AMB Express*, *9*(1). https://doi.org/10.1186/s13568-019-0788-3

Akpan, U. G., & Hameed, B. H. (2009). Parameters affecting the photocatalytic degradation of dyes using TiO2-based photocatalysts: A review. In *Journal of Hazardous Materials* (Vol. 170, Issues 2–3, pp. 520–529). https://doi.org/10.1016/j.jhazmat.2009.05.039

Aksu, Z., & Tezer, S. (2005). Biosorption of reactive dyes on the green alga Chlorella vulgaris. *Process Biochemistry*, *40*(3–4), 1347–1361. https://doi.org/10.1016/j.procbio.2004.06.007

Atalay, S., & Ersöz, G. (2016). *Novel Catalysts in Advanced Oxidation of Organic Pollutants*. 23–34. https://doi.org/10.1007/978-3-319-28950-2

Bai, Y., Wang, X., Zhang, F., & Zeng, R. J. (2022). Acid Orange 7 degradation using methane as the sole carbon source and electron donor. *Frontiers of Environmental Science and Engineering*, *16*(3). https://doi.org/10.1007/s11783-021-1468-5

Banat, I. M., Nigam, P., Singh, D., & Marchant, R. (1996). Microbial decolorization of textile-dye-containing effluents: A review. *Bioresource Technology*, *58*(3), 217–227. https://doi.org/10.1016/S0960-8524(96)00113-7

Barragán, B. E., Costa, C., & Carmen Márquez, M. (2007). Biodegradation of azo dyes by bacteria inoculated on solid media. *Dyes and Pigments*, *75*(1), 73–81. https://doi.org/10.1016/j.dyepig.2006.05.014

Basitere, M., Rinquest, Z., Njoya, M., Sheldon, M. S., & Ntwampe, S. K. O. (2017). Treatment of poultry slaughterhouse wastewater using a static granular bed reactor (SGBR) coupled with ultrafiltration (UF) membrane system. *Water Science and Technology*, *76*(1), 106–114. https://doi.org/10.2166/wst.2017.179

Bhad, R. M., Das, A., & Kodape, S. M. (2022). Ozonation of Procion Blue Reactive Dye and its Kinetics Study. *Pollution*, *8*(2), 529–541. https://doi.org/10.22059/POLL.2021.330871.1191

Bouacem, K., Rekik, H., Jaouadi, N. Z., Zenati, B., Kourdali, S., El Hattab, M., Badis, A., Annane, R., Bejar, S., Hacene, H., Bouanane-Darenfed, A., & Jaouadi, B. (2018). Purification and characterization of two novel peroxidases from the dye-decolorizing fungus Bjerkandera adusta strain CX-9. *International Journal of Biological Macromolecules*, *106*, 636–646. https://doi.org/10.1016/j.ijbiomac.2017.08.061

Bustos-Terrones, Y. A., Bandala, E. R., Moeller-Chávez, G. E., & Bustos-Terrones, V. (2022). Enhanced biological wastewater treatment using sodium alginate-immobilized microorganisms in a fluidized bed reactor. *Water Science and Engineering*, *15*(2), 125–133. https://doi.org/10.1016/j.wse.2022.02.002

Carvalho, C., Fernandes, A., Lopes, A., Pinheiro, H., & Gonçalves, I. (2007). Electrochemical degradation applied to the metabolites of Acid Orange 7 anaerobic biotreatment. *Chemosphere*, *67*(7), 1316–1324. https://doi.org/10.1016/j.chemosphere.2006.10.062

Chakravarthi, B., Mathkala, V., & Palempalli, U. M. D. (2021). Degradation and detoxification of congo red azo dye by immobilized laccase of streptomyces sviceus. *Journal of Pure and Applied Microbiology*, *15*(2), 864–876. https://doi.org/10.22207/JPAM.15.2.41

Chang, J. S., Chou, C., Lin, Y. C., Lin, P. J., Ho, J. Y., & Lee Hu, T. (2001). Kinetic characteristics of bacterial azo-dye decolorization by Pseudomonas luteola. *Water Research*, *35*(12), 2841–2850. https://doi.org/10.1016/S0043-1354(00)00581-9

Chen, S., Qin, C., Wang, T., Chen, F., Li, X., Hou, H., & Zhou, M. (2019). Study on the adsorption of dyestuffs with different properties by sludge-rice husk biochar: Adsorption capacity, isotherm, kinetic, thermodynamics and mechanism. *Journal of Molecular Liquids*, *285*, 62–74. https://doi.org/10.1016/j.molliq.2019.04.035

Chung, K.-T., & Stevens, S. E. (1993). DEGRADATION OF AZO DYES BY ENVIRONMENTAL MICROORGANISMS AND HELMINTHS. In *Envrronmenlol Toxrcology and Chemorry* (Vol. 12).

Corona-Bautista, M., Picos-Benítez, A., Villaseñor-Basulto, D., Bandala, E., & Peralta-Hernández, J. M. (2021). Discoloration of azo dye Brown HT using different advanced oxidation processes. *Chemosphere*, *267*. https://doi.org/10.1016/j.chemosphere.2020.129234

Daly, R., & Hearn, M. T. W. (2005). Expression of heterologous proteins in Pichia pastoris: A useful experimental tool in protein engineenring and production. In *Journal of Molecular Recognition* (Vol. 18, Issue 2, pp. 119–138). https://doi.org/10.1002/jmr.687

DeVito, S. C. (1993). Predicting Azo Dye Toxicity. *Critical Reviews in Environmental Science and Technology*, *23*(3), 249–324. https://doi.org/10.1080/10643389309388453

dos Santos, A. B., Cervantes, F. J., & van Lier, J. B. (2007). Review paper on current technologies for decolourisation of textile wastewaters: Perspectives for anaerobic biotechnology. *Bioresource Technology*, *98*(12), 2369–2385. https://doi.org/10.1016/j.biortech.2006.11.013

Elbanna, K., Sarhan, O. M., Khider, M., Elmogy, M., Abulreesh, H. H., & Shaaban, M. R. (2017). Microbiological, histological, and biochemical evidence for the adverse effects of food azo dyes on rats. *Journal of Food and Drug Analysis*, *25*(3), 667–680. https://doi.org/10.1016/j.jfda.2017.01.005

Firmino, P. I. M., da Silva, M. E. R., Cervantes, F. J., & dos Santos, A. B. (2010). Colour removal of dyes from synthetic and real textile wastewaters in one- and two-stage anaerobic systems. *Bioresource Technology*, *101*(20), 7773–7779. https://doi.org/10.1016/j.biortech.2010.05.050

Forgacs, E., Cserháti, T., & Oros, G. (2004). Removal of synthetic dyes from wastewaters: A review. In *Environment International* (Vol. 30, Issue 7, pp. 953–971). Elsevier Ltd. https://doi.org/10.1016/j.envint.2004.02.001

Foroutan, R., Mohammadi, R., Sohrabi, N., Sahebi, S., Farjadfard, S., Esvandi, Z., & Ramavandi, B. (2020). Calcined alluvium of agricultural streams as a recyclable and

cleaning tool for cationic dye removal from aqueous media. *Environmental Technology and Innovation*, *17*. https://doi.org/10.1016/j.eti.2019.100530

Fujita,'* Akira Era,', M., Ike,', M., Soda, S., Miyata, N., & Hira04, T. (2000). Decolorization of Heat-Treatment Liquor of Waste Sludge by a Bioreactor Using Polyurethane Foam-Immobilized White Rot Fungus Equipped with an Ultramembrane Filtration Unit. In *JOURNAL OF BIOSCIENCE AND BIOENGINEERING* (Vol. 90, Issue 4).

Garg, N., Garg, A., & Mukherji, S. (2020). Eco-friendly decolorization and degradation of reactive yellow 145 textile dye by Pseudomonas aeruginosa and Thiosphaera pantotropha. *Journal of Environmental Management*, *263*(March), 110383. https://doi.org/10.1016/j.jenvman.2020.110383

Gharbani, P., Tabatabaii, S. M., & Mehrizad, A. (2008). Removal of Congo red from textile wastewater by ozonation. *International Journal of Environmental Science and Technology*, *5*(4), 495–500. https://doi.org/10.1007/BF03326046

Gomi, N., Yoshida, S., Matsumoto, K., Okudomi, M., Konno, H., Hisabori, T., & Sugano, Y. (2011). Degradation of the synthetic dye amaranth by the fungus Bjerkandera adusta Dec 1: Inference of the degradation pathway from an analysis of decolorized products. *Biodegradation*, *22*(6), 1239–1245. https://doi.org/10.1007/s10532-011-9478-9

Guembri, M., Neifar, M., Saidi, M., Ferjani, R., Chouchane, H., Mosbah, A., Cherif, A., Saidi, N., & Ouzari, H. I. (2021). Decolorization of textile azo dye Novacron Red using bacterial monoculture and consortium: Response surface methodology optimization. *Water Environment Research*, *93*(8), 1346–1360. https://doi.org/10.1002/wer.1521

Hai, F. I., Yamamoto, K., & Fukushi, K. (2006). Development of a submerged membrane fungi reactor for textile wastewater treatment. *Desalination*, *192*(1–3), 315–322. https://doi.org/10.1016/j.desal.2005.06.050

Hai, F. I., Yamamoto, K., Nakajima, F., & Fukushi, K. (2012). Application of a GAC-coated hollow fiber module to couple enzymatic degradation of dye on membrane to whole cell biodegradation within a membrane bioreactor. *Journal of Membrane Science*, *389*, 67–75. https://doi.org/10.1016/j.memsci.2011.10.016

Harichandran, G., & Prasad, S. (2016). SonoFenton degradation of an azo dye, Direct Red. *Ultrasonics Sonochemistry*, *29*, 178–185. https://doi.org/10.1016/j.ultsonch.2015.09.005

Hassan, M. M., & Carr, C. M. (2018). A critical review on recent advancements of the removal of reactive dyes from dyehouse effluent by ion-exchange adsorbents. *Chemosphere*, *209*, 201–219. https://doi.org/10.1016/j.chemosphere.2018.06.043

Hayat, H., Mahmood, Q., Pervez, A., Bhatti, Z. A., & Baig, S. A. (2015). Comparative decolorization of dyes in textile wastewater using biological and chemical treatment. *Separation and Purification Technology*, *154*, 149–153. https://doi.org/10.1016/j.seppur.2015.09.025

Hema, N., & Suresha, S. (2014). BIOREMEDIATION OF TEXTILE DYE EFFLUENT BY SHEWANELLA PUTREFACIENS. In *International Journal of Pharmacy and Biological Sciences*. Volume 4| Issue 2|109-116. www.ijpbs.comorwww.ijpbsonline.com

Hein¯ing, A., Bergbauer, M., & Szewzyk, U. (1997). Biodegradation of azo and phthalocyanine dyes by Trametes versicolor and Bjerkandera adusta. *Appl Microbiol Biotechnol*. 48: 261-266

Ibrahim, A., El-Fakharany, E. M., Abu-Serie, M. M., Elkady, M. F., & Eltarahony, M. (2022). Methyl Orange Biodegradation by Immobilized Consortium Microspheres: Experimental Design Approach, Toxicity Study and Bioaugmentation Potential. *Biology*, *11*(1). https://doi.org/10.3390/biology11010076

Jadhav, S. B., Phugare, S. S., Patil, P. S., & Jadhav, J. P. (2011). Biochemical degradation pathway of textile dye Remazol red and subsequent toxicological evaluation by cytotoxicity, genotoxicity and oxidative stress studies. *International Biodeterioration and Biodegradation*, *65*(6), 733–743. https://doi.org/10.1016/j.ibiod.2011.04.003

Jayapal, M., Jagadeesan, H., Shanmugam, M., Danisha J, P., & Murugesan, S. (2018). Sequential anaerobic-aerobic treatment using plant microbe integrated system for degradation of azo dyes and their aromatic amines by-products. *Journal of Hazardous Materials*, *354*, 231–243. https://doi.org/10.1016/j.jhazmat.2018.04.050

Kalyani, D. C., Telke, A. A., Dhanve, R. S., & Jadhav, J. P. (2009). Ecofriendly biodegradation and detoxification of Reactive Red 2 textile dye by newly isolated Pseudomonas sp. SUK1. *Journal of Hazardous Materials*, *163*(2–3), 735–742. https://doi.org/10.1016/j.jhazmat.2008.07.020

Kamdod, A. S., & Kumar, M. V. P. (2022). Adsorption of Methylene Blue, Methyl Orange, and Crystal Violet on Microporous Coconut Shell Activated Carbon and Its Composite with Chitosan: Isotherms and Kinetics. *Journal of Polymers and the Environment*, *30*(12), 5274–5289. https://doi.org/10.1007/s10924-022-02597-w

Kaneshiro, W. S., Burger, M., Vine, B. G., De Silva, A. S., & Alvarez, A. M. (2008). Characterization of Erwinia chrysanthemi from a bacterial heart rot of pineapple outbreak in Hawaii. *Plant Disease*, *92*(10), 1444–1450. https://doi.org/10.1094/PDIS-92-10-1444

Kapdan, I. K., Kargia, F., McMullan, G., & Marchant, R. (2000). Effect of environmental conditions on biological decolorization of textile dyestuff by C. versicolor. *Enzyme and Microbial Technology*, *26*(5–6), 381–387. https://doi.org/10.1016/S0141-0229(99)00168-4

Kaskote, E., Rinquest, Z., Williams, Y., & Njoya, M. (2019). *Performance and Statistical Comparison of the Expanded and Static Granular Sludge Bed Reactors Treating Poultry Slaughterhouse Wastewater*. *May*, 16–18. https://doi.org/10.17758/eares8.eap1119137

Khalid, A., Arshad, M., & Crowley, D. E. (2008). Decolorization of azo dyes by Shewanella sp. under saline conditions. *Applied Microbiology and Biotechnology*, *79*(6), 1053–1059. https://doi.org/10.1007/s00253-008-1498-y

Knapp, J. S., & Newby, P. S. (1995). THE MICROBIOLOGICAL DECOLORIZATION OF AN INDUSTRIAL EFFLUENT CONTAINING A DIAZO-LINKED CHROMOPHORE. In *War. Res* (Vol. 29, Issue 7).

Knapp, J. S., Zhanga, F.-M., & Tapleyb, K. N. (1997). Decolourisation of II by a Wood-Rotting Orange Fungus. In *289È296 J. Chem. T ech. Biotechnol* (Vol. 69).

Krishnan, J., Arvind Kishore, A., Suresh, A., Madhumeetha, B., & Gnana Prakash, D. (2017). Effect of pH, inoculum dose and initial dye concentration on the removal of azo dye mixture under aerobic conditions. *International Biodeterioration and Biodegradation*, *119*, 16–27. https://doi.org/10.1016/j.ibiod.2016.11.024

Kumar Garg, S., Tripathi, M., Singh, S. K., & Tiwari, J. K. (2012). Biodecolorization of textile dye effluent by Pseudomonas putida SKG-1 (MTCC 10510) under the conditions optimized for monoazo dye orange II color removal in simulated minimal salt medium.

International Biodeterioration and Biodegradation, *74*, 24–35. https://doi.org/10.1016/j.ibiod.2012.07.007

Kurade, M. B., Waghmode, T. R., Jadhav, M. U., Jeon, B. H., & Govindwar, S. P. (2015). Bacterial-yeast consortium as an effective biocatalyst for biodegradation of sulphonated azo dye Reactive Red 198. *RSC Advances*, *5*(29), 23046–23056. https://doi.org/10.1039/c4ra15834b

Lade, H., Govindwar, S., & Paul, D. (2015). Mineralization and detoxification of the carcinogenic azo dye Congo red and real textile effluent by a polyurethane foam immobilized microbial consortium in an upflow column bioreactor. *International Journal of Environmental Research and Public Health*, *12*(6), 6894–6918. https://doi.org/10.3390/ijerph120606894

Lade, H., Kadam, A., Paul, D., & Govindwar, S. (2015). A low-cost wheat bran medium for biodegradation of the benzidine-based carcinogenic dye trypan blue using a microbial consortium. *International Journal of Environmental Research and Public Health*, *12*(4), 3480–3505. https://doi.org/10.3390/ijerph120403480

Lade, H. S., Waghmode, T. R., Kadam, A. A., & Govindwar, S. P. (2012). Enhanced biodegradation and detoxification of disperse azo dye Rubine GFL and textile industry effluent by defined fungal-bacterial consortium. *International Biodeterioration and Biodegradation*, *72*, 94–107. https://doi.org/10.1016/j.ibiod.2012.06.001

Lie, T. J., Leadbetter, J. R., & Leadbetter, E. R. (1998). Metabolism of sulfonic acids and other organosulfur compounds by sulfate-reducing bacteria. *Geomicrobiology Journal*, *15*(2), 135–149. https://doi.org/10.1080/01490459809378070

Lin, H., Zhang, H., & Hou, L. (2014). Degradation of c. i. acid orange 7 in aqueous solution by a novel electro/fe3o4/pds process. *Journal of Hazardous Materials*, *276*, 182–191. https://doi.org/10.1016/j.jhazmat.2014.05.021

Lourenco, N. D., Novais, J. M., & Pinheiro, H. M. (2000). Reactive textile dye colour removal in a sequencing batch reactor. *Water Science and Technology*, *42*(5–6), 321–328. https://doi.org/10.2166/wst.2000.0531

Mahmoud, M. S. (2016). Decolorization of certain reactive dye from aqueous solution using Baker's Yeast (Saccharomyces cerevisiae) strain . *HBRC Journal*, *12*(1), 88–98. https://doi.org/10.1016/j.hbrcj.2014.07.005

Martorell, M. M., Rosales Soro, M. del M., Pajot, H. F., & de Figueroa, L. I. C. (2018). Optimization and mechanisms for biodecoloration of a mixture of dyes by Trichosporon akiyoshidainum HP 2023. *Environmental Technology (United Kingdom)*, *39*(24), 3169–3180. https://doi.org/10.1080/09593330.2017.1375024

Melin, T., Jefferson, B., Bixio, D., Thoeye, C., De Wilde, W., De Koning, J., van der Graaf, J., & Wintgens, T. (2006). Membrane bioreactor technology for wastewater treatment and reuse. *Desalination*, *187*(1–3), 271–282. https://doi.org/10.1016/j.desal.2005.04.086

Melissa Denchak. (2018). *Water Pollution: Everything You Need to Know*. https://www.nrdc.org/stories/water-pollution-everything-you-need-know

Miao, S., Xia, H., Gao, H., Mao, X., Shi, M., & Zhang, Y. (2022). Metal-organic frameworks-derived CoFeN-NC materials with the enhanced catalytic activity and selectivity for the degradation of organic dyes via adsorption and heterogeneous photo-Fenton. *Applied Surface Science*, *601*. https://doi.org/10.1016/j.apsusc.2022.154028

Mukkera Vamshi Krishna, S Srinath, Katuri Srivani. Predicting the biodegradation of the Azo Dye Tertracid Red E using Residual Plots, Materials Today Proceedings, Volume 72, Part 1, 2023, pp. 317-323, Elsevier, https://doi.org/10.1016/j.matpr.2022.07.405

Narayanan, C. M., & Narayan, V. (2019). Biological wastewater treatment and bioreactor design: A review. In *Sustainable Environment Research* (Vol. 1, Issue 1). BioMed Central Ltd. https://doi.org/10.1186/s42834-019-0036-1

Naz, I., Khatoon, N., Ali, M. I., Saroj, D. P., Batool, S. A. ul, Ali, N., & Ahmed, S. (2014). Appraisal of the tire derived rubber (TDR) medium for wastewater treatment under aerobic and anaerobic conditions. *Journal of Chemical Technology and Biotechnology*, *89*(4), 587–596. https://doi.org/10.1002/jctb.4161

Ngo, A. C. R., Devanadera, M. K. P., & Dedeles, G. R. (2016). Decolorization of Selected Synthetic Textile Dyes by Yeasts from Leaves and Fruit Peels. *Journal of Health and Pollution*, *6*(10), 42–55. https://doi.org/10.5696/2156-9614-6-10.42

Olawoye, B. (2020). *A comprehensive handout on central composite design (ccd)*. *July*.

Patil, N. K., Veeranagouda, Y., Vijaykumar, M. H., Anand Nayak, S., & Karegoudar, T. B. (2006). Enhanced and potential degradation of o-phthalate by Bacillus sp. immobilized cells in alginate and polyurethane. *International Biodeterioration and Biodegradation*, *57*(2), 82–87. https://doi.org/10.1016/j.ibiod.2005.11.007

Pearce, C. I., Lloyd, J. R., & Guthrie, J. T. (2003). The removal of colour from textile wastewater using whole bacterial cells: A review. In *Dyes and Pigments* (Vol. 58, Issue 3, pp. 179–196). Elsevier BV. https://doi.org/10.1016/S0143-7208(03)00064-0

Popli, S., & Patel, U. D. (2015). Destruction of azo dyes by anaerobic–aerobic sequential biological treatment: a review. In *International Journal of Environmental Science and Technology* (Vol. 12, Issue 1, pp. 405–420). Center for Environmental and Energy Research and Studies. https://doi.org/10.1007/s13762-014-0499-x

Pulicherla, K. K., Kumar, P. S., Manideep, K., Rekha, V. P. B., Ghosh, M., & Rao, K. R. S. S. (2013). Statistical approach for the enhanced production of cold-active β-galactosidase from thalassospira frigidphilosprofundus: A novel marine psychrophile from deep waters of bay of bengal. *Preparative Biochemistry and Biotechnology*, *43*(8), 766–780. https://doi.org/10.1080/10826068.2013.773341

Qu, Y., Shi, S., Ma, F., & Yan, B. (2010). Decolorization of Reactive Dark Blue K-R by the synergism of fungus and bacterium using response surface methodology. *Bioresource Technology*, *101*(21), 8016–8023. https://doi.org/10.1016/j.biortech.2010.05.025

Rajamohan, N., & Rajasimman, M. (2013). Kinetic Modeling of Dye Effluent Biodegradation by Pseudomonas Stutzeri. In *Technology & Applied Science Research* (Vol. 3, Issue 2). www.etasr.com

Rajmohan K S, Ramya A, Murali Mohan Seepana (2019). Recent advancements and perspectives on biological degradation of Azo Dye. *Biochemical and Environmental Bioprocessing: Challenges and Developments*. 17, 17-31

Ramsay, J. A., Mok, W. H. W., Luu, Y. S., & Savage, M. (2005). Decoloration of textile dyes by alginate-immobilized Trametes versicolor. *Chemosphere*, *61*(7), 956–964. https://doi.org/10.1016/j.chemosphere.2005.03.070

Saqib, S., Akram, A., Halim, S. A., & Tassaduq, R. (2017). Sources of β-galactosidase and its applications in food industry. In *3 Biotech* (Vol. 7, Issue 1). Springer Verlag. https://doi.org/10.1007/s13205-017-0645-5

Saratale, G. D., Saratale, R. G., Chang, J. S., & Govindwar, S. P. (2011). Fixed-bed decolorization of Reactive Blue 172 by Proteus vulgaris NCIM-2027 immobilized on Luffa cylindrica sponge. *International Biodeterioration and Biodegradation*, *65*(3), 494–503. https://doi.org/10.1016/j.ibiod.2011.01.012

Saratale, R. G., Saratale, G. D., Chang, J. S., & Govindwar, S. P. (2011). Journal of the Taiwan Institute of Chemical Engineers Bacterial decolorization and degradation of azo dyes : A review. *Journal of the Taiwan Institute of Chemical Engineers*, *42*(1), 138–157. https://doi.org/10.1016/j.jtice.2010.06.006

Saravanan, P., Kumaran, S., Bharathi, S., Sivakumar, P., Sivakumar, P., Pugazhvendan, S. R., Aruni, W., & Renganathan, S. (2021). Bioremediation of synthetic textile dyes using live yeast Pichia pastoris. *Environmental Technology and Innovation*, *22*(February), 101442. https://doi.org/10.1016/j.eti.2021.101442

Sen, S. K., Raut, S., Bandyopadhyay, P., & Raut, S. (2016). Fungal decolouration and degradation of azo dyes: A review. *Fungal Biology Reviews*, *30*(3), 112–133. https://doi.org/10.1016/j.fbr.2016.06.003

Sharma, V. K. (2009). Aggregation and toxicity of titanium dioxide nanoparticles in aquatic environment-a review. In *Journal of Environmental Science and Health - Part A Toxic/Hazardous Substances and Environmental Engineering* (Vol. 44, Issue 14, pp. 1485–1495). https://doi.org/10.1080/10934520903263231

Shindhal, T., Rakholiya, P., Varjani, S., Pandey, A., Ngo, H. H., Guo, W., Ng, H. Y., & Taherzadeh, M. J. (2021). A critical review on advances in the practices and perspectives for the treatment of dye industry wastewater. In *Bioengineered* (Vol. 12, Issue 1, pp. 70–87). Bellwether Publishing, Ltd. https://doi.org/10.1080/21655979.2020.1863034

Singh, G., Dwivedi, S. K., & Mishra, J. (2020). *Role of Fungal Enzymes in the Removal of Azo Dyes* (pp. 231–257). https://doi.org/10.1007/978-981-15-1710-5_9

Singh, R. L., Singh, P. K., & Singh, R. P. (2015). Enzymatic decolorization and degradation of azo dyes - A review. In *International Biodeterioration and Biodegradation* (Vol. 104, pp. 21–31). Elsevier Ltd. https://doi.org/10.1016/j.ibiod.2015.04.027

Solís, M., Solís, A., Pérez, H. I., Manjarrez, N., & Flores, M. (2012). Microbial decolouration of azo dyes: A review. In *Process Biochemistry* (Vol. 47, Issue 12, pp. 1723–1748). https://doi.org/10.1016/j.procbio.2012.08.014

Song, Q., Sun, Z., Chang, Y., Zhang, W., Lv, Y., Wang, J., Sun, F., Ma, Y., Li, Y., Wang, F., & Chen, X. (2021). Efficient degradation of polyacrylate containing wastewater by combined anaerobic–aerobic fluidized bed bioreactors. *Bioresource Technology*, *332*. https://doi.org/10.1016/j.biortech.2021.125108

Stolz, A. (2001). Basic and applied aspects in the microbial degradation of azo dyes. *Applied Microbiology and Biotechnology*, *56*(1–2), 69–80. https://doi.org/10.1007/s002530100686

Sudarshan, S., Harikrishnan, S., RathiBhuvaneswari, G., Alamelu, V., Aanand, S., Rajasekar, A., & Govarthanan, M. (2023). Impact of textile dyes on human health and bioremediation of textile industry effluent using microorganisms: current status and future prospects. In *Journal of applied microbiology* (Vol. 134, Issue 2). NLM (Medline). https://doi.org/10.1093/jambio/lxac064

Telke, A., Kalyani, D., Jadhav, J., & Govindwar, S. (2008). Kinetics and mechanism of reactive red 141 degradation by a bacterial isolate Rhizobium radiobacter MTCC 8161. *Acta Chimica Slovenica*, *55*(2), 320–329.

Torres, M., & Dickson, A. J. (2021). Overexpression of transcription factor BLIMP1/prdm1 leads to growth inhibition and enhanced secretory capacity in Chinese hamster ovary cells. *Metabolic Engineering*, *67*, 237–249. https://doi.org/10.1016/j.ymben.2021.07.004

Vamshi Krishna Mukkera (a), Srivani Katuri and Rajmohan K. Soundararajan. Study of Biodegradation of Chrysophenine: Using bacteria *Thalassospira Frigidphilosprofundus* and *Erwinia Chrysanthemi Burkholder*. Journal of Water Chemistry and Technology (JWCT), Vol. 44, No. 5, pp. 381–388. © Allerton Press, Inc., 2022, DOI: 10.3103/S1063455X22050071

Vamshi Krishna Mukkera (b), Srivani Katuri. Biodegradation of the Azo Dye AIREDALE YELLOW CHD: Understanding using residuals, Journal of Experimental Biology and Agricultural Sciences (JEBAS), Horizon Publisher India [HPI], 10(2), 430-439, 2022, DOI: https://dx.doi.org/10.18006/2022.10(2).430.439

Van Der Zee, F. P., & Villaverde, S. (2005). Combined anaerobic-aerobic treatment of azo dyes - A short review of bioreactor studies. *Water Research*, *39*(8), 1425–1440. https://doi.org/10.1016/j.watres.2005.03.007

Vandevivere, P. C., Bianchi2, R., & Verstraete1, W. (1998). Review Treatment and Reuse of Wastewater from the Textile Wet-Processing Industry: Review of Emerging Technologies. In *J. Chem. T echnol. Biotechnol* (Vol. 72).

Varjani, S., Rakholiya, P., Ng, H. Y., You, S., & Teixeira, J. A. (2020). Microbial degradation of dyes: An overview. *Bioresource Technology*, *314*(June). https://doi.org/10.1016/j.biortech.2020.123728

Xu, M., Guo, J., & Sun, G. (2007). Biodegradation of textile azo dye by Shewanella decolorationis S12 under microaerophilic conditions. *Applied Microbiology and Biotechnology*, *76*(3), 719–726. https://doi.org/10.1007/s00253-007-1032-7

Yang, C., Luo, H., Cheng, W., Jiang, K., Lu, L., & Ling, L. (2022). Decolorization characteristics and mechanism of methyl orange dye by using Stenotrophomonas acidaminiphila EFS1. *International Journal of Environmental Science and Technology*, *19*(10), 10353–10362. https://doi.org/10.1007/s13762-021-03846-6

Zhao, L. C., He, Y., Deng, X., Yang, G. L., Li, W., Liang, J., & Tang, Q. L. (2012). Response surface modeling and optimization of accelerated solvent extraction of four lignans from fructus schisandrae. *Molecules*, *17*(4), 3618–3629. https://doi.org/10.3390/molecules17043618

List of Publications

Journal Publications based on the thesis work

1. **Vamshi Krishna Mukkera,** Srivani Katuri and Rajmohan K. Soundararajan. Study of Biodegradation of Chrysophenine: Using bacteria *Thalassospira Frigidphilosprofundus* and *Erwinia Chrysanthemi Burkholder*. Journal of Water Chemistry and Technology (JWCT), Vol. 44, No. 5, pp. 381–388. © Allerton Press, Inc., 2022, DOI: 10.3103/S1063455X22050071
2. **Vamshi Krishna Mukkera**, Srivani Katuri. Biodegradation of the Azo Dye AIREDALE YELLOW CHD: Understanding using residuals, Journal of Experimental Biology and Agricultural Sciences (JEBAS), Horizon Publisher India [HPI], 10(2), 430-439, 2022, DOI: https://dx.doi.org/10.18006/2022.10(2).430.439
3. **Mukkera Vamshi Krishna**, S Srinath, Katuri Srivani. Predicting the biodegradation of the Azo Dye Tertracid Red E using Residual Plots, Materials Today Proceedings, Volume 72, Part 1, 2023, pp. 317-323, Elsevier, https://doi.org/10.1016/j.matpr.2022.07.405
4. **Vamshi Krishna Mukkera**, Srivani Katuri, Usha Sri Musham. Biodegradation of Chrysophenine GX using *Candida Albicans* (NCIM 3665), Materials Today Proceedings, Volume 77, Part 1, 2023, pp. 350-357, Elsevier, https://doi.org/10.1016/j.matpr.2022.11.495

Book Chapter

1. **Vamshi Krishna Mukkera**, Srivani Katuri. Decolorization of Azo Dye-Contaminated Water using Microbes: A Review, in the book titled Innovative Trends in Hydrological and Environmental Systems, Springer, pp. 821-835, Print ISBN: 978-981-19-0303-8, 2022, https://doi.org/10.1007/978-981-19-0304-5_57

Conferences proceedings

1. Mukkera Vamshi Krishna, Dr. K. Srivani. Decolorization of azo dyed water using microbes: a review, National conference on “Advances in Food processing for Sustainable Food security”, organized by Department of Food Process Engineering, NIT Rourkela, May 17-18, 2019 “Best Paper Award”.
2. Vamshi Krishna Mukkera, Srivani Katuri. Biodegradation of Acid Red 13: A study using bacteria *Thalassospira Frigidphilosprofundus* and *Erwinia Chrysanthemi Burkholder*, International Conference on Advances in Sustainable Research for Energy

and Environmental Management (ASREEM-2021), NIT Surat, Gujarat, India, August 6-8, 2021.

3. Mukkera Vamshi Krishna, Dr S Srinath, Dr Katuri Srivani. Predicting The Biodegradation of the Azo Dye Tertracid Red E Using Residual Plots, International conference on Novel Materials and Technologies for Energy and Environmental Applications, Birla Institute of Technology & Science, Pilani – Hyderabad Campus, 18th and 19th February 2022.
4. Vamshi Krishna Mukkera, Srivani Katuri, Usha Sri Musham Biodegradation of Chrysophenine GX using Candida Albicans (NCIM 3665), 1st International Conference on Advances in Water Treatment and Management (ICAWTM 22), 25th and 26th March 2022, organized by Pandit Deendayal Energy University, Gandhinagar, Gujarat, India

Conferences / Workshops attended

1. A five-day Workshop on "Advanced computer aided modelling of chemical and biochemical processes" organized Department of Chemical engineering at National Institute of Technology Warangal, September 3 to 7, 2018
2. “Modelling and Control of Wastewater Treatment plants”, 19-23 November, 2018, Department of Chemical Engineering, NIT Warangal, Course Code: 171036B12.
3. Conference on “Advances in Food processing for Sustainable Food security”, organized by Department of Food Process Engineering, NIT Rourkela, May 17-18, 2019
4. International conference on Advances in Chemical Sciences and Technologies (Under TEQIP-III) 23-25 September, 2019, Department of Chemistry, NIT Warangal.
5. Young scientist conference -India International Science festival, on the theme of Frontier areas of research. November 5-8, 2019
6. International Conference on Innovative Trends in Hydrological and Environmental systems (ITHES), April 28-30, 2021, NIT Warangal.
7. Advances in Sustainable Research for Energy and Environmental Management (ASREEM-2021).
8. A five-day Workshop on software in Mathematics and Statistics (WSMS-2021) organized by National Institute of Technology Tiruchirappalli

9. Third international conference on ENVIRONMENTAL, AGRICULTURAL, CHEMICAL AND BIOLOGICAL SCIENCES (ICEACBS) in support of United Nations- SDGS, 22-26 January 2022
10. International conference on Novel Materials and Technologies for Energy and Environmental Applications (NMTEEA), Department of Chemical Engineering, Birla Institute of Technology & Science, Pilani – Hyderabad Campus, 18th and 19th February 2022.
11. 1st International Conference on Advances in Water Treatment and Management (ICAWTM 22), 25th and 26th March 2022 , organized by Pandit Deendayal Energy University, Gandhinagar, Gujarat, India